Dear Prof. Nunzio Romano,

A detailed sheet showing the changes and progress regarding our manuscript is provided as follows:

- in order to better explain the rationale of our study, the introduction has been improved. Moreover, in the paper, a new test comparing the recharge-displacement correlation between the recharge estimated with our method and a recharge obtained with a common simplification in landslide studies (recharge = precipitation minus non-calibrated ET_0) has been added. This test shows that our method more faithfully allows to estimate the groundwater recharge. We also propose to slightly modify the title as follows: AN EFFICIENT WORKFLOW TO ACCURATELY COMPUTE GROUNDWATER RECHARGE FOR THE STUDY OF RAINFALL-TRIGGERED DEEP-SEATED LANDSLIDES, APPLICATION TO THE SÉCHILIENNE UNSTABLE SLOPE (WESTERN ALPS).
- a clarification of the data needed to implement the proposed workflow has been added
- the section dealing with the estimation of the recharge-area parameters has been completely rewritten and the figure 1 has been updated accordingly
- the site description (and especially hydrogeology functioning) as well as the explanation of the delimitation of the recharge area have been improved
- the section dealing with the correlation between precipitation-recharge and displacement has been clarified
- results and discussions are now separated
- the benefit of the study regarding the Séchilienne landslide (site specific) has been moved to a new appendix
- the manuscript structure has been simplified:

Number of section	Title 1	Title 1.1	Title 1.1.1	Appendix
Old version	5	15	14	2
New version	5	15	4	3
Difference	0	0	-10	+1

- the manuscript has been shortened:

Number of word	Manuscript	Appendix	Captions	Total
Old version	9814	928	987	11729
New version	8165	1821	971	10957
Difference	-1649	+893	-16	-772

- most of the technical corrections from the two referees have been taken into account
- the manuscript have been proofread a second time by an English hydrogeologist

A detailed point-to-point reply to the comments received is provided in appendix 1 for referee 1 and in appendix 2 for referee 2 of this letter. These appendices are a copy of our answers from the interactive discussion which have been updated with the last changes we made to the submitted manuscript. A marked-up manuscript version is provided in appendix 3.

We agree with most of the referees's comments. For those we disagree with, reasons are developed in Appendices 1 and 2. However, we would like to insist on the fact that our research can bring a great contribution in the landslide community and can lead to a significant improvement of the knowledge of the rainfall-destabilisation relationship of numerous landslide sites. The proposed study is intended for non-hydrologists and shows that an accurate estimation of the recharge is crucial. We provide a guideline workflow to remove this scientific obstacle. We believe that our manuscript should be published as an original research article rather than a technical brief note.

Please let us know if you require further details about the revised manuscript.

Yours sincerely, Aurélien Vallet

Appendix 1: detailed point-to-point reply to the referee#1's comments

We would like to thank Referee #1 for his/her interest in the topic and for valuable comments to improve the manuscript. A point-by-point response to the comments is as follows:

General comments:

1: The site description, deformation mechanism and rainfall triggering have been improved to explain how the geology and the structural setting influence groundwater circulation and how the groundwater flow path is developed.

The recharge area is defined following geological and hydrogeochemical studies of Vengeon (1998), Guglielmi et al. (2002) and Mudry et Etievant (2007). The following figure shows a sketch of the conceptual groundwater flow defined by Guglielmi et al. (2002). In addition the sensitivity analysis allows to refine the estimation of the recharge parameters if a bias is introduced by the delimitation of the recharge area.

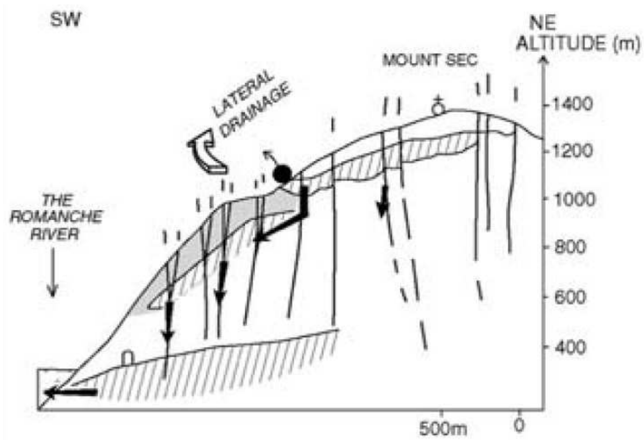

To clarify how the recharge area is delimited, we propose to modify the first paragraph of the section 3.2 (section 4.2 in the initial submitted manuscript) as follow:

*'The delimitation of the recharge area of the two-layer hydrosystem (*Fig. 3*) of the Séchilienne landslide is based on the geological and hydrochemical studies of Vengeon* (1998)*, Guglielmi et al.* (2002) *and Mudry and Etievant* (2007)*. The recharge area is delimited by the spatial extent of the sedimentary cover of which the hosting perched aquifer recharges the two-layer hydrosystem. Groundwater flow of the entire Mont-Sec massif is controlled by faults and fractures. The N20 fault bordering the sedimentary cover to the east as well as the N-S fault zone bordering the landslide to the east are structures which delimitate the recharge area. The scarcity of information does not allow to accurately define the actual extent of the recharge area. The sensitivity analysis mentioned in Section* 2.5 *allows to compensate for the possible biases introduced by this uncertainty.'*

Further, the figure 3 will integrate the spatial extent of the sedimentary cover:

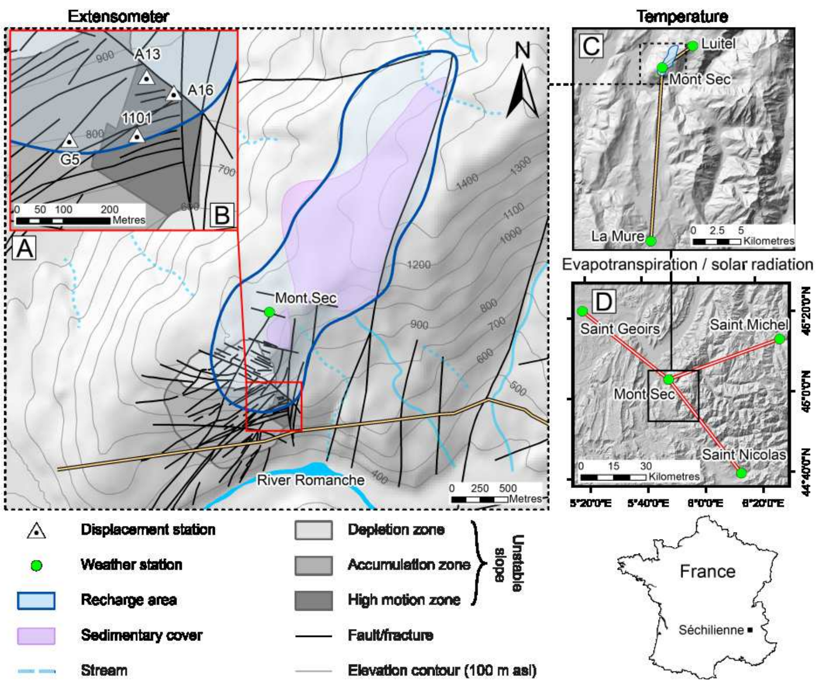

2: In this study, we analyse displacements measured once a day. This measurement is actually a daily displacement and is equivalent to a displacement velocity in mm/day. For the sake of simplicity we propose to use the term displacement instead of daily displacement. We propose to modify the section 2.1 with the following sentences:

'Similarly, this study is based on displacement recorded at a daily time-step. For the sake of simplicity, the daily displacement, equivalent to a velocity measurement in mm/day, is hereafter referred to as displacement.'

In the part of the text preceding these sentences, the displacement will be referred to as displacement velocity.

The method develop to approximate the groundwater saturation state allows to provide a landslide response-time analysis with the shift factor and the cumulative period from the decreasing sum. We propose to elaborate on this point in the appendix C (new appendix of the revised manuscript) with the following sentences and the table 2 (table 6 in the initial submitted manuscript):

'The cumulative period and the shift factor deduced from the antecedent cumulative sum allow to determine the response-time of the Séchilienne landslide to rainfall events. Displacement stations located in the high motion zone show homogenous time delays with shift factors of 2 to 3 days. The average cumulative periods beyond which precipitation or R_{LRIW} have no longer any influence on the landslide destabilisation are estimated at about 50 days for precipitation and 75 days for R_{LRIW}. The station G5 shows significantly different time delays and cumulative periods, whatever the precipitation or R_{LRIW} data used. This difference can be explained by the low signal-to-noise ratio which makes the correlations difficult to interpret.'

Table 2: Statistics of the displacement records and results of the best linear correlation between precipitation/R_{LRIW} and displacement records for 4 displacement stations (1101, A13, A16 and G5). The displacement column indicates basic statistics of the displacement records: 1st quartile (Q1), median and 3rd quartile (Q3). Cumulative period (n), shift factor (β) and weighting factor (α) are the terms of the equation (3). P stands for precipitation, R_1 stands for R_{PMNE} and R2 stands for R_{LRIW}.

Station	Displacement mm/day	Cumulative period (n)			Shift factor (β)			Weighting factor (α)			R^2		
	Q1/median/Q3	P	R_1	R_2	P	R_1	R_2	P	R_1	R_2	P	R_1	R_2
1101	1.75 / 2.50 / 3.84	42	54	68	2	2	2	0.071	0.065	0.091	0.28	0.35	0.50
A13	1.18 / 1.75 / 3.41	52	80	82	3	2	2	0.102	0.070	0.091	0.28	0.37	0.52
A16	1.94 / 2.98 / 4.39	64	71	76	2	2	2	0.163	0.125	0.168	0.34	0.44	0.59
G5	0.02 / 0.05 / 0.08	8	169	132	0	6	6	0.039	0.003	0.011	0.001	0.08	0.24

3: We agree with this comment about our paper, but we prefer to wait for the comments of the other referees before addressing this comment

4: The revised manuscript will be proof-read by an English native speaker.

Specific comment:

1: modified in the revised manuscript

2: reference added in the revised manuscript

3: modified in the revised manuscript

4: Typesetting error, corrected in the revised manuscript

5: modified to earth flow in the revised manuscript

Appendix 2: detailed point-to-point reply to the referee#2's comments

We appreciate the thorough and helpful comments of Anonymous Referee #2. A point-by-point response to the comments is as follows:

General comments:

A: Foremost, the rationale for the study is not strongly communicated.…the authors do not provide a convincing case that the current practice of predicting land-mass movement is inadequate specifically due to the failure to accurately represent groundwater recharge. The reader is left wondering if this work is really needed in the specific case study discussed in this paper.

We agree with this comment. In the introduction, the incriminated sentences are replaced by:

'These approaches can over-estimate the groundwater recharge and can thus bias the characterisation of the relationship between rainfall and destabilisation. A more accurate estimation of the groundwater recharge signal can improve the accuracy of these studies.'

Please refer to additional answers to this comment in the answers to the specific comments 3 and 22.

B: The authors also present this work as a method that can be readily adapted and used by practitioners and non-hydrologist… it is doubtful that this method can be easily adapted and used by practitioners or other researchers.

We agree with this comment. The revised manuscript has been modified accordingly (please refer to the answer to the specific comment 1).

C: The soil-water-balance model is used in this paper to estimate groundwater recharge.

There is no evidence provided to indicate if the model is even remotely accurate (e.g. measurements of water table fluctuations)… of the utility of their more complicated scheme. These points are further discussed in specific comment 22.

Please refer to the answer to the specific comment 22

D: In my opinion, a workflow, which presents no new quantitative representation of any process, does not constitute new scientific knowledge. It could be a potentially useful tool for practitioners. As such, I recommend that when this article is resubmitted, it is resubmitted as a technical brief rather than an original research article.

Although the proposed workflow does not constitute a new scientific progress for hydrologists for who the recharge characterisation is a common knowledge, this is not the case of the scientific community working on landslides. Indeed, several studies estimate the recharge without calibration of the ET_0 reduced-set methods and without soil-water balance by only subtracting the evapotranspiration from the precipitation data or by the use of empirical methods (Canuti et al., 1985; Alfonsi, 1997; Hong et al., 2005; Binet et al., 2007b; Durville et al., 2009; Pisani et al., 2010; Prokešová et al., 2013). In addition, several studies use precipitation data instead of recharge (Rochet et al., 1994; Zêzere et al., 2005; Meric et al., 2006; Helmstetter and Garambois, 2010; Belle et al., 2013). The proposed study is intended for non-hydrologists and aims at showing that an accurate estimation of the recharge is crucial and we provide a guideline workflow to remove this scientific obstacle. For all these reasons, we consider that our manuscript should be published as an original research article rather a technical brief note. In addition, this manuscript was initially submitted to NHESS at the intention of the landslide scientific community, but was rejected before review. The reason of the rejection was “out of scope for NHESS”, and the editor told us to submit our manuscript to HESS.

I would strongly encourage the authors to develop a simple software tool (in Microsoft Excel, or other readily available platform like R). The authors suggest this was one of their primary motivations. Providing a readily usable tool might prompt people to use this workflow, otherwise it is doubtful that many people will wade through this 18-page methods section and appendices and develop their own software to execute the workflow.

We are aware that the implementation of the workflow for a non-hydrologist mainly interested in characterising the rainfall-destabilisation relationship can be laborious. We have been planning to develop a free software is the near future but, before starting this development, we logically wait for the validation of the scientific rationale of the proposed workflow. The software will be based on this manuscript and will require an additional detailed user guide. The software in the form of either a standalone software or a toolbox from an available platform such as R or Matlab (still in discussion). As the purpose of this work is to provide a readily usable tool, we will develop this software with a software engineer in order to design an easy-to-use and friendly interface. This clarification is added in the conclusion:

'*Within this scope, a software is planned to be developed in the near future in order to provide a user-friendly tool for recharge estimation.*'

Specific comments/questions:

1: We agree with this comment. It is modified in the revised manuscript as follows:

'*A workflow to compute daily groundwater recharge is developed. This workflow requires the records of precipitation, air temperature, relative humidity, solar radiation and wind speed within or close to the landslide area. The determination of the parameters of the recharge area is based on a spatial analysis requiring field observations and spatial datasets (digital elevation models, aerial photographs and geological maps).*'

2: We agree with this comment. It is modified in the revised manuscript.

3: We agree with this comment. The introduction of the revised manuscript has been modified.

Regarding the already published studies, given the difficulty to obtain the complete dataset and the details of the methods used in these studies, we could not recalculate the recharge and therefore we cannot determine the benefit of our method for these studies. Moreover, to carry out such recalculations would require several months and would bring the manuscript to an unacceptable length. We rather propose a new test, based on a suggestion in the specific comment 22, which allows the reader to realize the benefit of our method with respect to one common assumption related to the estimation of the recharge (please refer to answer to the specific comment 22).

Regarding the following comment: **Again, more detail is needed here about what exactly is wrong with the assumption that the infiltration rate at the soil surface is equivalent to precipitation.**

We apologise for this ambiguous wording. By "infiltration", we mean "deep percolation". This was modified in the revised manuscript and replaced by recharge.

4: We agree with this comment. It is modified in the revised manuscript.

5: We agree with this comment and we follow the recommendation of Referee 2 by inserting his suggested sentences in the revised manuscript. However we do not insert the following sentence "**In principle, the actual groundwater recharge flux controls the dynamics of**

pore-water pressures and water table fluctuations, rather than the precipitation flux at the land surface”. Instead, we suggest to insert the following sentence in the introduction of the revised manuscript ‘*In the absence of piezometric measurements, the groundwater recharge is used as the most relevant parameter to characterize the pore water pressure of the landslide aquifers’*.

6: We agree with this comment. The entire section 2.1 is deleted in the revised manuscript. Only the sentences from lines 5 to 12 (p 6347) and from lines 24 (p 6347) to 2 (p 6348) are kept and moved to the section 2.2.

7: We partly agree with this comment.

In the revised manuscript, the standard equation FAO-56 PM is now defined in the introduction. Appendix A with the details equations is now announced in the beginning of the sub-sections 2.2.1 and 2.2.2.

The calibration of the reduced-set equations is a common method acknowledged by the scientific community (Allen et al., 1994; Itenfisu et al., 2003; Alkaeed et al., 2006; Lu et al., 2005; Tabari et al., 2013; Alexandris et al., 2008; Shahidian et al., 2012). We refer the reader to these studies. However, we agree with Referee 2 to move the statement from page 6345 (line 18-20) and to be more explicit. The following sentence is added to the section 2.2 (section 2.3 in the initial submitted manuscript):

‘ET_0 reduced-set and R_S temperature methods were initially developed for given regions or sites with their own climatic conditions and must be calibrated to take into account the weather conditions of the study site. Details about calibration can be found in the literature (Allen et al., 1994; Itenfisu et al., 2003; Lu et al., 2005; Alkaeed et al., 2006; Alexandris et al., 2008; Shahidian et al., 2012; Tabari et al., 2013).’

The purpose of the calibration is to account for the weather conditions specific to the study site. Although three stations can appear as a small sample size, the network density of weather stations recording the required parameters at a daily rate is generally weak. Increasing the number of reference stations can lead to use remote stations that might be located in remote areas not representative of the climatic conditions of the study site. The user has to maintain a balance between the sample size and the representativeness of the reference weather stations. One reference weather station can be sufficient, provided that the weather conditions are the same at the reference station as at the study site. In the case of the Séchilienne landslide, in order to rely on three stations, we had to look for stations located as 60 kilometres from the study site. The section 2.2 (section 2.3 in the initial submitted manuscript) is modified as follows in the revised manuscript:

'The user has to maintain a balance between the number of selected reference stations and the necessity for these stations to be located in areas with climatic conditions similar to those of the study site.'

The median is an interesting estimator if the data number is significantly high or if the studied dataset shows outliers. In the proposed calibration, the number of required weather reference stations can be limited. The selected reference weather station(s) should be representative of the study site conditions and the calibration coefficient should be within the same range. Consequently, the median estimator is not relevant and the calibration parameters should be within the same range (no outliers). The average estimator allows integrating in one estimator small variations between the various reference stations used. We do not think we need to elaborate on that point in the required effort to reduce the manuscript length.

8: We agree with this comment. The paragraph is clarified in the revised manuscript as follows:

'The performance assessment of regional-scale calibrated methods is based on the comparison between observed measurements and calibrated estimates for R_s and between FAO-56 PM estimates and calibrated estimates for ET_0 for each reference weather station.'

Regarding the sub-comment "**though again, we have not yet seen the actual Equations**" in the revised manuscript, the standard equation FAO-56 PM is now defined in the introduction. Appendix A with detailed equations is now announced in the beginning of the sub-sections 2.2.1 and 2.2.2.

9: We agree with this comment. The revised manuscript has been revised accordingly.

10: We agree with this comment. The equations pertaining to solar radiation have been moved to the Appendix A.

11: We agree with this comment. The manuscript has been revised as follows:

‘*The α coefficient is applied for the two first rain-event days since, for a rain period longer than two days, the value of the Rs estimated from* ΔT *and the actual* R_s *value become almost identical.*’

12: We agree with this comment. The first part of this comment **(Page 6353; lines 10-18: The description of methods here is wholly inadequate. You say, “For one given parameter, the recharge area was divided into sub-areas, each being characterized by a constant value estimated according to field measurements, literature values or calculation.” A methods section should be written with sufficient detail that another scientist could replicate your work based solely on its description within the manuscript. That would be impossible given only this description of how the average parameter values were determined based on landscape characteristics. The subsections that follow (within section 2.4) are similarly vague. For example, in section 2.4.2 the authors state that “SAWC is deduced from soil properties (type of horizon, texture and bulk density) and depth extent from auger hole cores, using a pedotransfer function.” Did you actually measure the soil texture and bulk density using a laboratory method, or did you assume a value based on some soil survey data?)** has been addressed by a complete rewriting of the incriminated section and by a modification of the figure 1.

Regarding the second part of this comment (**Did you assume that the maximum depth of your auger hole was the maximum depth of the soil? Or do you have other information that indicates the depth of the soil? What is the depth to bedrock, and is the bedrock impermeable, fractured, other? Do you think one core is sufficient to extrapolate to the entire sub-area for which you are estimating the SAWC parameter? Soil texture and hydraulic properties can vary by orders of magnitude over small distances.),** our answer is as follows:

All these questions need no longer to be asked because our analysis just requires rough estimates of the various parameters. These estimates will subsequently be refined by a sensitivity analysis.

Regarding the third part of this comment **(Last, you state that the dependency of SAWC on vegetation species is taken into account through the Kc coefficient. More detail is needed here. The description of Kc in the preceding section indicates that it is a function of vegetation height, albedo, canopy resistance and soil evaporation. It is not immediately**

apparent how any of those factors are related to the SAWC, which is a theoretical (and questionable) value indicating the fraction of the total soil-pore volume that can be utilized by plants for solution uptake. Also, you already stated that the SAWC was estimated from a pedotransfer function (all of which are rough approximations for any individual soil), so how is that estimate of SAWC from the pedotransfer function modified based on the Kc coefficient?), our answer is as follows:

The K_c coefficient takes into account the specificity of the vegetation involved in the evapotranspiration process and therefore integrates the specific extent of the root zone. This point is not necessary to understand the method and is removed from the revised manuscript.

13: The estimated runoff in our study includes both the overland flow and the subsurface flow. The distinction between the two is therefore useless.

14: We do not entirely agree with this comment. Since this study also targets non-hydrologists, we believe it is important to keep this section to help the reader to understand the soil-water balance procedure.

15: We agree with this comment. The revised manuscript has been modified accordingly.

16: According to Verstraeten et al. (2005), the specific vegetation evapotranspiration (ET_c) is a lumped parameter including potential transpiration, potential soil evaporation and canopy interception evaporation. This is why, in our approach, the interception component does not appear on the diagram of Figure 2b since it is taken into account by the ET_C. We agree with Referee 2 that this paragraph is confusing regarding the interception component. The paragraph is modified as follows:

'*The ET_c is a lumped parameter including potential transpiration, potential soil evaporation and canopy interception evaporation (Verstraeten et al., 2005). In the proposed computation diagram workflow (Fig. 2B) the interception component is therefore integrated in the ET_c component.*'

17: We agree with this comment and we modified the revised manuscript accordingly.

18: We agree with this comment. The phrase 'aquifer saturation state' has been removed from the manuscript. Same for 'decreasing sum'.

19: We agree with this comment and the manuscript is modified accordingly as follows:

'The correlation between water input and displacement requires measurements of landslide displacements at the same temporal frequency (daily frequency in this study) as the measurements of water input (precipitation or recharge). The groundwater hydrodynamic processes in aquifers are non-linear. A former rainfall event displays less impact (though not negligible) than a recent one on the aquifer hydrodynamic fluctuations (Canuti et al., 1985; Crozier, 1986; Diodato et al., 2014). The daily precipitation/recharge time series cannot therefore be used without appropriate corrections. An antecedent cumulative sum of precipitation/recharge weighted by a factor α is applied as a moving window to the daily precipitation/recharge time series (Eq. (3)). The antecedent cumulative sum allows to approximate the daily triggering impact of the aquifer ATI on the landslide destabilisation. In order to take into account the groundwater transit time, a β time-lag factor is introduced. This factor can shift the moving window from the target date t.

$$ATI_t = \sum_{i=t+\beta}^{t+\beta+n} \frac{W_i}{1+\alpha\ (\mathrm{i} - (\mathrm{t}+\beta))} \tag{3}$$

where:

ATI_t *Aquifer Triggering Impact at the date t (in mm)*

β *time shift of the moving window (in days)*

i *i^{th} day from the date t (i=t+β: start of the moving window and i= t+β +n: end of the moving window)*

n *length of the moving window of the cumulative period (in days)*

W_i *water input, i.e., precipitation or recharge at the i^{th} day (in mm)*

α *weighting factor*

An iterative grid search algorithm is used to find the optimal set of parameters of the antecedent cumulative sum. The optimal set of parameters is the set that maximizes the correlation performance itself based on the R^2 indicator. The grid search algorithm investigates the following parameter ranges: n from 1 to 250 days (increment: 1 day), α from 0 to 0.5 (increment: 0.0001) and β from 1 to 10 days (increment: 1 day).'

20: The site description is improved in the revised manuscript. For further details please refer to the answer to the general comment 1 of Referee 1.

21: We partly agree with this comment which is actually more general than specific. We added a one-page long “general workflow” section that summarizes the workflow. So far, the revised manuscript is more than one thousand words shorter than the previous submission. We prefer to separate the method details from the application of the method to the Séchilienne landslide. By doing so, any reader who is interested either by the method or by the results for the Séchilienne landslide can select the relevant part.

22: We are aware of the existence of recharge-weighting functions, but these functions are used in the case of tracer-based studies. In our opinion, relying only on ET_0 and precipitation data, and without tracer data, the recharge-weighting functions cannot be used in this study.

Regarding the comment (**Comparing estimated recharge versus precipitation is a fairly weak test. We know, in principle, that recharge is more relevant than simply precipitation for influencing pore-water pressure.**), we answer as follows:

First, several landslide studies use precipitation data instead of the recharge (Rochet et al., 1994; Zêzere et al., 2005; Meric et al., 2006; Helmstetter and Garambois, 2010; Belle et al., 2013). This demonstrates that our precipitation vs. recharge test is not an useless effort.

Furthermore, following Referee 2 comment, we carried out an additional test to compare the performance of our proposed method with an estimated recharge signal itself obtained with the commonly used simplification: Recharge = precipitation minus ***non-calibrated*** ET_0, as used by the following authors (Canuti et al., 1985; Binet et al., 2007b; Pisani et al., 2010; Prokešová et al., 2013). In this additional test, we use the non-calibrated Turc evapotranspiration equation as it is the most appropriate equation for the Séchilienne site. Indeed, the Turc equation has been developed initially for the French climate.

In the revised manuscript, the recharge estimated with our workflow (named LRIW in the revised manuscript: Landslide Recharge Input Workflow) is called R_{LRIW} and the recharge estimated by subtracting the non-calibrated ET_0 from precipitation is called R_{PMNE} (PMNE standing for Precipitation Minus Non-calibrated ET_0).

Accordingly, new Null Hypothesis tests have been performed as follows:

To estimate whether the R_{PMNE}/displacement correlation R^2 is significantly better than the precipitation/displacement correlation R^2 value, the Null Hypothesis 1 (NH1) is tested. The

NH1 states that the R_{PMNE}/displacement correlation R^2 value is not significantly greater than the R^2 value obtained from precipitation. In other words, the NH1 statistic test is the difference between the R_{PMNE} R^2 value and the precipitation R^2 value, expected to be 0 if no difference. Similarly, the Null Hypothesis 2 (NH2) and the Null Hypothesis 3 (NH3) are tested. NH2 estimates whether the R_{LRIW}/displacement correlation R^2 is significantly better than the precipitation/displacement correlation R^2 value. NH3 estimates whether the R_{LRIW}/displacement correlation R^2 is significantly better than the R_{PMNE}/displacement correlation R^2 value.

The results of this additional test are added in the revised manuscript and Figure 10 is modified as follows:

'Figure 10 *summarizes the comparison of the performances between the precipitation, the R_{PMNE} and the R_{LRIW} based on the NH1, NH2 and NH3 tests for the four extensometers. All LBCI values from bootstrap testing of NH1, NH2 and NH3 are greater than zero, allowing to reject the three null hypotheses for the four stations (*Fig. 2*A). Rejection of the NH1 null hypothesis shows that R^2 obtained with R_{PMNE} are significantly higher than those computed with precipitation. Rejection of the NH2 null hypothesis shows that the R^2 obtained with R_{LRIW} are significantly higher than those computed with precipitation. Similarly, rejection of the NH3 null hypothesis shows that R^2 obtained with R_{LRIW} are significantly higher than those computed with R_{PMNE}. R^2 values vary from 0.0006 to 0.343 for precipitation, from 0.076 to 0.444 for R_{PMNE} and from 0.243 to 0.586 for R_{LRIW}, for G5 and A16 extensometer respectively (*Table 2*). On average, R_{PMNE} allows to increase the R^2 value by 29% relatively to precipitation, while R_{LRIW} allows to increase the R^2 by 78% (*Fig. 2*B). The R^2 obtained with R_{LRIW} are 38% higher on average than those obtained with R_{PMNE}.*

*These results are confirmed by the LBCI and by the observed values of the NH2 test which are always greater than those from the NH1 test as well as by the positive LBCI values of the NH3 test (*Fig. 10*). The correlation performance for the recharge estimated with the LRIW method significantly exceeds the performances of the two other signals, making the LRIW method particularly appropriate to be used in landslide studies. A discussion about the benefit of this study for the understanding of the rainfall-displacement relationship in the case of the Séchilienne landslide can be found in appendix C.'*

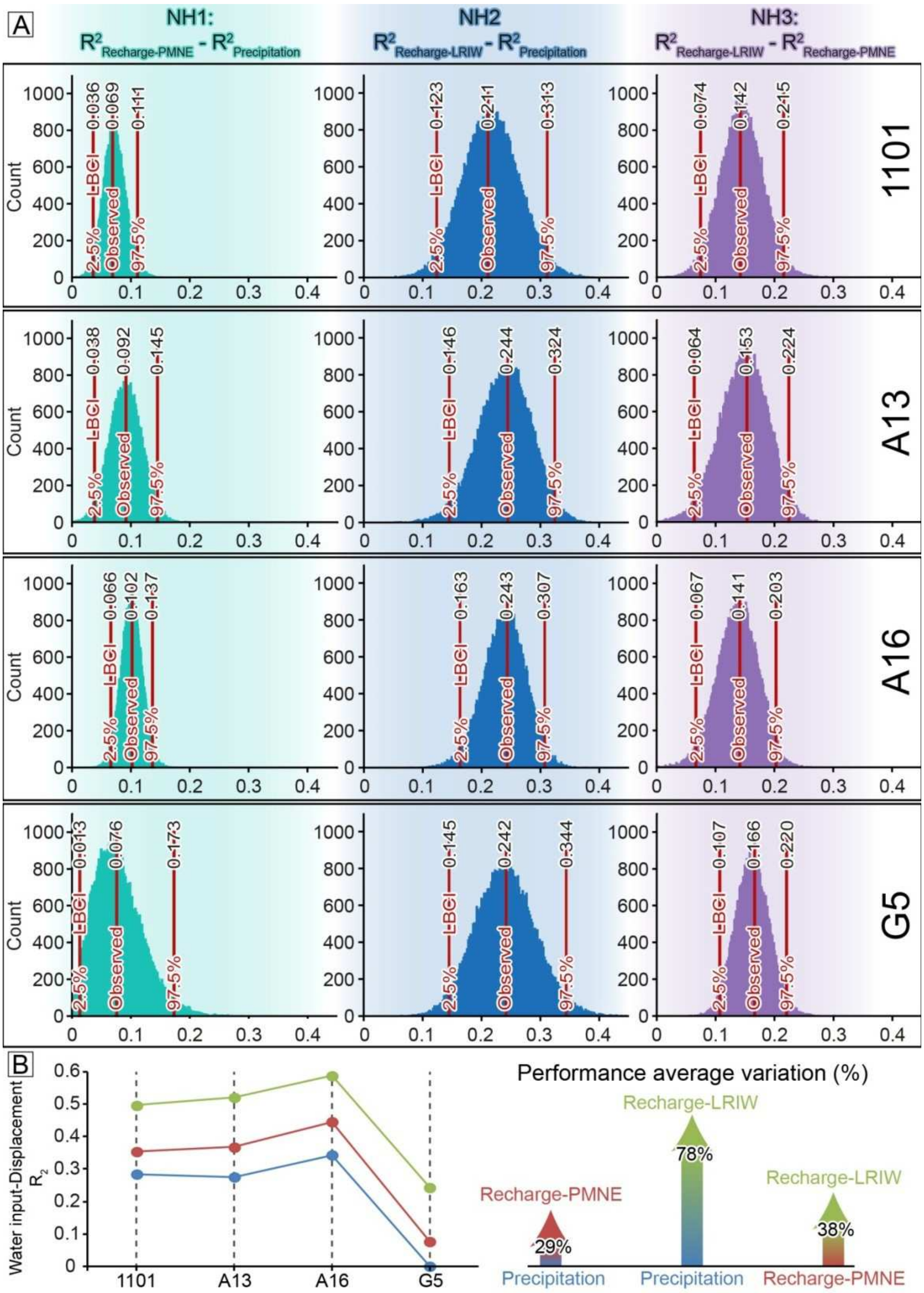

Figure 10: Performance of the LRIW workflow. A: Bootstrap distribution of null hypothesis NH1, NH2 and NH3 tests for four displacement recording stations. LBCI is the lower bound of the confidence interval. B: R^2 values for the four displacement recording stations obtained with the precipitation, recharge-PMNE, and recharge-LRIW. LBCI is the lower bound of the confidence interval. G5 station is disregarded in the calculation of the performance average variation calculation since the R^2 value obtained at G5 from precipitation is close to 0, therefore leading to a non-representative variation.

Technical corrections:

Most technical corrections have been taken into account. Those not taken into account are discussed below:

Page 6366: methods rather than results. We partly agree with this comment.

Lines 5 to 10 are moved to the section 'Application to the Séchilienne landslide'. The rest is kept at the same place as it is the result of the GIS composite analysis.

Page 6389: relative error of 25% seems non-trivial.

We misused the phrase 'relative error'. In the former manuscript, the coefficient of variation of the RMSE (root mean square error) should have been used instead of 'relative error'. The CV(RMSE) is equal to RMSE divided by the observed dataset mean. The CV(RMSE) indicator is used to compare models with different units, which is not the case of this study. In the revised manuscript, the CV(RMSE) is replaced by the RMSE performance indicator. Table 3 is modified as follows:

Table 3: Calibration and performance of the five tested ET_0 methods relatively to the FAO-56 PM ET_0 standard (Penman-Monteith method defined in the FAO-56 paper). All the ET_0 methods are detailed in the appendix A. a, b and R^2 are the results of linear regression between FAO-56 PM ET_0 and tested ET_0 methods. RMSE is the root mean square error

Method	a	b	R^2	RMSE
HS Et_0	0.920	0.130	0.917	0.548
Turc ET_0	0.880	0.434	0.900	0.588
PS ET_0	0.352	0.365	0.919	0.533
M ET_0	1.107	-0.018	0.910	0.565
PM_{red} ET_0	0.994	0.013	0.932	0.505

Appendix 3: marked-up manuscript version

~~A new method to compute the groundwater recharge for the study of rainfall-triggered deep-seated landslides. Application to the Séchilienne unstable slope (western Alps).~~

~~**A. Vallet[1], C. Bertrand[1], O. Fabbri[1], J. Mudry[1]**~~

~~[1] {CNRS:~~

AN EFFICIENT WORKFLOW TO ACCURATELY COMPUTE GROUNDWATER RECHARGE FOR THE STUDY OF RAINFALL-TRIGGERED DEEP-SEATED LANDSLIDES, APPLICATION TO THE SÉCHILIENNE UNSTABLE SLOPE (WESTERN ALPS)

Vallet A.[1], Bertrand C.[1], Fabbri O.[1], Mudry J.[1]

[1] UMR6249 Chrono-Environnement - Université de Franche-Comté - 16 route de Gray - F-25030 Besançon cedex ~~-~~ – France~~}~~

~~Correspondence to: A. Vallet (aurelien.vallet@univ-fcomte.fr)~~

Abstract

Pore water pressure ~~built~~build-up by recharge of underground hydrosystems is one of the main triggering factors of deep-seated landslides. ~~Groundwater recharge, which is the contribution of the precipitation to the recharge of the saturated zone, is a significant parameter. However, in landslide studies, methods and recharge area parameters used to determine the groundwater recharge amount are rarely detailed. Currently, no turnkey method has been proposed to simply and accurately estimate the groundwater recharge. In this study, the groundwater recharge is estimated with a soil water balance based on characterization of evapotranspiration, soil available water capacity and runoff. Although evapotranspiration estimation is a data-demanding method, many landslide sites have limited meteorological datasets. A workflow method is developed to compute daily groundwater recharge. The method requires only temperature and precipitation as inputs. Soil available water capacity and runoff quantities are determined from field observations and spatial datasets using a spatial composite approach before being refined with a sensitivity analysis. The proposed method is developed to be as versatile as possible in order to be readily applied to other landslide sites, and to be sufficiently simple to be used by any specialist who intends to characterise the relationship between rainfall and landslide displacements. Moreover, this method can be applied to any other parameters, as long as these parameters have a relationship with groundwater recharge. This study demonstrates that, for the Séchilienne landslide, the performance of the correlation between rainfall and displacement is significantly improved with groundwater recharge (average R^2 of 0.46) compared to results obtained with precipitation data (average R^2 of 0.25).~~

~~1. Introduction~~

~~Groundwater recharge (hereinafter called recharge) is the part of the precipitation which recharges the saturated zone (aquifer).~~ In most~~Patwardhan et al.~~ ~~(1990) showed that the soil-water balance method is an accurate way to estimate recharge. Recharge computation with a soil-water balance depends mainly on the surface runoff, the soil available water capacity (SAWC) and the specific vegetation (so-called crop) evapotranspiration (ET_c, also referred as potential evapotranspiration) which is deduced from reference vegetation evapotranspiration (ET_0). The Penman-Monteith method (Allen et al., 1998) is the widely acknowledged standard method to estimate ET_0. This method requires the knowledge of the relative humidity, the temperature, the wind speed and the solar radiation.~~

~~However, most weather stations in landslide areas record only temperature and rainfall. Additionally, solar radiation and relative humidity measurements are subject to drift and inaccuracies leading to bias in evapotranspiration computation (Samani, 2000; Droogers and Allen, 2002). Alternate methods based on empirical or physical equations using a reduced meteorological dataset (reduced-set in short) allow a simpler expression of ET_0 based only on temperature and/or solar radiation (Tabari et al., 2013). Alongside, reduced-set methods have also been developed to estimate solar radiation based on temperature records only (Almorox, 2011). Combination of ET_0 and solar radiation reduced-set methods allow an estimation of ET_0 suitable for landslide analyses by requiring only temperature records. Reduced-set methods were developed under specific site conditions and must be calibrated in order to improve accuracy (Allen et al., 1994; Shahidian et al., 2012).~~

~~Pore water pressure built-up by recharge of the aquifer(s) is one of the main triggering factors of motion of deep-seated landslides (Noverraz et al., 1998; Van Asch et al., 1999; Bonzanigo et al., 2001; Guglielmi et al., 2005; Bogaard et al., 2007). In most natural~~ deep-seated landslides, pore water pressure data are not available since piezometers, if any, have a very short lifespan because of slope movements. As a consequence, indirect parameters, such as the calculated recharge, are the only data which enable to understand landslide hydrodynamic behaviour. ~~In this context, recharge is a crucial parameter to estimate.~~ However, in landslide studies, methods and recharge-area parameters used to determine the groundwater recharge are rarely detailed. In this study, the groundwater recharge is estimated with a soil-water balance based on characterization of evapotranspiration and parameters characterising the recharge area (soil-available water-capacity, runoff and vegetation coefficient). A workflow to compute daily groundwater recharge is developed. This workflow requires the records of precipitation, air temperature, relative humidity, solar radiation and wind speed within or close to the landslide area. The determination of the parameters of the recharge area is based on a spatial analysis requiring field observations and spatial datasets (digital elevation models, aerial photographs and geological maps). This study demonstrates that the performance of the correlation with landslide displacement velocity data is significantly improved using the recharge estimated with the proposed workflow. The coefficient of determination obtained with the recharge estimated with the proposed workflow is 78% higher on average than that obtained with precipitation, and is 38% higher on average than that obtained with recharge computed with a commonly used simplification in landslide studies (recharge = precipitation minus non-calibrated evapotranspiration method).

~~In most cases, deep-seated landslide studies take into account recharge, either without calibration of the ET_0 reduced-set methods~~

1. Introduction

Pore water pressure build-up by recharge of aquifers is one of the main triggering factors of destabilisation of deep-seated landslides (~~Binet~~Noverraz et al.,~~ 2007; Durville~~ 1998; Van Asch et al.,~~ 2009; Pisani~~ 1999; Guglielmi et al.,~~ 2010~~ 2005; Bogaard et al., 2007; Bonzanigo et al., 2007)~~, or with the use of elaborate or indirect methods~~. In most deep-seated landslides, pore water pressure data are not available since piezometers, if any, have a very short lifespan because of slope movements. In addition, landslides show heterogeneous, anisotropic and discontinuous properties (~~Hong et al., 2005;~~ Cappa et al., ~~2006; Prokešová~~2004; Binet et al., ~~2013~~2007a)~~. Some studies have used precipitation data as an infiltration input signal~~ and local measurements are rarely representative of the overall behaviour of the landslide aquifers. In the absence of piezometric measurements, the groundwater recharge is used as the most relevant parameter to characterize the pore water pressure of the landslide aquifers. Groundwater recharge (hereafter recharge), also referred to as deep percolation, is the part of the precipitation which recharges the saturated zones (aquifers).

Landslide studies involve a wide range of specialities (sub-surface geophysics, structural geology, modelling, geotechnics, and geomechanics). Scientists or engineers in charge of landslides may not have the required hydrology knowledge to accurately estimate the recharge. In most cases, deep-seated landslide studies devoted to characterise the rainfall-destabilisation relationships do not take into account recharge with enough accuracy. In particular, some studies estimate the recharge without calibration of the evapotranspiration estimation methods and without soil-water balance (~~Rochet~~Canuti et al., ~~1994~~1985; Alfonsi, 1997; ~~Zêzere~~Hong et al., 2005; ~~Merie~~Binet et al., ~~2006; Zizioli~~2007b; Durville et al., 2009; Pisani et al., 2010; Prokešová et al., 2013)~~. These approaches can lead to significant errors in estimates of infiltration and tend to under-estimate or over-estimate the destabilisation triggered by rainfall. In addition, in these studies, the methods and the recharge area parameters used to determine the recharge are rarely detailed and no turnkey method has so far been proposed to estimate simply and accurately the recharge.~~

~~The purpose of this study is to develop an efficient method in order to take into consideration the recharge in the studies of landslides with limited meteorological dataset. The objective of the method is to improve the reliability in calculation for the widest possible audience, by balancing the technical complexity and the accuracy. Indeed, landslide studies involve a wide~~

~~range of specialities (sub-surface geophysics, structural geology, modelling, geotechnics, and geomechanics), for which scientists do not necessarily have the required hydrology training, but are nevertheless capable of following a simplified and robust method to compute the recharge.~~

~~To demonstrate that an accurate estimation of the recharge improves the characterization of the groundwater conditions which trigger the motion of deep-seated landslides, a simple linear correlation between recharge and displacement signals is carried out. The aim of the demonstration is to prove that recharge is a more relevant parameter than precipitation for accounting for the motion of deep-seated landslides, and is performed with no intention to model or to quantify the displacement.~~

~~2. Strategy and Methods~~

~~2.1. Recharge computation strategy~~

~~The computation of the recharge has been simplified and detailed to increase its utility for the widest possible audience, without losing the accuracy required for its intended purpose (the prediction of slope displacement). The concept of requisite simplicity~~ . Lastly, several studies use precipitation data instead of the recharge ~~(Stirzaker et al., 2010)~~(Rochet et al., 1994; Zêzere et al., 2005; Meric et al., 2006; Helmstetter and Garambois, 2010; Belle et al., 2013). These approaches can over-estimate the groundwater recharge and can thus bias the characterisation of the relationship between rainfall and destabilisation. A more accurate estimation of the groundwater recharge signal can improve the accuracy of these studies. So far, no computation workflow has been proposed to estimate simply and accurately the recharge in the context of landslide studies.

Patwardhan et al. ~~has been central to the design of an efficient method, balancing technical accuracy with utility for non-hydrologist users. It is thought that the method developed in this study is suitable for a typical scenario concerning both the availability of data for the site and the technical background of the user.~~

~~With respect to this aim, only the soil available water capacity (SAWC), the runoff coefficient, the vegetation coefficient and the evapotranspiration have been taken into account over the recharge area (averaged estimation for the whole recharge area). Evapotranspiration is the major factor influencing the recharge signal. Surface runoff is also a significant process to determine in order to accurately estimate the recharge. This is particularly true in mountainous areas or in areas prone to intense storms. Additional parameters such as the exposure to solar radiation or the influence of the unsatured zone and discrete calculation could be taken into account, but at the expense of a greater complexity, with no guarantee of significantly improving the accuracy.~~

~~Typically, the deeper the aquifer, the slower the recharge and the more smoothed the recharge signal. However, a landslide is not a homogeneous medium. A part of the groundwater flows is slow and occur over several months, while another part is rapid and occur over a few days (Mudry and Etievant, 2007)~~(1990)~~. Both slow and rapid flows play a role in landslide destabilization. A monthly resolution is therefore too long to take the groundwater response into account in the analysis. For a deep-seated landslide triggered by a deep water-saturated zone, the impact of a multi-day cumulative rainfall is far more significant than rainfall duration or intensity (Guzzetti et al., 2008). The hourly rainfall input signal is smoothed through hydrogeologic processes, depending on the hydrosystem inertia and connectivity. For these reasons, this study is based on a daily time-step. The availability of the environmental~~

~~data on a daily resolution determines which weather stations should be selected to supply the input data.~~

~~2.2. Method workflow~~

~~The recharge method workflow (Figure 1) includes three steps. The first step~~ showed that the soil-water balance method is an accurate way to estimate groundwater recharge. Recharge computation with a soil-water balance depends mainly on the surface runoff, the soil-available water-capacity (SAWC) and the specific vegetation (so-called crop) evapotranspiration (ET_c, also referred to as potential evapotranspiration), itself being deduced from reference vegetation evapotranspiration (ET_0) with a vegetation coefficient (K_c). The Penman-Monteith method (Eq. (A6) in appendix A)), hereafter referred to as the ET_0 standard equation or FAO-56 PM, developed in the paper FAO-56 (Food and Agriculture Organization of the United Nations) is considered by the scientific community as a global standard method to estimate ET_0 worldwide (Jensen et al., 1990; Allen et al., 1998). This method requires the knowledge of the air relative humidity, the air temperature, the wind speed and the solar radiation. However, most weather stations in landslide areas record only air temperature and rainfall. Unlike the FAO-56 PM method, methods based only on air temperature and solar radiation (R_s) allow a simpler expression of ET_0 (Tabari et al., 2013). Besides, R_s can also be estimated only from air temperature (Almorox, 2011), thus allowing ET_0 to be obtained only from air temperature records. These reduced-set methods are developed under specific site conditions and must be calibrated in order to improve accuracy (Allen et al., 1994; Shahidian et al., 2012).

The objective of this study is to develop a parsimonious, yet robust, guideline workflow to calculate time series of groundwater recharge at the scale of the recharge area, time series that can subsequently be used as a deterministic variable in landslide studies. To maximize the accessibility to diverse user groups, we strive to develop an efficient method, balancing technical accuracy with operational simplicity. The proposed workflow is applied on the deep-seated Séchilienne landslide. To test its utility, a correlation analysis is used to evaluate whether the calculated groundwater recharge is more strongly correlated with measured land mass displacement velocities than with precipitation or with recharge estimated with a common simplification in landslide studies (recharge = precipitation minus non-calibrated ET_0; Canuti et al., 1985; Binet et al., 2007; Pisani et al., 2010; Prokešová et al., 2013). The significance of the correlations is assessed with bootstrap tests. The proposed study aims at showing that an accurate estimation of the recharge can significantly improve the results of rainfall-displacement studies.

2. Method

2.1. General workflow

In the case of deep-seated landslides triggered by deep water-saturated zones, the impact of a multi-day cumulative rainfall is far more significant than rainfall duration or intensity (Van Asch et al., 1999; Guzzetti et al., 2008). For these reasons, the workflow is developed to compute daily groundwater recharge. Similarly, this study is based on displacement recorded at a daily time-step. For the sake of simplicity, the daily displacement, equivalent to a velocity measurement in mm/day, is hereafter referred to as displacement. The groundwater recharge is estimated with a soil-water balance based on characterization of ET_0 and parameters characterising the recharge area (SAWC, runoff and K_c). The computation workflow (Fig. 1), hereafter referred to as LRIW (Landslide Recharge Input Workflow), includes four steps.

The estimation of the ET_0 requires the records of air temperature within the landslide area and relative humidity, solar radiation and wind speed within or close to the landslide area. In the case of a landslide-located weather station recording only the temperature, the first step (detailed in section 1.1) consists of a regional calibration of ~~reference vegetation evapotranspiration (~~ET_0~~)~~ and ~~solar radiation (~~R_S~~)~~ reduced-set ~~methods, with respect to the standard evapotranspiration method and direct measurements using reference weather stations recording all required parameters (~~equations (equations detailed in ~~section 2.3). Calibrated~~appendix A). The calibrated methods then allow to estimate evapotranspiration ~~at the landslide site equipped with a weather station measuring~~based only on temperature records. In the case of a landslide weather station recording the full set of parameters, the first step can be skipped and the FAO-56 PM method can then be used to estimate ET_0. The second step (detailed in section 2.3) consists in estimating the ~~vegetation coefficient, the SAWC, and the~~recharge-area parameters (surface runoff~~ coefficient across the recharge area~~, SAWC and K_c) using a GIS (Geographic Information Systems) composite method ~~(detailed in section 2.4~~requiring field observations and spatial datasets (digital elevation models, aerial photographs and geological maps). The third step (detailed in section 2.4) uses a soil-water balance to estimate the recharge with ~~calibrated~~the estimated ET_0 and ~~R_S reduced-set methods, and~~ the estimation of the recharge~~-~~-area parameters. The fourth step (detailed in section ~~2.5). Besides,~~0) consists of a sensitivity analysis based on a recharge-displacement velocity correlation and is performed in order to refine the estimations of SAWC and runoff coefficient~~ estimations~~.

~~2.3.Methods calibration –~~ Step 1
2.2.~~The regional method~~ : Regional calibration of ET_0 and R_S methods

ET_0 reduced-set and R_S temperature methods were initially developed for given regions or sites with their own climatic conditions and must be calibrated to take into account the weather conditions of the study site. Details about calibration can be found in the literature (Allen et al., 1994; Itenfisu et al., 2003; Lu et al., 2005; Alkaeed et al., 2006; Alexandris et al., 2008; Shahidian et al., 2012; Tabari et al., 2013).

The regional calibration method (Fig. 1– Step 1) is performed using the records of nearby weather stations (~~Figure 1 – Step 1). These stations record the necessary meteorological parameters and will be~~hereafter referred to as reference weather stations~~. Calibrations~~) having similar climatic conditions as the study site and recording the required meteorological parameters. The calibration of R_S and ET_0~~ reduced-set~~ methods are performed for each reference weather station (local scale). The local adjustment coefficients of the reference stations~~, deduced from the local calibration,~~ are then averaged in order to define a regional calibration~~ for sites where more than one reference station can be used. The elevation and the latitude of the reference weather stations should be within the range of the studied landslide~~. The user has to maintain a balance between the number of selected reference stations and the necessity for these stations to be located in areas with climatic conditions similar to those of the study site~~ elevation and latitude~~. For sites with a sparse weather station network, one reference station can be sufficient for the calibration, provided that this station has the same weather conditions as those of the studied site.

The performance assessment ~~and ranking~~ of ~~each of the regionally~~regional-scale calibrated methods is based on the comparison between observed measurements and calibrated estimates for R_s and between FAO-56 PM estimates and calibrated estimates for ET_0 for each reference weather station. Performance indicators are the coefficient of determination (R^2), the slope and the intercept from linear regression (independent variable: estimated parameter; dependant variable: ~~observed~~reference parameter), and the ~~relative error RE (~~root mean square error~~, or~~ (RMSE~~, divided by the observed dataset mean~~).

~~2.3.1.~~2.2.1. Solar radiation methods

Bristow and Campbell (1984) and Hargreaves and Samani (1985)~~ proposed each a reduced-set method to compute solar radiation (R_S) based on temperature (equations A1 and A2 in appendix A). Castellvi (2001) demonstrated that both methods show good results for daily frequencies. Almorox (2011) compared the performance of a more extensive list of temperature-based R_S methods which might be more suitable to local conditions at other landslide sites. In this study, the calibration of the Rs reduced-set method was performed using the following modified equations of which a constant is added to take into account eventuality of a R_S estimation shift from the original method:~~

~~Bristow-Campbell modified equation (~~ $\cancel{BC_{mod}\ R_s}$ ~~):~~

$$\cancel{BC_{mod}\ R_s = A_{BC}\ Ra\left[1 - exp\left(-B_{BC}\ \left(\alpha \Delta T\right)^{C_{BC}}\right)\right] + D_{BC}} \qquad \cancel{(1)}$$

~~Hargreaves-Samani modified equation (~~ proposed methods to compute R_S based solely on the air temperature measurement (Eq. (A1) and Eq. (A2) in appendix A). Castellvi (2001) demonstrated that both methods show good results for daily frequencies. The coefficients of the Bristow-Campbell method have to be evaluated. The coefficients of the Hargreaves-Samani method have default values. However, Trajkovic (2007) showed that the regional calibration of the Hargreaves-Samani method is significantly improved by an adjustment of the coefficients rather than by a linear regression. Therefore, all the $HS_{mod}\ R_s$ ~~):~~

$$\cancel{HS_{mod}\ R_s = A_{HS}\ Ra\left(\alpha\ \Delta T\right)^{B_{HS}} + C_{HS}} \qquad \cancel{(2)}$$

~~where~~

$\cancel{A_{BC}, B_{BC}, C_{BC}, D_{BC}}$ ~~are~~coefficients are adjusted. In this study, modified forms of the Bristow-Campbell ~~regional calibration coefficients~~

$\cancel{A_{HS}, B_{HS}, C_{HS}}$ method (Eq. (A3)) and Hargreaves-Samani method (Eq. (A4)) are ~~the Hargreaves-Samani regional~~used. For the R_S equations, the adjustment of the local calibration coefficients

$\cancel{\alpha}$ ~~is the cloud cover adjustment factor~~

~~The Bristow-Campbell coefficients have to be evaluated. The Hargreaves-Samani method coefficients have default values. However, Trajkovic (2007) showed that the regional calibration of the Hargreaves-Samani method (combining ET_0 and R_S methods) is significantly improved by coefficient adjustments rather than by linear regression. Therefore, all the~~ $\cancel{HS_{mod}\ R_s}$ ~~coefficients are adjusted.~~

~~A cloud cover adjustment factor α is furthermore applied to~~ $\cancel{\Delta T}$ ~~since, for cloudy conditions,~~ $\cancel{\Delta T}$ ~~can produce an estimate larger than the incoming solar radiation (Bristow and Campbell, 1984). The α coefficient is applied for the two first rain event days since, for a rain period longer than two days, the temperature and R_s get equilibrated. If~~ $\cancel{\Delta T}$ ~~on the day before a rain event (~~$\cancel{\Delta T_{j-1}}$~~) is less than~~ $\cancel{\Delta T_{j-2}}$ ~~by more than 2°C, the coefficient α is also applied assuming that cloud cover was already significantly present. For the remaining days, α is not applied (α = 1). The 2°C threshold and the 2 days period are based on Bristow and Campbell (1984). In~~

~~this study, the cloud cover adjustment factor α is calibrated according to site conditions. This approach is based on the principle that if this adjustment is not relevant, a calibrated α coefficient would be equal to 1 (no effect).~~

~~Adjustment of coefficients (including α) for the R_S regional calibration~~ is non-linear. To adjust the calibration coefficients, a grid search iterative algorithm is used to maximise the R^2 value ~~of R_S performance (equation 3).~~

$$\cancel{R_S\, performance = \frac{\sum_{i=1}^{m}\left(R_m^2 - RE_m\right)}{m}} \qquad \cancel{(3)}$$

~~where m is~~while minimizing the ~~number of weather stations used for the calibration, R^2 is the coefficient of determination and RE is the relative error, both R^2 and RE being computed between measured and estimated values~~RMSE at each reference weather station.

~~2.3.2.~~2.2.2. Evapotranspiration methods

~~The reference vegetation evapotranspiration (~~ET_0~~)~~ is the evapotranspiration from a reference grass surface and is used as a standard from which ~~specific vegetation evapotranspiration~~ET_c is deduced~~. The Penman-Monteith method has been extensively evaluated worldwide and is considered~~ as ~~the most widely accepted method for ET_0 estimation~~follows (~~Jensen~~Allen et al., ~~1990~~1998)~~. Following this work, Allen et al. (1998) in the paper FAO-56 (Food and Agriculture Organization of the United Nations) developed a modified form of the Penman-Monteith method (FAO-56 PM ET_0), which is adopted by the scientific community as a global standard method to estimate ET_0 worldwide.~~

~~Several reference vegetation evapotranspiration (ET_0) methods using a reduced dataset in comparison to FAO-56 PM ET_0, have been developed worldwide. Only a few methods are commonly used. This is the case with the five ET_0 methods selected for this study, which have shown good performance when using daily to weekly frequencies (Trajkovic, 2005; Yoder et al., 2005; Alexandris et al., 2008; Shahidian et al., 2012; Tabari et al., 2013). The five ET_0 methods include one temperature-based method, that is the Hargreaves-Samani method~~ :

$$ET_c = ET_0 \times K_c \qquad (1)$$

where K_c is the vegetation coefficient.

Several ET_0 methods using a reduced dataset in comparison to the FAO-56 PM method have been developed worldwide. Only a few methods are commonly used. This is the case with the five ET_0 methods selected for this study, which have shown good performance when using daily to weekly frequencies ~~(1985)~~(Trajkovic, 2005; Yoder et al., 2005; Alexandris et al., 2008; Shahidian et al., 2012; Tabari et al., 2013)~~, four solar radiation/temperature-based~~. The five selected ET_0 methods, namely the methods of ~~Makkink~~Hargreaves-Samani (~~1957~~1985), ~~Turc~~Makkink (~~1961~~1957)~~, and Priestley and Taylor~~ , Turc (~~1972~~1961), Priestley and ~~the Penman-Monteith reduced-set method~~Taylor ~~(Allen et al., 1998)~~(1972) ~~(equations A4 to A10 in appendix A). The estimation of solar radiation with a R_S temperature-based method allows to compute the evapotranspiration with the five above ET_0 methods based only with temperature. The reference vegetation evapotranspiration (ET_0) corresponds to the maximum possible water loss by evaporation and transpiration from an actively growing grass with an extensive and uniform surface~~ , and the Penman-Monteith reduced-set method (Allen et al., 1998)~~. The Priestley-Taylor and Penman-Monteith ET_0 reduced-set methods use net solar~~

~~radiation (R_n) instead of R_S, which can be deduced from R_S with the Penman-Monteith reduced-set method assumptions (Allen et al., 1998). The foregoing ET_0 methods were developed for irrigation scheduling, for which the scope of application involves positive temperatures (plant water supply during the spring-summer growing period). However, in mountainous sites, winter temperatures are often below 0°C, and ET_0 empirical methods can compute negative ET_0 values. Negative ET_0 computed values do not have any physical meaning and are therefore set to zero.~~

~~Previously cited ET_0 methods were developed for specific weather conditions. FAO-56 PM calculated data at reference weather stations are used as standards to calibrate the ET_0 reduced-set methods, in order to take into account the landslide site weather conditions. A linear regression is performed for each of the reduced-set evapotranspiration methods and for each weather station (Eq. 4). The slope *a* and the intercept *b* of the best-fit regression line obtained for each reference weather station are used as local calibration coefficients. Regional calibration coefficients are calculated by averaging the local coefficients of each reference weather station.~~

$$\cancel{ET_{0\,FAO-56\,PM} = a\,ET_{0\,method} + b} \qquad \cancel{(4)}$$

~~where $ET_{0\,FAO\text{-}56\,PM}$ is the reference vegetation evapotranspiration and $ET_{0\,method}$ is obtained by any of the five reduced-set methods tested in this study. The linear regression method has been widely used to calibrate ET_0 reduced-set methods~~ , require records of R_S and temperature (Eq. (A7) to Eq. (A12) in appendix A). As R_S can be estimated with a calibrated R_S temperature-based method, ET_0 can thus be obtained with temperature records only.

ET_0 is calculated using data collected at each reference weather stations (independent ET_0 estimates). These calculations follow FAO-56 PM method outlined in the FAO-56 document (Allen et al., ~~1994; Trajkovic, 2005; Shahidian et al., 2012~~ 1998)~~.~~

~~Reduced-set ET_0 methods do not take into account the wind speed variations. By removing saturated air from the boundary layer, wind increases evapotranspiration (Shahidian et al., 2012). Several studies show the influence of the wind speed on reduced-set ET_0 method performance and therefore on calibration (Itenfisu et al., 2003; Trajkovic, 2005; Trajkovic and Stojnic, 2007). For this study, the days with wind speed above the 95^{th} percentile of the dataset (extreme values) were disregarded for the calibration.~~

~~The combination of calibrated ET_0 and R_S methods allows the estimation of ET_0 based only on temperature. The specific vegetation evapotranspiration (ET_c) is calculated by applying a vegetation coefficient (K_c) to ET_0 (i.e. $ET_c = ET_0 \times K_c$).~~

~~2.4. Recharge area: Composite GIS – Step 2~~

~~No attempt of discrete calculation of recharge over the recharge area is undertaken in this study. The recharge area parameters (soil available water capacity SAWC, runoff coefficient, vegetation coefficient K_c) were assumed to be spatially uniform and constant over time (except for K_c which varies in time). However, the spatial heterogeneity of the recharge area was taken into account in order to estimate an average value for each parameter over the recharge area by performing a GIS composite method (Figure 1 – Step 2). For one given parameter, the recharge area was divided into sub-areas, each being characterised by a constant value estimated according to field measurements, literature values or calculation. For each parameter, the matching sub-area is estimated by combining the different land use sub-areas which have an influence on the target parameter (for example vegetation + geology substratum). Sub-areas can be continuous or discontinuous, and their number and their~~

~~geometry can differ according to land use spatial distribution. The parameters are subsequently estimated at the scale of the recharge area according to the sub-area surface (Equation in Figure 1 – Step 2). A wide range of input data (digital elevation model (DEM), aerial photographs, geological maps, field investigations and auger holes) were analysed and combined to estimate the three recharge area parameters required for recharge computation.~~

~~2.4.1. Vegetation coefficient (K_e)~~

~~The K_e coefficient gather together four primary characteristics that distinguish the vegetation from the reference grass: vegetation height, albedo, canopy resistance and evaporation from soil~~. These independent ET_0 estimates are then used as pseudo-standards for the purpose of calibrating the regional-scale ET_0 methods. A linear regression is performed for each of the evapotranspiration methods and for each reference weather station (Eq. (2)). The slope *a* and the intercept *b* of the best-fit regression line are used as local calibration coefficients.

$$ET_{0\,FAO-56\,PM} = a\,ET_{0\,method} + b \qquad (2)$$

where $ET_{0\ FAO\text{-}56\ PM}$ is the ET_0 estimated with the standard method and $ET_{0\ method}$ is the ET_0 obtained by any of the five methods tested in this study. The linear regression method has been widely used to calibrate ET_0 methods (Allen et al., ~~1998~~ 1994; Trajkovic, 2005; Shahidian et al., 2012)~~. As a consequence, the sub-areas were defined according to vegetation cover deduced from aerial photographs, with the main vegetation species described through field observations. Because the K_e coefficient is dependent on the vegetation development stages, it varies from a minimum during winter to a maximum during summer. For each sub-area, minimum and maximum K_e values were estimated from the literature and assigned respectively to 4th of February (middle of winter) and 6th of August (middle of summer) of each year. A daily linear interpolation was performed for K_e between these two dates (Verstraeten et al., 2005).~~

~~2.4.2. Soil available water capacity (SAWC)~~

~~SAWC is mainly affected by soil texture and thickness, which primarily depends on geological substratum and vegetation cover. SAWC is also dependent on the root zone extent and the permanent wilting point, both variables according to vegetation type. Sub-areas were defined according to vegetation cover (deduced from aerial photographs) and according to geological substratum (deduced from geological maps). For each sub-area type, one auger hole was drilled at a representative location. SAWC is deduced from soil properties (type of horizon, texture and bulk density) and depth extent from auger hole cores, using a pedotransfer function (Jamagne et al., 1977; Bruand et al., 2004). SAWC values of auger holes are then assigned to the sub-area. The SAWC varies over time since water demand depends on the plant growing season. The SAWC dependency to vegetation species is taken into account through the K_e coefficient.~~

~~2.4.3. Runoff coefficient~~

~~Several rainfall-runoff models (Jakeman et al., 1990; Tan and O'Connor, 1996; Chiew et al., 2002; Brocca et al., 2011) have been designed for the purpose of hydrology, i.e. to characterise catchment outlet. They are not tailored for recharge estimation. Rainfall-runoff models require temporal flow calibration at the catchment outlet. In this study, there is no such outlet flow data, as most of the recharge area discharges into an alluvial aquifer at the~~

~~landslide foot. As such, rainfall-runoff model calibration is not possible and this technique cannot be employed to estimate the recharge. The soil conservation service curve number runoff method (SCS) designed for storm rainfall events rather than daily continuous estimation is also not suitable.~~

~~The runoff estimation method applied in this study is similar to the well-known and commonly used 'runoff rational method'. The runoff coefficient depends mainly on the slope gradient and the vegetation cover. Sub-areas are defined according to vegetation cover deduced from aerial photographs. For each sub-area, an average slope gradient value is assigned, utilising DEM slope gradient analysis. For each sub area, runoff coefficients are deduced from vegetation cover and slope gradient magnitude based on the Sautier chart~~ .

2.3. Step 2: Estimation of the parameters of the recharge area

The estimation of the recharge with the soil-water balance (step 3 – section 2.4) requires the calculation, at the scale of the recharge area, of three parameters which are SAWC, runoff coefficient R_{coeff}, and K_c. These three parameters are controlled by one or several factors which are, in this study, the slope gradient, the geological nature of the substratum and the type of vegetation cover. Besides, at the scale of the recharge area, the controlling factors are commonly heterogeneous and thus the recharge-area parameters cannot be readily computed. For each of the controlling factors, the recharge area is divided into sub-areas (hereafter referred to as factor sub-areas) characterized by homogenous factor properties. Factor sub-areas can be either continuous or discontinuous, and their number and shape can differ, depending of the spatial distribution of the factors. Relevant factor sub-areas are in turn used to define parameter sub-areas. For a given parameter sub-area, the value of the parameter is estimated from either field measurements or from the literature. The parameter values at the scale of the recharge area are then calculated by taking into account the relative surface of the parameter sub-areas (Fig. 1 – Step 2). Lastly, if preferential infiltration structures (hereafter referred to as infiltration structures) such as sinkholes, cracks, reverse slope areas, bare ground or any topographical depression which can collect the surface runoff are present in the recharge area, the above-mentioned parameters have to be adjusted. For such areas, the SAWC and R_{coeff}, being very low, will be set at zero in the calculations. Similarly, for such areas, ET_0 is negligible and therefore the surface of these areas is disregarded for the K_c computation. The parameter values are afterwards refined by a sensitivity analysis (step 4- section 0) in order to find the optimal set of recharge-area parameters.

The K_c parameter takes into account four key characteristics (vegetation height, albedo, canopy resistance and evaporation from soil) that distinguish the vegetation type of a given sub-area from the reference grass used to estimate ET_0 ~~(Musy and Higy, 2011)~~(Allen et al., 1998)~~. This chart was developed for Switzerland where environmental conditions are similar to the French Alps.~~

. The K_c sub-areas are defined according to the type of vegetation (e.g., meadow, forest…) obtained from aerial photographs. The dominant vegetation species assigned to each vegetation type can be obtained from literature (e.g., forest agency data) or from field observations. Since the K_c parameter depends on the stage of development of the vegetation, it varies from a minimum value during winter to a maximum value during summer. The minimum and maximum K_c values are estimated from the literature and are assigned respectively to the 4th of February (middle of winter) and the 6th of August (middle of summer) of each year. A daily linear interpolation is performed for K_c between these two dates (Verstraeten et al., 2005).

The SAWC parameter refers to the difference between a maximum water content above which all free water is drained through gravity (field capacity) and a minimum moisture content below which plant roots cannot extract any water (permanent wilting point). The SAWC is mainly affected by soil texture and thickness, both depending primarily on the geological substratum and the vegetation. The SAWC sub-areas are defined according to the type of vegetation (obtained from aerial photographs) and to the geological substratum (obtained from geological maps). SAWC values can be either calculated with pedotransfer functions (Bruand et al., 2004; Pachepsky and Rawls, 2004) from soil properties (type of horizon, texture and bulk density) and thickness or obtained directly from the literature. Soil properties and thickness can be obtained from the literature (e.g., pedological maps) or from morphological description or laboratory measurements of auger hole cores.

The method used to estimate the surface runoff is similar to the commonly used ‘runoff rational method’. The R_{coeff} parameter depends mainly on topography and vegetation. The R_{coeff} sub-areas are defined according to the vegetation (obtained from aerial photographs). An average slope gradient obtained from the DEM is assigned to each vegetation sub-area. The R_{coeff} values can then be calculated from vegetation cover and slope gradient through the use of charts such as the Sautier chart (Musy and Higy, 2011).

~~2.4.4.~~ Infiltration ~~structure~~

~~An additional sub-area type is defined to take into account preferential infiltration~~ structures ~~such as sinkholes, cracks, reverse slope areas, bare ground and any topographical depressions which can collect runoff. For such sub-areas, SAWC and runoff coefficient are very low and are considered to be null in the calculation at the scale of the recharge area. The consequence of preferential infiltration structures is a global decrease of SAWC and runoff coefficient values at the scale of recharge area. Infiltration structures are defined through inspection~~are first located through examination of aerial photographs (lineaments~~),~~ analysis) and geological ~~mapping~~maps, and are then inspected in the field ~~observations~~.

~~2.5.~~2.4. ~~Soil-water balance: recharge~~ Step 3: Recharge computation ~~- Step 3~~with soil-water balance

~~Recharge is estimated according to the following~~**The soil-water balance workflow used to estimate the recharge at a daily frequency is detailed in Fig. 2. All terms required for the soil-water balance estimation are expressed in water amount (millimetres), except for R_{coeff} expressed in %. The soil-water balance** ~~with the ET_0 computed with the combination of R_S and ET_0 reduced-set calibrated methods and the SAWC, the vegetation coefficient and the runoff coefficient deduced from the GIS method (Figure 1 – Step 3).~~

~~The precipitation (P) is the amount of liquid (rain) or solid (snow) water which falls on the recharge area.~~is based on ET_c, SAWC, K_c and R_{coeff}. The precipitation (P) is the amount of liquid (rain) or solid (snow) water which falls on the recharge area. ~~**However, in the remaining part of the paper, the**~~ The precipitation will be ~~**considered to be the same**~~taken here as the sum of snow melt and rainfall. A part of this water amount is intercepted by the vegetative canopy (interception~~) (**Figure 2**~~; Fig. 2A). The remainder of precipitation reaches the ground surface and forms~~:~~ (i) the runoff (Rf), which is the water joining the surface drainage network~~;~~ and (ii) the infiltration (I) into the soil layer which supplies the SAWC ~~**(also called soil available moisture capacity). The SAWC is the maximum soil water content available for evapotranspiration**~~. The remaining part of the precipitation ~~**which has**~~

not ~~been taken off~~uptaken by evapotranspiration and runoff and ~~which has~~ not ~~been~~ stored in the SAWC is called the recharge (R). It corresponds to deep percolation and ~~it~~ is the component of the ~~rainfall~~precipitation which recharges the saturated zone ~~(Figure 2~~(Fig. 2A).

~~SAWC refers to the difference between a maximum water content above which all free water is drained through gravity (field capacity) and a minimum moisture content below which plant roots cannot extract anymore water (permanent wilting point).The difference between the maximum of SAWC and the actual SAWC is called the SAWC deficit ($SAWC_{max}$-$SAWC_{j-1}$ in Figure 2B).~~

~~The~~The ET_c is a lumped parameter including potential transpiration, potential soil evaporation and canopy ~~reservoir capacity was not evaluated in this study and therefore water evaporated by the~~ interception ~~process is taken off the SAWC reservoir (Figure 2B). Evapotranspiration is the total evaporative loss from the surface, i.e.~~ evaporation ~~from soil and plants (~~(Verstraeten et al., 2005). In the proposed computation diagram workflow (Fig. 2B) the interception~~), and transpiration from plants. Interception is the part of precipitation which is caught by leaves and branches, and which is subsequently evaporated.~~

~~The specific vegetation evapotranspiration (ET_e), deduced from ET_0 method and vegetation coefficient,~~ component is therefore integrated in the ET_c component. The ET_c is the water evapotranspired without any other restrictions ~~other~~ than the atmospheric demand (assuming unlimited soil water availability). However, field conditions do not always fulfil these requirements, particularly during low rainfall periods~~,~~ when water supplies are inadequate to support vegetation uptakes. ~~Actual~~The actual evapotranspiration (ET_a) corresponds to the actual amount of evapotranspired water.

Runoff takes place when the intensity of a precipitation event exceeds the soil infiltration capacity. The use of a daily measurement frequency for precipitation does not allow an accurate estimation of rainfall intensity ~~(hourly rainfall resolution is not available).~~. Instead, a ~~runoff coefficient (~~R_{coeff}~~)~~ is applied only for days when precipitation is greater than the average. Such days are considered as high intensity rainfall days. The ~~runoff coefficient~~R_{coeff} is applied only to excess precipitation, after the demands of evapotranspiration and SAWC are met ~~(~~, i.e., when SAWC is fulfilled~~) (Figure 2B~~ (Fig. 2B).

~~The soil-water balance workflow used to estimate the recharge at a daily frequency is detailed in Figure 2B. Each term (P, Rf, I, Et_a, ET_e, SAWC and R) is expressed in water amount (millimetres), except for R_{coeff} which is expressed in %.~~

~~2.6.~~2.5. Step 4: Sensitivity analysis of the recharge~~—~~-area parameters

In the landslide recharge area, ~~infiltration~~recharge can be ~~assumed to be~~considered as spatially heterogeneous. Indeed, in fractured ~~rock hydrogeology~~rocks, the groundwater flow is mainly driven by an anisotropic fracture network. The proportion of infiltrated water which flows toward the landslide aquifer can ~~be~~ significantly ~~different~~differ between two zones of the recharge area. Nevertheless, the GIS composite method considers that any part of the recharge area has the same ~~weigh relatively~~weight with respect to the ~~infiltrated water~~groundwater which flows toward the landslide aquifer ~~(i.e., homogeneous infiltration).~~. This homogeneous recharge assumption can lead to ~~a bias estimation~~biased estimations of the recharge~~-~~-area parameters. On the other hand, uncertainties in the delimitation of the recharge area can also lead to biased estimations.

~~On~~A sensitivity analysis evaluates the ~~other hand, numerous uncertainties remain about the recharge area delimitation, the SAWC~~ possible over-estimation ~~and~~or under-estimation of the ~~canopy reservoir influence. These uncertainties can also lead to biases in the~~set of recharge~~-~~-area parameters~~ estimation. First, the delimitation of the recharge area only approximates the boundary of the actual recharge area. Secondly, the SAWC is deduced from soil properties and depth extent. However, variations in the root zone of different vegetation types have not been evaluated. Finally, for this study, the canopy reservoir is not evaluated in the soil-water balance which considers, by default, that the SAWC reservoir combines the water storage of both soil and canopy.~~

~~A sensitivity analysis is performed to evaluate the overestimation or underestimation of recharge area parameters. Infiltration structures~~. The infiltration-structure sub-areas are used as ~~a~~ fitting ~~factor~~factors (varying from 0 to 100% of the recharge area surface) to adjust the ~~recharge area parameter~~ estimation ~~based on a heterogeneous assumption (identical land use properties but different infiltration contribution weight to~~of the ~~landslide aquifer).~~set of recharge-area parameters. A variation of the infiltration structure percentage corresponds to a variation of the contribution weight of the infiltration structures ~~contribution weight~~ to the recharge of the landslide aquifer. ~~As a consequence, a percentage~~ Consequently, a variation of the infiltration structure percentage does not affect the relative proportion of the other sub-area surfaces~~, which remain the same,~~ but only their contribution weights. ~~In summary, with the assumption of an homogeneous infiltration, the recharge area parameters are defined from sub-area surfaces, while in the case of the heterogeneous infiltration assumption, the recharge area parameters are defined according to the sub-area infiltration contribution proportion (weighting) to the landslide aquifer.~~

The sensitivity analysis is based on ~~rainfall~~ the performance of a linear correlation between daily time series of recharge and displacement ~~correlation performance~~. The landslide displacement ~~velocity of the landslide~~ triggered by ~~rainfall depends on the groundwater saturation state and~~ pore water pressure is therefore ~~representative of~~related to the hydrodynamic variations of the landslide aquifers. For this reason, ~~rainfall~~ the performance of the correlation between recharge and displacement ~~correlation performance~~ informs whether the recharge~~-~~-area parameters are ~~suitable to characterise the water infiltration flowing toward the landslide aquifer.~~

satisfactorily estimated. The sensitivity analysis allows to determine the optimal set of recharge~~-~~-area parameters which maximize the ~~rainfall/displacement correlation performance. The SAWC estimation deduced from the sensitivity analysis will take into account the contribution of canopy storage and vegetation cover~~performance of the correlation.

~~2.6.1. Saturation state approximation of the landslide triggering aquifer~~

2.6. ~~The groundwater hydrodynamic processes due to aquifer drainage are non-linear. An ancient rainfall event displays less impact (though not null) than the most recent one on the aquifer saturation state~~ Correlation between water input and displacement

2.6.1. Antecedent cumulative sum

The correlation between water input and displacement requires measurements of landslide displacements at the same temporal frequency (daily frequency in this study) as the measurements of water input (precipitation or recharge). The groundwater hydrodynamic processes in aquifers are non-linear. A former rainfall event displays less impact (though not negligible) than a recent one on the aquifer hydrodynamic fluctuations (Canuti et al., 1985; Crozier, 1986; Diodato et al., 2014). ~~As a consequence, in this study, the aquifer saturation state is approximated by an~~The daily precipitation/recharge time series cannot therefore be used without appropriate corrections. An antecedent cumulative sum ~~amount~~ of precipitation/recharge weighted by a ~~decreasing~~ factor ~~(~~α~~) (Equation 5).~~ is applied as a moving window to the daily precipitation/recharge time series (Eq. (3)). The antecedent cumulative sum ~~corresponds~~allows to approximate the ~~total amount~~daily triggering impact of ~~rainfall that occurred over a defined period prior to a~~the aquifer *ATI* on the landslide destabilisation. In order to take into account the groundwater transit time, a β time-lag factor is introduced. This factor can shift the moving window from the target date~~. In equation 5, for α equalling zero, the decreasing sum matches a classic arithmetic sum of rainfall~~ *t*.

$$\cancel{Decreasing\ \ sum = \sum_{i=1}^{n} \frac{W_{i+\beta}}{1+\alpha\left(i-1\right)} \qquad (5)}$$

$$ATI_t = \sum_{i=t+\beta}^{t+\beta+n} \frac{W_i}{1+\alpha\ (\mathrm{i} - (\mathrm{t} + \beta))} \qquad (3)$$

where:

ATI_t ~~cumulative period (day~~Aquifer Triggering Impact at the date t (in mm)

β time shift of the moving window (in days)

i ~~ith day~~ith day from the date t (i=t+β: start of the moving window and i= t+β +n: end of the moving window)

n length of the moving window of the cumulative period (in days)

W_i water input~~:~~, i.e., precipitation or recharge at the ith day (in mm)

α weighting factor

~~β shift factor (day)~~

~~2.6.2. Rainfall-displacement correlation~~

~~Linear regressions between cumulative precipitation and displacement and/or between~~An iterative grid search algorithm is used to find the optimal set of parameters of the antecedent cumulative ~~recharge and displacement are performed for each decreasing sum type, with n ranging~~sum. The optimal set of parameters is the set that maximizes the correlation performance itself based on the R² indicator. The grid search algorithm investigates the following parameter ranges: n from 1 to 250 days (~~1 day~~ increment: 1 day), α ~~ranging~~ from 0 to 0.5 (increment: 0.~~001~~0001) and β ~~ranging~~ from 1 to 10 days (increment~~ 1). The coefficient~~

~~of determination (R^2) is used to assess the performance of rainfall-displacement correlation. An iterative grid search algorithm is used to find the best solution based on R^2.~~: 1 day).

~~Between two correlation performance solutions, a small improvement of the R^2 value can be the result of adding an extra long computation period to which very low weighting factors are associated. The increase of the period computation to which low weights are applied acts as a smoothing function. The correlation improvement is explained by the randomness/noise smoothing of input signal rather than by a physical process. A R^2 tolerance of 0.001 for the best correlation performance is implemented. The correlation performance which ranges within the R^2 tolerance window and which has the lowest computation period is then selected as the best solution.~~

~~2.6.3.~~2.6.2. Significance of ~~rainfall~~the water input-displacement correlation

~~The significance is evaluated only for the characterization of the relationship between precipitation/recharge and displacement. The significance of R^2 for solar radiation and evapotranspiration calibration is not evaluated, because the purpose of the calibration was only to tune adjustment coefficients and the significance of the relationship is not on purpose.~~

The bootstrap method, which is an inference statistical resampling method, is used to estimate the confidence interval (CI) of estimated parameters and to perform statistical hypothesis tests (Chernick, 2008). The bootstrap method uses resampling with replacement and preserves the pair-wise relationship. However, for inter-dependent data (such as time series), the structure of the dataset has to be preserved during the resampling. The moving block bootstrap is a variant of the bootstrap method. It divides data into blocks for which the structure is kept~~, which makes it suitable for times series~~ (Cordeiro and Neves, 2006). The moving block bootstrap method is performed with a 90-day block size (season) and 50,000 iterations for each run.

To estimate the significance of the linear regression, the lower bound of the confidence interval (LBCI) of R^2 is used at the level of confidence of 95%. An LBCI value greater than 0 means that the relationship is significant.

Particular to statistical hypothesis tests is the definition of the tested null hypothesis which is often a default position opposite to the aim of the test, i.e. by stating that "there is no relationship between the two considered quantities". The null hypothesis is assumed to be true until it is rejected by statistical evidence in favour of the alternative ~~hypothesis (that is the contrary).~~opposite hypothesis. The recharge estimated with the LRIW workflow is hereafter called R_{LRIW}. The recharge estimated by subtracting a non-calibrated ET_0 from precipitation is hereafter called R_{PMNE}, PMNE standing for Precipitation Minus Non-calibrated ET_0.

To estimate whether the ~~recharge~~R_{PMNE}/displacement correlation R^2 is significantly better than the precipitation/displacement correlation R^2 value, the Null Hypothesis 1 (NH1) ~~was~~is tested. The NH1 states that the ~~recharge~~R_{PMNE}/displacement correlation R^2 value is not significantly greater than the R^2 value obtained ~~with~~from precipitation. In other words, the NH1 statistic test is the difference between the ~~recharge~~R_{PMNE} R^2 value and the precipitation R^2 value, expected to be 0 if no ~~differences~~difference. Similarly, the Null Hypothesis 2 (NH2) and the Null Hypothesis 3 (NH3) are tested. NH2 estimates whether the R_{LRIW}/displacement correlation R^2 is significantly better than the precipitation/displacement correlation R^2 value. NH3 estimates whether the R_{LRIW}/displacement correlation R^2 is significantly better than the R_{PMNE}/displacement correlation R^2 value.

To estimate whether the best ~~rainfall~~precipitation-R_{LRIW}/displacement correlation R^2 value computed from the sensitivity analysis is significantly better than the other R^2 values obtained, the Null Hypothesis ~~2 (NH2) was~~4 (NH4) is tested. The ~~NH2~~NH4 states that the best R^2 value is not significantly greater than the ones obtained with all the remaining combinations. In other words, the ~~NH2~~NH4 statistic test is the difference between the best R^2 value and the R^2 values obtained with the remaining combinations, expected to be 0 if no ~~differences~~difference.

For ~~both~~all null hypotheses~~ NH1 and NH2~~, the decision ~~to reject the null hypothesis~~of rejection is made by determining how much of the bootstrap distribution (among 50,000 iterations) falls below zero by using the lower bound of the confidence interval (LBCI) at the level of confidence of 95%. An LBCI value greater than 0 ~~allow~~allows to reject the null hypotheses.

3. Application to the Séchilienne landslide

~~Several studies on the Séchilienne landslide concerning the rainfall trigger use precipitation or indirect infiltration estimates (Rochet et al., 1994; Alfonsi, 1997; Meric et al., 2006; Helmstetter and Garambois, 2010). Similarly, the warning system of Séchilienne is partly based on precipitation. Séchilienne landslide investigations and the warning system could be significantly improved by evaluating recharge instead of precipitation.~~

~~3.1.Context~~

3.1.~~The Séchilienne landslide is located 25 km south-east of Grenoble, (France), on the right bank of the Romanche River, on the southern slope of the Mont-Sec Massif. The site is located in the external part of the French Alps, in the Belledonne crystalline range. The geological nature of the area is composed of vertical N-S foliated micaschists unconformably covered by Carboniferous to Liassic sedimentary deposits along the massif ridge line above the unstable zone (Figure 3). Locally, Quaternary glacio-fluvial deposits overlie these formations. The landslide is delineated to the east by a major N20° trending fault zone. Two major wrench faults, N140° dextral and N20° sinistral, compartmentalize the disturbed zone into blocks. The slope is cut by a dense network of two conjugate sub-vertical fracture sets, striking N140° and N50-70° ~~Geological settings and rainfall triggering

The Séchilienne landslide is located in the French Alps on the right bank of the Romanche river, on the southern slope of the Mont-Sec Massif (Fig. 3). The climate is mountainous with a mean annual precipitation height of 1200 mm. The geological nature of the area is composed of vertical N-S foliated micaschists unconformably covered by Carboniferous to Liassic sedimentary deposits along the massif ridge line above the unstable zone. Quaternary glacio-fluvial deposits are also present. The Séchilienne landslide is limited eastwards by a N-S fault scarp and northwards by a major head scarp of several hundred meters wide and tens of meters high below the Mont Sec. The slope is cut by a dense network of two sets of near-vertical open fractures trending N110 to N120 and N70 ~~(Vengeon, 1998)~~(Le Roux et al., 2011).

The ~~latter divides~~Séchilienne landslide is characterized by a deep progressive deformation controlled by the ~~slope into numerous sub-vertical compartments.~~

~~3.2.Deformation mechanism~~network of faults and ~~rainfall triggering~~

~~An originality~~fractures. A particularity of the Séchilienne landslide is the absence of a well~~-~~-defined basal sliding surface. The ~~Séchilienne landslide deep-seated progressive deformation is controlled by the main discontinuities (faults/fractures). The slope~~landslide is affected by a deeply rooted (about 100-150 m) toppling movement of the N50-70°~~E striking blocks toward~~ slabs to the valley~~,~~ (accumulation zone) coupled with the ~~subsidence~~sagging of the upper ~~part of the~~ slope ~~near~~ (depletion zone) beneath the Mont~~-~~ Sec~~. This mechanism has been described by Vengeon (1998)~~(Vengeon, 1998; Durville et al., 2009; Lebrouc et al., 2013)~~ as an internal rupture mechanism. The landslide displacement velocity smoothes progressively toward the west and the slope foot, whereas it drops abruptly beyond the N20° trending fault zone delimiting the eastern boundary.~~

~~The groundwater flow is mainly driven through a network of fractures with relatively high flow velocities (km/day). The moving zone, about 150 m deep~~. A very active moving zone is distinguishable from the unstable slope where high displacement velocities can be 10-time higher than the rest of the landslide.

The landslide shows a higher hydraulic conductivity than the underlying stable bedrock (Vengeon, 1998; Meric et al., 2005; Le Roux et al., 2011)~~, shows a higher hydraulic conductivity than the bedrock~~, thus leading to a landslide perched aquifer ~~(Vengeon, 1998)~~(Guglielmi et al., 2002)~~ and constitutes a perched aquifer~~. The recharge of the landslide perched aquifer is essentially local, enhanced by the trenches and the counterscarps which tend to limit the runoff and to facilitate groundwater infiltration in the landslide area. However, the hydrochemical analyses of Guglielmi et al. (~~Guglielmi et al.,~~ 2002)~~. The landslide displacement has caused a wide opening of the fractures. The groundwater flow mechanisms that are responsible for recharge in the disturbed zone are not agreed upon. Vengeon~~ shows that the sedimentary deposits distributed above the landslide hold a perched aquifer which can recharge the landslide perched aquifer. The fractured metamorphic bedrock beneath the landslide contains a deep satured zone at the base of the slope and an overlying vadose zone. The groundwater flow of the entire massif is mainly controlled by the network of fractures with high flow velocities (up to a few kilometres per day; Mudry and Etievant, 2007). The hydromechanical study of Cappa et al. (~~1998~~2014)~~ shows that the moving zone perched aquifer is recharged by water level rise of the deep saturated zone whereas Guglielmi et al.~~ shows that the deep aquifer can also trigger the Séchilienne landslide destabilization as a result of stress transfer and frictional weakening. Thus, the Séchilienne landslide destabilisation is likely triggered by a two-layer hydrosystem: the landslide perched aquifer and the deep aquifer. The Séchilienne landslide behaviour is characterized by a good correlation between precipitations and displacement velocities ~~(2002)~~(Rochet et al., 1994; Alfonsi, 1997; Durville et al., 2009; Chanut et al., 2013)~~ showed that the main recharge originates from the top sedimentary perched aquifer. Increases in pore water pressure originate in the disturbed zone, leading to landslide displacement. As a result, the Séchilienne landslide shows a good correlation between antecedent cumulative precipitation and average displacements (Rochet et al., 1994; Alfonsi, 1997). Helmstetter and Garambois (2010) showed a weak but significant correlation between rainfall signals and rock fall micro-seismicity. Instability in the Séchilienne slope is mainly triggered by rainfall events.~~

~~3.3.Dataset~~

~~The selected weather stations satisfy two conditions: (i) they~~ .The seasonal variations of the daily displacements are clearly linked to the seasonal variations of the recharge (high displacements during high flow periods and low displacements during low flow periods).

3.2.Method implementation

The recharge computation uses the daily rainfall recorded at the weather station located at Mont-Sec, a few hundred meters above the top of the landslide (Table 1 and Fig. 3). This station is equipped with rain and snow gauges and a temperature sensor. However, the temperature measurements at the Mont-Sec station are considered unreliable because of a non-standard setting of the temperature sensor and numerous missing data. Consequently, the temperature at the Mont-Sec station has to be estimated in order to estimate the evapotranspiration at the landslide site (see details about the computation in appendix B).

Since the Mont-Sec station does not record ~~all~~ the ~~required~~full set of parameters ~~to compute ET_0 with standard FAO-56 PM (wind speed,~~ (relative humidity, temperature, wind speed and solar radiation ~~or relative sunshine duration, measured daily); and (ii) they are~~), a regional calibration of ET_0 and R_S reduced-set methods is required. Three weather stations located at less than 60 kilometres from the studied site~~. Three~~ are used as reference weather stations~~, managed by MétéoFrance, fulfil these requirements~~: Grenoble-Saint-Geoirs, Saint-Jean-Saint-Nicolas and Saint-Michel-Maur (Table 1 ~~and Figure 3).~~ and Fig. 3). The Saint-Michel-Maur weather station does not measure R_S~~. However R_S can be calculated~~, which is estimated with the Angström formula (~~equation A3~~Eq. (A5) in Appendix A) using sunshine duration data recorded at the station ~~(FAO-56 guidelines, Allen et al., 1998).~~. The Angström formula empirical default coefficients ~~were~~are tuned with the two others weather stations (a_S = 0.232 and b_S = 0.574). ~~The recharge computation was based on the rainfall recorded at the weather station located at Mont-Sec, a few hundred meters above the top of the disturbed zone (Table 1 and Figure 3). This station is equipped with rain and snow gauges.~~

~~Although this study aims at estimating recharge using only temperature and precipitation dataset, temperature measurements at the Mont Sec station are considered unreliable because of temperature sensor non-standard setting and numerous missing data. In order to estimate a representative daily temperature dataset for the site, the two nearest weather stations measuring temperature, named Luitel and La Mure, were used~~ (The delimitation of the recharge area of the two-layer hydrosystem (Fig. 3 ~~and Figure 3). The estimation of the Mont-Sec temperature is detailed in appendix B.~~

~~Aerial photographs of 0.5 m resolution and a digital elevation model (DEM) of 25 m resolution were provided by the "Institut National de l'Information Géographique et Forestière" (IGN). Geological maps from the French Geological Survey (BRGM) were used to determine the geology and faults within the recharge area.~~

) of the Séchilienne landslide is based on the geological and hydrochemical studies of Vengeon (1998), Guglielmi et al. (2002) and Mudry and Etievant (2007). The recharge area is delimited by the spatial extent of the sedimentary cover of which the hosting perched aquifer recharges the two-layer hydrosystem. Groundwater flow of the entire Mont-Sec massif is controlled by faults and fractures. The N20 fault bordering the sedimentary cover to the east as well as the N-S fault zone bordering the landslide to the east are structures which delimitate the recharge area. The scarcity of information does not allow to accurately define the actual extent of the recharge area. The sensitivity analysis mentioned in Section 0 allows to compensate for the possible biases introduced by this uncertainty. The following spatial datasets are used for the estimation of the parameters of the recharge area. The aerial photographs (0.5 m resolution) and a DEM of 25 m resolution are provided by the "Institut National de l'Information Géographique et Forestière" (IGN) and geological maps are provided by the French Geological Survey (BRGM).

The Séchilienne landslide is permanently monitored by ~~several displacement stations using a variety of techniques (extensometers, radar,~~a dense network of displacement stations managed by the CEREMA Lyon (Duranthon et al., 2003). In this study, one infra-red~~, inclinometers, GPS). This dense network has been implemented by the CEREMA Lyon (Duranthon et al., 2003). For the present study, one infra-red (named~~ station (1101) and three extensometer ~~(named~~ stations (A16, A13 and G5) ~~stations have been~~ are used. Stations 1101, A13 and A16 ~~and A13 are located on the surface~~are representative of the most active ~~unstable~~ zone ~~which is also the most reactive zone with respect to rainfall events (Figure 3). The A16 extensometer was used for the sensitivity analysis whereas the three other stations were only used for rainfall~~ (median displacement ~~correlation purposes.~~ of 2.5, 1.75 and 2.98 mm/day, respectively), while G5 is located on a much less active zone (median displacement of 0.05 mm/day, Fig. 3 and Table 2).

The sensitivity analysis is performed on the A16 extensometer on the period from 01 May 1994 to 01 January 2012, period during which both A16 extensometer and recharge datasets are available.~~ In order to compare the rainfall-displacement correlation~~ The performance test of the ~~four selected stations, the correlation~~LRIW workflow against precipitation and R_{PMNE} is performed on the four displacements stations on the period from 01 January 2001 to 01 January 2012, period during which the ~~fours extensometers and recharge datasets are available.~~ four stations and recharge datasets are available. The R_{PMNE} is estimated with the non-calibrated Turc equation (Eq. (A8)) which is the most appropriate ET_0 reduced-set equation for the Séchilienne site. Indeed, the Turc equation was developed initially for the climate of France. The Turc equation requires the estimation of R_S which is performed with the non-calibrated Hargreave-Samani equation (Eq. (A2)).

~~3.4.~~3.3. Displacement data detrending

~~The long term displacement monitoring of the most active zone of the Séchilienne landslide shows that displacement rates and amplitudes have significantly increased over time as illustrated with the records of the extensometer A16 (Figure 6A). This increase is also observed for all the records even the G5 station located in a less active zone. The trend could be the result of a deterioration of near-surface rock mechanical properties or of a change of behaviour in groundwater hydrodynamics (Rutqvist and Stephansson, 2003). It means that for the same amount of rainfall, the displacement rate and the displacement amplitude are not the same over time. In terms of time series analysis, the displacement data series shows a trend on the variance amplitude as well as on the average. The observed trend is not dependent on rainfall, but finds its origin in the modification of landslide mechanical properties. In order to perform a pluri-annual comparison between the rainfall signal and the displacement signal, the trend of displacement data for the four stations has been removed (detrending).~~

~~The trend was defined by fitting a fourth-order polynomial to the recorded displacement. Removal of the trend was performed with the multiplicative method (i.e., time series is divided by the trend) which results in a unitless time series with both variance and mean trend removed. The trend characterization is a statistical process which is enhanced by increasing the amount of data used in the process. Using a larger framing interval allows to reduce edge effects, which can be particularly high for the upper bounds of the interval (exponential pattern). For this reason, the detrending was performed on a larger interval than the one used for rainfall-displacement correlation. An example of trend removal by the multiplicative method is shown in Figure 6 for the extensometer A16 record. A16 record trend is defined from 06 March 1994 to 30 June 2012 whereas detrending is performed from 01 May 1994 to~~

~~31 December 2011. The detrended displacement data of the four displacement stations are then used for the correlation with precipitation and recharge.~~

~~4. Results and discussion~~

The long-term displacement monitoring shows that displacement rate and amplitude exponentially increased with time as illustrated by the records of extensometer A16 (Fig. 4A). The rainfall data series does not show any trend over the year, meaning that the displacement trend is independent of the recharge amount. Consequently, on the Séchilienne landslide, for the same amount of rainfall, the displacement rate and magnitude responses increase steadily with time. The observed trend is the consequence of a progressive weakening of the landslide due to long-term repetitive stresses. The accumulating deformation can be assimilated to long-term creep (Brückl, 2001; Bonzanigo et al., 2007) and can be explained by a decrease of the slope shear strength (Rutqvist and Stephansson, 2003). As shown by the detrended displacement, the Séchilienne landslide is constantly moving and shows large daily to seasonal variations which seem to be the landslide response to the precipitation trigger. Consequently, the precipitation-displacement correlation is performed on the detrended displacement.

The exponential trend is removed with the statistical multiplicative method ($y_t = T_t S_t I_t$) where the time series (y_t) is composed of three components (Madsen, 2007; Cowpertwait and Metcalfe, 2009; Aragon, 2011): trend (T_t), seasonal (S_t) and irregular (I_t). In this study, the irregular and seasonal components are both assumed to be linked to the rainfall triggering factor ($y_t = T_t D_t \ with \ D_t = S_t I_t$). The trend is determined by curve fitting of a fourth-order polynomial (parametric detrending). The result is a detrended unitless time series (D_t) with both variance and mean trend removed. The time series decomposition process is illustrated with the A16 extensometer in Fig. 4.

4. Results of the recharge estimation with the LRIW method

4.1. Calibration of R_S and ET_0 methods

~~4.1.1. Solar radiation methods~~

~~Data used for calibration are from 08 July 2009 to 01 January 2012 at Grenoble Saint-Geoirs (907 records) and from 01 January 2004 to 01 January 2012 for both Saint-Jean-Saint-Nicolas (2876 records) and Saint-Michel-Maur (2864 records) weather stations. The~~ The two calibrated R_S methods show good results with respect to R_S measured at the reference weather stations ~~(Table 2).~~. The BC_{mod} R_s method is selected as it shows a better performance (R^2 = 0.864; ~~RE = 0.119~~RMSE = 1.567) than the HS_{mod} R_s method (R^2 = 0.847; ~~RE = 0.123). Equation 6~~RMSE = 1.625). The equation (4) presents the calibrated BC R_s method with all the calibrated coefficients.

$$\cancel{BC_{mod}\ R_s = 0.669\ Ra\left[1-\exp\left(-0.010\ (\alpha\Delta T)^{2.053}\right)\right]+1.733} \qquad \cancel{(6)}$$

$$BC_{mod}\ R_s = 0.669\ Ra\left[1-\exp\left(-0.010\ (\alpha\Delta T)^{2.053}\right)\right]+1.733 \qquad (4)$$

The cloud cover adjustment factor α is either equal to 0.79 (~~calibrated) or to 1, according to the conditions mentioned in Section 2.5.~~cloud impact) or to 1. All the equation terms are described in the ~~respective references (~~Appendix A~~).~~. The BC_{mod} R_s calibrated method is then used to compute R_s input data of the five ET_0 reduced-set methods.

~~4.1.2. Evapotranspiration methods~~

~~The data period used for ET_0 method regional calibration was the same as the one for R_S calibration. However strong wind days were removed.~~ Overall, all of the ET_0 methods tested show good results for regional calibration~~,~~ and are all suitable for the Séchilienne site (Table 3~~). PS ET_0, Turc ET_0 and M ET_0 methods *a* and *b* coefficients show that the regional calibration is required (Table 3). Conversely, PM red ET_0 and HS ET_0 methods *a* and *b* coefficients show that these methods have reliable performance even without regional calibration for the Séchilienne site.~~

). Among the ET_0 methods tested, the PM_{red} ET_0 method shows the best performance (R^2 = 0.932; ~~RE~~RMSE=0.~~221~~505) and requires only a low regional adjustment~~.~~ (a = 0.994 and b = 0.013). Therefore, the PM_{red} ET_0 method ~~was~~is selected to compute ET_0 for the Séchilienne site (hereafter referred to as ET_0 Séch). Figure ~~4~~5 displays the estimated ~~PM_{red}~~ ET_0 Séch versus the FAO-56 PM computation for each reference weather station. ~~Equation 7~~

The equation (5) is the final ~~calibrated PM_{red} ET_0 method with all the~~ calibrated PM_{red} ET_0 method with all the calibrated coefficients. The input R_n term is deduced from the calibrated BC_{mod} R_S method~~.~~ (Eq. (4)).

$$ET_{0\ \text{Séch}} = 0.994\,\frac{0.408\,\Delta(R_n - 0) + \gamma \frac{900}{T_{avg}+273} 1.5 (e_s - e_a)}{\Delta + \gamma(1 + 0.34\ 1.5)} + 0.013 \qquad (7)$$

~~Although the HS ET_0 method does not produce a performance as good as the PM red ET_0 method, it is one of the simplest methods from the five methods tested. The HS ET_0 method constitutes a simpler alternative for ET_0 estimation on the Séchilienne site. The HS ET_0 method shows an acceptable performance when used for rough ET_0 estimation without calibration. Equation 8 presents the combination of calibrated BC_{mod} R_S and calibrated HS ET_0 methods with all the calibrated coefficients. All the equation terms are described in the respective equation references (Appendix A).~~

$$ET_0 = 0.920\ 0.0135\ 0.408\left(0.669\ Ra\left[1 - \exp\left(-0.010\ (\alpha\Delta T)^{2.053}\right)\right] + 1.733\right)\left(T_{avg} + 17.8\right) + 0.130 \qquad (8)$$

~~In the remaining part of this paper, the evapotranspiration component ET_c will be computed with the calibrated PM red ET_0 method (Equation 7), of which the R_n term is deduced from the calibrated BC_{mod} R_S method (Equation 6) and K_c coefficients.~~

$$ET_{0\ \text{Séch}} = 0.994\,\frac{0.408\,\Delta(R_n - 0) + \gamma \frac{900}{T_{avg}+273} 1.5 (e_s - e_a)}{\Delta + \gamma(1 + 0.34\ 1.5)} + 0.013 \qquad (5)$$

4.2. Recharge-area parameters

~~The overall recharge area is delimited by taking into account: (i) the results of natural tracing combined with a tracer test which demonstrates that the highest summits of the massif contribute to the recharge area (Mudry and Etievant, 2007); (ii) the results of a $\delta^{18}O$ survey, which confirm that remote, high elevation areas (up to 3km away) fall within the recharge area of the landslide (Guglielmi et al., 2002); and (iii) topographical and geological maps.~~

Sub-areas are expressed in percentages of the whole recharge area ~~(Table 4 and Figure 5).~~(Table 4 and Fig. 6). Two types of vegetation cover, pasture and forest, are ~~delineated~~defined using aerial photographs, with proportions of 23% and 53%, respectively. The Séchilienne forest is mainly composed of beeches (*Fagus sylvatica*) and conifers (*Picea excelsa*), which are associated occasionally with ashes (*Fraxinus*) and sweet chestnuts (*Castanea sativa*). Three main geology sub-areas, micaschist bedrock (15%), sedimentary cover (20%) and superficial formations (41%), are defined through examination of the geological map and field investigations. Infiltration structures are ~~centred~~centered on the major faults ~~as~~ identified on the geological map, ~~the~~on lineaments deduced from ~~an~~aerial-photograph analysis ~~of the aerial photographs~~ and ~~the~~on geomorphological features (sinkholes, cracks~~...) for which a~~...). A 50-meter wide influence zone ~~surrounding~~is added to the identified objects~~ is added~~, leading to ~~a~~an infiltration-structure sub-area representing 24% of the recharge area.

~~**4.2.1.**~~ **For K_c estimation, the proportion of beeches and conifers is assumed to be identical for the Séchilienne forest (each 50% of forest sub-area) and other species are ignored. K_c are set to 0.71 and 0.97 for conifers, and to 0.78 and 0.9 for beeches according to Verstraeten et al. (2005). Most pastures are anthropogenic and consist of grass. K_c are set to 0.85 and 1 according to Allen et al. (1998). Infiltration structure sub-areas are not taken into account in the K_c estimation, so the relative proportions of pasture and forest become 30% and 70%, respectively.** ~~**Vegetation coefficient (K_c)**~~

~~The Séchilienne forest is mainly composed of beech (*Fagus sylvatica*) and conifer (*Picea excelsa*) trees, which can be associated occasionally with ash (*Fraxinus*) and sweet chestnut (*Castanea sativa*) trees. The proportion of beech and conifer was assumed to be identical for the Séchilienne forest (each 50% of forest sub-area) and other species were ignored for K_c estimation. Vegetation coefficient (K_c) were set to 0.71 and 0.97 for conifer, and to 0.78 and 0.9 for beech trees (Verstraeten et al., 2005). Most of the pastures are anthropogenic and consist of grass (K_c = 0.85 to 1, Allen et al., 1998). Infiltration structure sub-areas are not taken into account in the K_c estimation, so the relative proportions of pasture and forest become 30% and 70%, respectively.~~ The contribution of each sub-area ~~is estimated (Table 4,~~(Table 4, column "K_c RA~~"), allowing~~") allows the determination of the recharge area K_c values at the scale of the recharge area (0.777 to 0.955).

~~**4.2.2. Soil available water capacity (SAWC)**~~

~~The combination of geology and vegetation sub-areas results in six combined sub-areas for the recharge area (Table 4). SAWC values based on soil auger investigations are assigned to each sub-area. The contribution of each sub-area to the average recharge area estimation is derived from the GIS composite method. The average estimation of SAWC at the recharge area scale is 106 ±10 mm (rounded to 105 mm).~~

~~**4.2.3. Runoff coefficient**~~

~~An~~The combination of geology and vegetation sub-areas results in six types of SAWC sub-areas (Table 4). For each SAWC sub-area, at least one auger hole was drilled. For each soil auger core, the soil texture, the stoniness and the organic-matter content are estimated by morphological description (Jabiol and Baize, 2011). Based on these estimations, the SAWC is then computed using the pedotransfer functions of Jamagne et al (1977) and Bruand et al. (2004). The average estimation of SAWC at the recharge area scale is 106 ±10 mm (rounded to 105 mm).

To estimate the R_{coeff}, an average slope gradient is computed from slope gradient analysis of the DEM and is assigned to each vegetation sub-area. Pasture and forest sub-areas show an average slope gradient of 14° and of 20.6° respectively. ~~Pasture and forest sub-areas show an average slope gradient of 14° and of 20.6° respectively.~~ ~~Runoff coefficients~~ R_{coeff} values of 22% for pasture and 15% for forest are deduced from ~~the~~ Sautier chart~~.~~ (Musy and Higy, 2011). This chart was developed for Switzerland where environmental conditions are similar to the French Alps. A 12.8% runoff coefficient is then estimated at the recharge area scale, according to the respective proportions of ~~sub-areas in the recharge area (Table 4).~~vegetation sub-areas (Table 4).

4.3. Sensitivity analysis of the parameters of the recharge area

~~The data period for rainfall-displacement correlation is from 01 May 1994 to 01 January 2012 (6454 records). This is a common data interval for A16 extensometer and Mont-Sec weather station records. Because the recharge is computed since 09 September 1992 onwards, there are no edge effects due to SAWC initial conditions (sufficient time to equilibrate in the soil-water balance process).~~

~~Although the sensitivity analysis is based on infiltration structure percentage, the results of the sensitivity analysis are described according to the corresponding estimated SAWC values. SWAC parameter is more informative than an infiltration structure percentage.~~ Sensitivity analysis is performed for SAWC ranging from 0 (100% of infiltration structures corresponding to precipitation) to 145 mm of SAWC (0% infiltration structures +10 mm of SAWC uncertainties measurement) with ~~an increment~~increments of 10 mm. The coupled surface ~~runoff coefficient~~R_{coeff} ranges from 0 to 16.3% (~~in~~with increments of about 1%). For each combination, recharge is computed according to the soil-water balance ~~(Figure 1~~(Fig. 1 – Step 3 and ~~Figure 2)~~Fig. 2) with: (i) the temperature estimated for the recharge area (Appendix B), (ii) the precipitation recorded at Mont-Sec weather station, and (iii) the parameters of the recharge area ~~(Appendix B), (ii) the precipitation recorded at Mont-Sec weather station, and (iii) the properties of the recharge area.~~.

All the best computations have a one-day lag, with periods ranging from 56 to 104 days ~~(Table 5).~~(Fig. 7A and Table 5). The best R^2 obtained from recharge is obtained with both the ~~homogeneous infiltration assumption (SAWC = 105 mm, R^2 = 0.618) and the heterogeneous infiltration assumption for SAWC from 85 (R^2 = 0.618) to 115 mm (R^2 = 0.617).~~ estimated recharge-area parameters (SAWC = 105 mm, R^2 = 0.618) and the recharge-area parameters for SAWC adjusted from 75 (R^2 = 0.616) to 115 mm (R^2 = 0.617, Fig. 7B and Table 5). One of the best correlation performances is obtained for the estimated recharge-area parameters. This shows that the delimitation of the recharge area properly reflects the actual field conditions. The best correlation performance is assumed to be obtained, with the estimated parameter-recharge parameters for the NH4 null hypothesis, i.e. testing R^2 obtained with the estimated recharge-area set (SAWC = 105 mm) minus R^2 obtained with each of the other adjusted recharge-parameter sets of the sensitivity analysis (Table 5).

For all the recharge combinations tested, the LBCI values from bootstrap testing of ~~NH1~~NH2 are greater than 0, allowing to reject the null hypothesis ~~NH1 (Figure 7C).~~NH2 (Fig. 7C). In other words, it shows that the R^2 obtained with recharge is always significantly higher than the one computed with precipitation (R^2 = 0.311) even for a SAWC of 5 mm (R^2 = 0.426~~) (Table 5).~~

~~One of the best correlation performances is obtained with the homogeneity assumption. This reveals that the delimitation of the recharge area reflects properly the Séchilienne landslide groundwater contributing recharge area. For the heterogeneous infiltration~~, Table 5). For the adjusted recharge-area parameters scenarios having SAWC values above ~~55~~45 mm, the LBCI values from bootstrap testing of ~~NH1from~~NH4 are lower than 0, not allowing to reject the null hypothesis ~~NH2 (Table 5 and Figure 7D~~NH4 (Table 5 and Fig. 7D). In other words, it shows that the R^2 obtained with ~~the homogeneous assumption (~~a SAWC ~~=~~of 105 mm~~)~~ is not significantly higher than the ones obtained from ~~the heterogeneous assumption with~~ SAWC above ~~55 mm. The best correlation from the sensitivity analysis can be influenced by local properties of the A16 extensometer location and it is possible that infiltration structures could gather a large proportion of the flow (up to 61% for SAWC = 55 mm) relative to their recharge surface area (24%) (Table 5). If so, fractures can play an important role in the groundwater drainage from the massif towards the landslide aquifer.~~

45 mm. Recharge-displacement correlations for SAWC values ranging from 75 (runoff = 9%) to 115 mm (runoff = 13.9%) show (i) a cumulative period computation (n) below 101 days, that is within the third quartile, (ii) an R^2 greater than 0.616, that is within the third quartile ~~and~~, (iii) LBCI values of NH2 greater than 0 ~~(Table 5~~and (iv) LBCI values of NH4 lower than 0 (Table 5 and ~~Figure 7). This~~Fig. 7). These SAWC and runoff ~~range seems~~values seem to statistically reflect the recharge area properties of the landslide~~,~~ and ~~is recommended~~are suggested for further work on the Séchilienne landslide. ~~For the remaining part of this paper, the homogeneous infiltration assumption (SAWC = 105 mm) will be preferred to the heterogeneous assumption because it is based on actual field observation data.~~

4.4. Estimation of the recharge for the Séchilienne landslide

For the remaining part of this paper, the R_{LRIW} is based on the estimated recharge-area parameters (infiltration structures = 24%, SAWC = 105 mm, and R_{coeff} = 12.8%). Indeed, among all solutions giving satisfying performances in the sensitivity analysis, these parameters arise from actual field data. The R_{LRIW} is compared with the precipitation signal in Fig. 8.

The R_{LRIW} signal differs significantly from the precipitation signals, marked by a high seasonal contrast. This is especially true during summer when ET_c is important. Indeed, the first rainfall events after a dry period do not reach the aquifer until the SAWC is exceeded. Figure ~~8~~9 shows the best correlation results ~~of cumulative~~for precipitation and ~~recharge (SAWC=105 mm)~~R_{LRIW}, together with A16 detrended ~~displacement~~daily displacements. The cumulative recharge signal reproduces well the displacement acceleration and deceleration phases, and especially the dry summers where displacement ~~dropped~~ dramatically dropped (summers 1997, 1998, 2003, 2004 and 2009, ~~Figure 8B~~Fig. 9B). On the contrary, the cumulative precipitation signal is more contrasted and more noisy, and does not manage to reproduce ~~many~~several peaks (in width ~~and~~as well as in intensity) of the detrended displacement signal (winters 1997, 2000, 2004, 2005 and 2010). In addition, the cumulative precipitation signal shows a weak correlation with displacement deceleration phases (summers 1998, 1999, 2000 2006, 2009 and 2010).

~~Because the displacements of deep-seated landslides are strongly correlated with pore water pressures, the weakness of the correlation performance (R^2 < 0.7) can be explained by the fact that all the displacement data are correlated, not only the displacement acceleration stages.~~

~~Indeed, the displacement rate depends on rock properties and aquifer hydrodynamics, which behave differently according to either acceleration or deceleration stages.~~

5. Discussion

~~4.4.~~5.1. Relevance of ~~recharge signal for the Séchilienne landslide~~the LRIW method

~~The recharge is computed according to the homogeneous assumption (i.e. infiltration structures = 24%, SAWC = 105 mm, and runoff coefficient = 12.8%) and is compared with the precipitation signal (~~Figure ~~9). The recharge signal differs significantly from~~10 summarizes the comparison of the performances between the precipitation~~ signal, especially during summer when ET$_e$ is important. Indeed, the first rainfall events after a dry period do not reach the aquifer until~~, the ~~SAWC is exceeded.~~

~~In order to assess whether~~ R_{PMNE} and the ~~recharge is a relevant parameter~~R_{LRIW} based on the NH1, NH2 and NH3 tests for the ~~Séchilienne landslide, the correlation between rainfall and displacement was tested against~~ four ~~displacement stations (Figure 3) on their common data interval (01 January 2001 to 01 January 2012). Stations 1101, A13 and A16 are representative of the most active zone (median displacement of 2.5, 1.75 and 2.98 mm/day, respectively), while G5 is located on a much less active zone (median displacement of 0.05 mm/day) (Table 6).~~extensometers. All LBCI values from bootstrap testing of NH1, NH2 and NH3 are greater than zero, allowing to reject the ~~null hypothesis NH1. Rejection of NH1~~ three null hypotheses for the four stations (Fig. 10A). Rejection of the NH1 null hypothesis shows that R^2 obtained with R_{PMNE} are significantly higher than those computed with precipitation. Rejection of the NH2 null hypothesis shows that the R^2 obtained with ~~recharge~~R_{LRIW} are significantly higher than ~~the ones~~those computed with precipitation~~ for the four stations (Figure 10). R^2 varies from 0.243 to 0.586 for recharge and from 0.~~. Similarly, rejection of the NH3 null hypothesis shows that R^2 obtained with R_{LRIW} are significantly higher than those computed with R_{PMNE}. R^2 values vary from 0.0006 to 0.343 for precipitation, from 0.076 to 0.444 for R_{PMNE} and from 0.243 to 0.586 for R_{LRIW}, for G5 and A16 extensometer respectively ~~(Table 6). However, the 2.5th and 97.5th percentile of NH1 bootstrap distribution and the observed~~ (Table 2). On average, R_{PMNE} allows to increase the R^2 value ~~of NH1 test are rather constant for the four displacement stations, respectively about 0.145, 0.250 and 0.325 (Figure 10). In other words, recharge is more significant than~~ by 29% relatively to precipitation~~ at the same level for the four stations whereas correlation with displacement is very variable. This may be explained by the fact that groundwater hydrodynamic probably triggers the entire Séchilienne landslide while the displacement velocity response depends on the damage level of the rock of the displacement station location. This interpretation is supported by the variability of the cumulative period, the shift factor, the weighting factor and the R^2 value especially between G5 and the three others stations (Table 6). Finally, concerning the A16 extensometer, R^2 is better on the short interval (0.343) than the one from the sensitivity analysis (0.311) for precipitation and inversely for the recharge (0.586 instead of 0.618 for the sensitivity analysis). This could be the consequence of a degradation of near-surface rock mechanical properties of the Séchilienne landslide (as suggested by the displacement trend, Figure 6) which makes the landslide more sensitive to precipitation events in the recent period~~, while R_{LRIW} allows to increase the R^2 by 78% (Fig. 10B). The R^2 obtained with R_{LRIW} are 38% higher on average than those obtained with R_{PMNE}.

These results are confirmed by the LBCI and by the observed values of the NH2 test which are always greater than those from the NH1 test as well as by the positive LBCI values of the NH3 test (Fig. 10). The correlation performance for the recharge estimated with the LRIW method significantly exceeds the performances of the two other signals, making the LRIW method particularly appropriate to be used in landslide studies. A discussion about the benefit of this study for the understanding of the rainfall-displacement relationship in the case of the Séchilienne landslide can be found in appendix C.

~~4.5.~~5.2. Applicability of the LRIW method to other landslides

~~Several studies have shown the relevance of recharge for coastal landslides (Maquaire, 2000; Bogaard et al., 2013), unstable embankment slope landslides~~ Several studies have shown the relevance of the recharge signal for various landslide types: coastal landslides (~~Cartier and Pouget, 1987; Delmas~~Maquaire, 2000; Bogaard et al., ~~1987; Matichard and Pouget, 1988~~2013)~~ and deep-seated earthflow~~, unstable embankment slope landslides ~~(Malet et al., 2003; Godt et al., 2006)~~(Cartier and Pouget, 1987; Delmas et al., 1987; Matichard and Pouget, 1988)~~. In addition, destabilization of shallow landslides is known to be influenced by antecedent soil moisture and precipitation~~ and deep-seated earth flow landslides (~~Brocca~~Malet et al., ~~2012; Garel~~2003; Godt et al., ~~2012; Ponziani et al., 2012~~2006).~~ Recharge, which implicitly gathers together~~ In addition, destabilization of shallow landslides is known to be influenced by antecedent soil moisture and precipitation ~~can be a significant parameter to consider. However, its relevance to landslide has to be evaluated in relation to classical methods~~ (~~Van Asch~~Brocca et al., ~~1999~~2012; Garel et al., 2012; Ponziani et al., 2012)~~. Although the appropriateness of using the recharge to better characterise the precipitation-displacement relationship is demonstrated in previous studies, the parameters used are rarely described and a state of uncertainty remains about the methods implemented~~. Recharge, which implicitly gathers antecedent soil moisture and precipitation, can be a significant parameter to consider.

Although the method proposed in this study has not yet been tested at other sites, there are several arguments which suggest its applicability elsewhere. First, the FAO Penman-Monteith method used in this study is considered worldwide as the evapotranspiration method standard (~~Maquaire, 2000; Binet~~Allen et al., ~~2007; Zizioli~~ 1998; Shahidian et al., ~~2013; Padilla et al., 2014~~ 2012).

~~Although the method proposed in this study has not been yet tested at other sites, there are several arguments which suggest its applicability to other sites. Firstly, the FAO Penman-Monteith method used in this study is used worldwide as the~~ Several evapotranspiration ~~method standard~~methods were developed locally and many of them can be calibrated against reference methods in other contexts (Hargreaves and Allen, 2003; Yoder et al., ~~1998~~ 2005; Alkaeed et al., 2006; Igbadun et al., 2006; Trajkovic, 2007; Alexandris et al., 2008; López-Moreno et al., 2009; Sivaprakasam et al., 2011; Tabari and Talaee, 2011; Shahidian et al., 2012; Tabari et al., 2013)~~. Several reduced-set evapotranspiration methods have been developed locally and many of them can be calibrated against reference method in other contexts~~. Otherwise, the Penman-Monteith or Hargreaves-Samani methods are recommended ~~(Hargreaves and Allen, 2003; Yoder et al., 2005; Alkaeed et al., 2006; Igbadun et al., 2006; Trajkovic, 2007; Alexandris et al., 2008; López-Moreno et al., 2009; Sivaprakasam et al., 2011; Tabari and Talaee, 2011; Shahidian et al., 2012; Tabari et al., 2013)~~(Allen et al., 1998)~~. Otherwise, Penman-Monteith reduced-set or Hargreaves-Samani methods are recommended~~. Several solar radiation methods were developed and can be applied worldwide if locally calibrated, allowing estimation of evapotranspiration from temperature alone (Allen et al., 1998; Almorox, 2011)~~. A number of reduced-set solar radiation methods have been developed and can be applied worldwide if locally calibrated, allowing estimation of vegetation evapotranspiration with temperature alone~~. Recharge-area parameters can be estimated locally or with local or global literature reference values. The use of global values will increase recharge estimation uncertainties. However, the implementation of a sensitivity analysis allows a refinement of recharge-area parameters in order to compensate for the lack of site-specific data. Pachepsky and Rawls ~~(Allen et al., 1998; Almorox, 2011)~~(2004)~~. Recharge area parameters can be estimated locally or with local or global literature reference values according to land use. The use of global values will increase recharge estimation uncertainties. However, the implementation of a sensitivity analysis allows a refinement of recharge area parameters, in order to compensate for the lack of site-specific data. Pachepsky and Rawls~~ developed pedotransfer functions to estimate SAWC for various regions of the world. R_{coeff} values from the widely used rational method can be applied, as well as most of the runoff coefficients from the literature ~~(2004)~~(McCuen, 2005; Musy and Higy, 2011)~~ have developed~~. In addition, pedotransfer functions ~~to estimate SAWC~~ can also be used for ~~different regions of the world. Runoff~~runoff estimation. Lastly, vegetation coefficients are available from ~~the widely used rational method can be applied, as well as most of the runoff coefficients from the literature~~local surveys ~~(McCuen, 2005; Musy and Higy, 2011)~~(Gochis and Cuenca, 2000; Verstraeten et al., 2005; Hou et al., 2010)~~. In addition, pedotransfer functions can also be used for runoff estimation. Finally, vegetation coefficients are available from local surveys~~, but can also be found in the literature for many species (~~Gochis and Cuenca, 2000; Verstraeten~~Allen et al., ~~2005; Hou et al., 2010~~ 1998)~~, but can also be found in the literature for many species (Allen et al., 1998).~~

.

~~5.~~6. Conclusion and perspectives

~~This study demonstrates that the performance of landslide displacement data correlation with rainfall is significantly enhanced using recharge (average R^2 of 0.46), compared to results obtained with precipitation (average R^2 of 0.25). Most landslide sites include weather stations with limited meteorological datasets. A workflow method~~A method based on a soil-water balance, named LRIW, is developed to compute recharge on a daily interval, requiring ~~only temperature and rainfall as inputs. Two solar radiation (R_S) methods and five commonly used reference vegetation~~the characterization of evapotranspiration ~~(ET_0) reduced-set methods are tested at the Séchilienne site. However, the method~~ and parameters characterising the recharge area (soil-available water-capacity and runoff). A workflow is developed to ~~be as universal as possible in order to be applied to other landslides. SAWC, vegetation coefficient and runoff coefficient are estimated at~~compute daily groundwater recharge and requires the records of precipitation, air temperature, relative humidity, solar radiation and wind speed within or close to the landslide. The determination of the parameters of the recharge area ~~scale with a GIS composite method, and~~is based on a spatial analysis requiring field observations and spatial datasets (digital elevation models, aerial photographs and geological maps). Once determined, the parameters are refined with a sensitivity analysis.

~~For the Séchilienne landslide, the performances of all R_S tested methods are similar once they are calibrated. The five ET_0 methods tested show acceptable to very good performance. The reduced-se equations of Bristow-Campbell (R_S) and Penman-Monteith (ET_0) show the best performances, and are used for the recharge computation. A sensitivity analysis allows definition of a bracketed estimation of SAWC (from 75 to 115 mm) and of surface runoff (from 9 to 13.9%). A vegetation factor is estimated from 0.777 (winter) to 0.955 (summer).~~

~~The sensitivity analysis~~The method has been tested on the Séchilienne landslide. The tests demonstrate that the performance of the correlation with landslide displacement velocity data is significantly enhanced using the LRIW estimated recharge. The R^2 obtained with the LRIW recharge are 78% higher on average than those obtained with precipitation and are 38% higher on average than those obtained with recharge computed with a commonly used simplification in several landslide studies (recharge = precipitation minus non-calibrated ET_0). The sensitivity analysis of the LRIW workflow appears to be an appropriate alternative to estimate or to refine soil-water balance parameters of the recharge area, especially in the case of insufficient field investigations or in the absence of the necessary spatial dataset. ~~For the Séchilienne site, temperature is missing and so has to be accurately estimated. Temperature estimation brings the greatest uncertainty in the estimation of ET_0. Fortunately, temperature is commonly measured at weather stations near landslides.~~

The ~~use of recharge improves the relationship between landslide displacement and rainfall signal~~LRIW workflow is developed to be as universal as possible in order to be applied to other landslides. The ~~proposed method for estimation of the recharge~~ workflow is developed in order to be sufficiently simple ~~for use by~~to guide any non-~~hydro~~hydrogeology specialist~~.~~ ~~The proposed method~~ who intends to estimate the recharge signal in the case of rainfall-landslide displacement studies. Within this scope, a software is planned to be developed in the near future in order to provide a user-friendly tool for recharge estimation. In addition, the LRIW workflow also enables the reconstruction of retrospective time series for sites recently equipped with weather stations designed to measure a full set of parameters. ~~This method can be adapted to any other scientific study attempting to correlate time series signals with recharge.~~ A further step will ~~be~~have to account for the spatial and temporal ~~variability~~variabilities of precipitation and recharge area properties, ~~which will provide~~thus providing a better estimation of the recharge. In addition, taking recharge ~~(i.e.~~into account can assist in determining a warning rainfall threshold for ~~water budget computation).~~the deep-seated slope movements.

~~In addition, taking into account recharge can assist in determining a warning rainfall threshold for Séchilienne slope movements. To our knowledge, no attempt has led to a successful determination of rainfall threshold for deep-seated landslides (Zizioli et al., 2013). Finally, an accurate estimation of the recharge will allow to better characterise the relationship between water and displacement. This would enable to determine the influence of groundwater on the seasonal variations of destabilisation (detrended displacement) and multi-annual trend behaviour. Such an understanding will be of great benefit for instance in the framework of global climate change.~~

Acknowledgments

This research was funded by the SLAMS program (Séchilienne Land movement: Multidisciplinary Studies) of the National Research Agency (ANR). The meteorological data were provided by MétéoFrance, LTHE, ONF and CEREMA Lyon. Aerial photographs and the digital elevation model were provided by IGN. Displacement data were supplied by CEREMA Lyon. The authors acknowledge the support of Jean-Pierre Duranthon and Marie-Aurélie Chanut from the CEREMA Lyon and Jean-Paul Laurent from the LTHE. Appreciation is also given to Eric Lucot of Chrono-Environnement for his kind ~~advises~~advices for soil log interpretation and to Patrick Giraudoux for his support to implement bootstrap ~~test. Finally~~tests. Lastly, the authors thank Peter Milmo for English and technical proof reading.

References

Alexandris, S., Stricevic, R. and Petkovic, S.: Comparative analysis of reference evapotranspiration from the surface of rainfed grass in central Serbia, calculated with six empirical methods against the Penman–Monteith formula, European Water, 21/22, 17–28, 2008.

Alfonsi, P.: Relation entre les paramètres hydrologiques et la vitesse dans les glissements de terrains. Exemples de La Clapière et de Séchilienne, Revue ~~française~~Française de ~~géotechnique~~Géotechnique, (79), 3–12, 1997.

Alkaeed, O. A., Flores, C., Jinno, K. and Tsutsumi, A.: Comparison of Several Reference Evapotranspiration Methods for Itoshima Peninsula Area, Fukuoka, Japan, Memoirs of the Faculty of Engineering, Kyushu University, 66(1), 1–14, 2006.

Allen, R. E., Pereira, L. S., Raes, D. and Smith, M.: Crop evapotranspiration : guidelines for computing crop water requirements, FAO Irrigation and drainage paper 56., Food and Agriculture Organization of the United Nations, Rome., 1998.

Allen, R. G., Smith, M., Pereira, L. S. and Perrier, A.: An Update for the Definition of Reference Evapotranspiration, ICID Bulletin of the International Commission on Irrigation and Drainage, 43(2), 1–34, 1994.

Almorox, J.: Estimating global solar radiation from common meteorological data in Aranjuez, Spain, Turkish Journal of Physics, 35(1), 53–64, 2011.

Aragon, Y.: Séries temporelles avec R: Méthodes et cas, Springer Science & Business Media., 2011.

Van Asch, ~~Th.~~T. W. J., Buma, J. and ~~Van~~van Beek, L. P.~~H~~ .: A view on some hydrological triggering systems in landslides, Geomorphology, 30(1–2), 25–32, doi:10.1016/S0169-555X(99)00042-2, 1999.

Belle, P., Aunay, B., Bernardie, S., Grandjean, G., Ladouche, B., Mazué, R. and Join, J.-L.: The application of an innovative inverse model for understanding and predicting landslide movements (Salazie cirque landslides, Reunion Island), Landslides, 1–13, doi:10.1007/s10346-013-0393-5, 2013.

Binet, S., Guglielmi, Y., Bertrand, C. and Mudry, J.: Unstable rock slope hydrogeology: insights from the large-scale study of western Argentera-Mercantour hillslopes (South-East France), Bulletin de la Société Géologique de France, 178(2), 159–168, doi:10.2113/gssgfbull.178.2.159, 2007a.

Binet, S., Mudry, J., Scavia, C., Campus, S., Bertrand, C. and Guglielmi, Y.: In situ characterization of flows in a fractured unstable slope, Geomorphology, 86(1–2), 193–203, doi:10.1016/j.geomorph.2006.08.013, ~~2007~~2007b.

Bogaard, T., Guglielmi, Y., Marc, V., Emblanch, C., Bertrand, C. and Mudry, J.: Hydrogeochemistry in landslide research: a review, Bulletin de la Société Géologique de France, 178(2), 113–126, doi:10.2113/gssgfbull.178.2.113, 2007.

Bogaard, T., Maharjan, L. D., Maquaire, O., Lissak, C. and Malet, J.-P.: Identification of Hydro-Meteorological Triggers for Villerville Coastal Landslide, in Landslide Science and Practice, edited by C. Margottini, P. Canuti, and K. Sassa, pp. 141–145, Springer Berlin Heidelberg. [online] Available from: http://link.springer.com.biblioplanets.gate.inist.fr/chapter/10.1007/978-3-642-31427-8_18 (Accessed 12 June 2014), 2013.

Bonzanigo, L., Eberhardt, E. and Loew, S.: ~~Hydromechanical~~ Long-term investigation of a deep-seated creeping landslide in crystalline rock. Part I. Geological and hydromechanical factors controlling the ~~creeping~~ Campo~~-~~Vallemaggia ~~landslide, in Symposium of landslides, Causes, Impacts and Countermeasures, 17-21 June 2001, Davos, Switzerland., pp. 13–22, 2001~~ landslide, Can. Geotech. J., 44(10), 1157–1180, doi:10.1139/T07-043, 2007.

Bristow, K. L. and Campbell, G. S.: On the relationship between incoming solar radiation and daily maximum and minimum temperature, Agricultural and Forest Meteorology, 31(2), 159–166, doi:10.1016/0168-1923(84)90017-0, 1984.

~~Brocca, L., Melone, F. and Moramarco, T.: Distributed rainfall-runoff modelling for flood frequency estimation and flood forecasting, Hydrol. Process., 25(18), 2801–2813, doi:10.1002/hyp.8042, 2011.~~

Brocca, L., Ponziani, F., Moramarco, T., Melone, F., Berni, N. and Wagner, W.: Improving Landslide Forecasting Using ASCAT-Derived Soil Moisture Data: A Case Study of the Torgiovannetto Landslide in Central Italy, Remote Sensing, 4(12), 1232–1244, doi:10.3390/rs4051232, 2012.

Bruand, A., Duval, O. and Cousin, I.: Estimation des propriétés de rétention en eau des sols à partir de la base de données SOLHYDRO : Une première proposition combinant le type d'horizon, sa texture et sa densité apparente, Etude et Gestion des Sols, 11, 3, 323–334, 2004.

Brückl, E. P.: Cause-Effect Models of Large Landslides, Natural Hazards, 23(2-3), 291–314, doi:10.1023/A:1011160810423, 2001.

Canuti, P., Focardi, P. and Garzonio, C.: Correlation between rainfall and landslides, Bulletin of Engineering Geology and the Environment, 32(1), 49–54, doi:10.1007/BF02594765, 1985.

Cappa, F., Guglielmi, Y., ~~Rutqvist~~Soukatchoff, V. M., Mudry, J., ~~Tsang~~Bertrand, C~~. F~~. and ~~Thoraval~~Charmoille, A.: Hydromechanical ~~modelling~~modeling of ~~pulse tests that measure fluid pressure and fracture normal displacement at~~ a large moving rock slope inferred from slope levelling coupled to spring long-term hydrochemical monitoring: example of the ~~Coaraze Laboratory site~~La Clapière landslide (Southern Alps, France~~, International~~), Journal of ~~Rock Mechanics and Mining Sciences, 43(7), 1062–1082~~Hydrology, 291(1–2), 67–90, doi:10.1016/j.~~ijrmms.2006.03.006, 2006~~jhydrol.2003.12.013, 2004.

Cappa, F., Guglielmi, Y., Viseur, S. and Garambois, S.: Deep fluids can facilitate rupture of slow-moving giant landslides as a result of stress transfer and frictional weakening, Geophys. Res. Lett., 41(1), 61–66, doi:10.1002/2013GL058566, 2014.

Cartier, G. and Pouget, P.: Corrélation entre la pluviométrie et les déplacements de pentes instables, in 9th European conference on soil mechanics and foundation engineering, vol. 1, CRC Press, Dublin. [online] Available from: http://www.crcpress.com/product/isbn/9789061917229 (Accessed 2 April 2014), 1987.

Castellvi, F.: A new simple method for estimating monthly and daily solar radiation. Performance and comparison with other methods at Lleida (NE Spain); a semiarid climate, Theoretical and Applied Climatology, 69(3), 231–238, doi:10.1007/s007040170028, 2001.

Chanut, M.-A., Vallet, A., Dubois, L. and Duranthon, J.-P.: Mouvement de versant de Séchilienne : relations entre déplacements de surface et précipitations – analyse statistique, in Journées Aléa Gravitaire 2013, Grenoble, France., 2013.

Chernick, M. R.: Bootstrap methods: ~~a~~A guide for practitioners and researchers, Wiley-Interscience, Hoboken, N.J., 2008.

~~Chiew, F. H. S., Peel, M. C., Western, A. W., Singh, V. P. and Frevert, D.: Application and testing of the simple rainfall-runoff model SIMHYD., Mathematical models of small watershed hydrology and applications, 335–367, 2002.~~

Cordeiro, C. and Neves, M.: The Bootstrap methodology in time series forecasting, in COMPSTAT 2006 - Proceedings in Computational Statistics, pp. 1067–1073, Springer, Italy, Rome. [online] Available from: http://www.springer.com.biblioplanets.gate.inist.fr/statistics/computational+statistics/book/978-3-7908-1708-9, 2006.

Cowpertwait, P. S. P. and Metcalfe, A.: Introductory Time Series with R, Édition : 2009., Springer-Verlag New York Inc., Dordrecht ; New York., 2009.

Crozier, M. J.: Landslides: ~~causes~~Causes, consequences et environment, Croom Helm, London ; Dover, N.H., 1986.

Delmas, P., Cartier, G. and Pouget, G.: Méthodes d'analyse des risques liés aux glissements de terrain, Bulletin ~~liaison~~Liaison Laboratoire Ponts et Chaussées, 150/151, 29–38, 1987.

~~Droogers, P. and Allen, R. G.: Estimating Reference Evapotranspiration Under Inaccurate Data Conditions, Irrigation and Drainage Systems, 16(1), 33–45, doi:10.1023/A:1015508322413, 2002.~~

Diodato, N., Guerriero, L., Fiorillo, F., Esposito, L., Revellino, P., Grelle, G. and Guadagno, F. M.: Predicting Monthly Spring Discharges Using a Simple Statistical Model, Water Resources Management, 28(4), 969–978, doi:10.1007/s11269-014-0527-0, 2014.

Duranthon, J.-P., Effendiaz, L., Memier, M. and Previtali, I.: Apport des méthodes topographiques et topométriques au suivi du versant rocheux instable des ruines de Séchilienne, Association Francaise de Topographie, (94), 31–38, 2003.

Durville, J.-L., Kasperki, J. and Duranthon, J.-P.: The Séchilienne landslide: monitoring and kinematics, in First Italian Workshop on Landslides, vol. 1, pp. 174–180, Napoli, Italia., ~~8 June 2009,~~ 2009.

Garel, E., Marc, V., Ruy, S., Cognard-Plancq, A.-L., Klotz, S., Emblanch, C. and Simler, R.: Large scale rainfall simulation to investigate infiltration processes in a small landslide under dry initial conditions: the Draix hillslope experiment, Hydrological Processes, 26(14), 2171–2186, 2012.

Gochis, D. and Cuenca, R.: Plant Water Use and Crop Curves for Hybrid Poplars, Journal of Irrigation and Drainage Engineering, 126(4), 206–214, doi:10.1061/(ASCE)0733-9437(2000)126:4(206), 2000.

Godt, J. W., Baum, R. L. and Chleborad, A. F.: Rainfall characteristics for shallow landsliding in Seattle, Washington, USA, Earth Surf. Process. Landforms, 31(1), 97–110, doi:10.1002/esp.1237, 2006.

Guglielmi, Y., Cappa, F. and Binet, S.: Coupling between hydrogeology and deformation of mountainous rock slopes: Insights from La Clapière area (~~Southern~~southern Alps, France), Comptes Rendus Geoscience, 337(13), 1154–1163, doi:10.1016/j.crte.2005.04.016, 2005.

Guglielmi, Y., Vengeon, J. M., Bertrand, C., Mudry, J., Follacci, J. P. and Giraud, A.: Hydrogeochemistry: an investigation tool to evaluate infiltration into large moving rock masses (case study of La Clapière and Séchilienne alpine landslides), Bulletin of Engineering Geology and the Environment, 61(4), 311 – 324, 2002.

Guzzetti, F., Peruccacci, S., Rossi, M. and Stark, C. P.: The rainfall intensity–duration control of shallow landslides and debris flows: an update, Landslides, 5(1), 3–17, doi:10.1007/s10346-007-0112-1, 2008.

Hargreaves, G. H. and Allen, R. G.: History and Evaluation of Hargreaves Evapotranspiration Equation, Journal of Irrigation and Drainage Engineering, 129(1), 53–63, doi:10.1061/(ASCE)0733-9437(2003)129:1(53), 2003.

Hargreaves, G. and Samani, Z.: Reference Crop Evapotranspiration from Temperature, Applied Engineering in Agriculture, 1(2), 96–99, 1985.

Helmstetter, A. and Garambois, S.: Seismic monitoring of Séchilienne rockslide (French Alps): Analysis of seismic signals and their correlation with rainfalls, Journal of Geophysical Research, 115(F3), F03016, doi:10.1029/2009JF001532, 2010.

Hong, Y., Hiura, H., Shino, K., Sassa, K., Suemine, A., Fukuoka, H. and Wang, G.: The influence of intense rainfall on the activity of large-scale crystalline schist landslides in Shikoku Island, Japan, Landslides, 2(2), 97–105, doi:10.1007/s10346-004-0043-z, 2005.

Hou, L. G., Xiao, H. L., Si, J. H., Xiao, S. C., Zhou, M. X. and Yang, Y. G.: Evapotranspiration and crop coefficient of Populus euphratica Oliv forest during the growing season in the extreme arid region northwest China, Agricultural Water Management, 97(2), 351–356, doi:10.1016/j.agwat.2009.09.022, 2010.

Igbadun, H., Mahoo, H., Tarimo, A. and Salim, B.: Performance of Two Temperature-Based Reference Evapotranspiration Models in the Mkoji Sub-Catchment in Tanzania, Agricultural Engineering International: the CIGR Ejournal, VIII [online] Available from: http://ecommons.library.cornell.edu/handle/1813/10573 (Accessed 15 April 2014), 2006.

Itenfisu, D., Elliott, R. L., Allen, R. G. and Walter, I. A.: Comparison of Reference Evapotranspiration Calculations as Part of the ASCE Standardization Effort, Journal of

Irrigation and Drainage Engineering, 129(6), 440–448, doi:10.1061/(ASCE)0733-9437(2003)129:6(440), 2003.

Jabiol, B. and Baize, D.: Guide pour la description des sols, Quae éditions., 2011.

Jacobson, P. M. Z.: Fundamentals of Atmospheric Modeling, Édition : 2., Cambridge University Press, Cambridge, UK; New York., 2005.

~~Jakeman, A. J., Littlewood, I. G. and Whitehead, P. G.: Computation of the instantaneous unit hydrograph and identifiable component flows with application to two small upland catchments, Journal of hydrology, 117(1), 275–300, 1990.~~

Jamagne, M., Bétrémieux, R., Bégon, J. C. and Mori, A.: Quelques données sur la variabilité dans le milieu naturel de la réserve en eau des sols, Bulletin Technique d'Information du Ministère de l'Agriculture, (324-325), 627–641, 1977.

Jensen, M. E., Burman, R. D. and Allen, R. G.: Evapotranspiration and irrigation water requirements : a manual, American Society of Civil Engineers, New York., 1990.

Lebrouc, V., Schwartz, S., Baillet, L., Jongmans, D. and Gamond, J. F.: Modeling permafrost extension in a rock slope since the Last Glacial Maximum: Application to the large Séchilienne landslide (French Alps), Geomorphology, 198, 189–200, doi:10.1016/j.geomorph.2013.06.001, 2013.

López-Moreno, J. I., Hess, T. M. and White, S. M.: Estimation of reference evapotranspiration in a mountainous mediterranean site using the Penman-Monteith equation with limited meteorological data, Pirineos, 164, 7–31, 2009.

Lu, J., Sun, G., McNulty, S. G. and Amatya, D. M.: A comparison of six potential evapotranspiration methods for regional use in the Southeastern United States, JAWRA Journal of the American Water Resources Association, 41(3), 621–633, doi:10.1111/j.1752-1688.2005.tb03759.x, 2005.

Madsen, H.: Time Series Analysis, 1 edition., Chapman and Hall/CRC, Boca Raton., 2007.

Makkink, G. .: Testing the Penman formula by means of lysimeters, Journal of the Institution of Water Engineers, 11, 277–288, 1957.

Malet, J. P., Maquaire, O. and Vanash, T. W.: Hydrological behaviour of earthflows developed in clay-shales: investigation, concept and modelling, The Occurrence and Mechanisms of Flows in Natural Slopes and Earthfills, Patron Editore, Bologna, 175–193, 2003.

Maquaire, O.: Effects of Groundwater on the Villerville-Cricqueboeuf Landslides , Sixteen Year Survey (Calvados, France), in 8th Landslides International symposium, pp. 1005–1010, Cardiff., 2000.

Matichard, Y. and Pouget, P.: Pluviométrie et comportement de versants instables, in Landslides : proceedings of the fifth International Symposium on Landslides, pp. 725–730, Lausanne, Switzerland., 1988.

McCuen, R. H.: Hydrologic analysis and design, Pearson Prentice Hall, Upper Saddle River, N.J., 2005.

Meric, ~~O., Garambois, S. and Orengo, Y.: Large Gravitational Movement Monitoring Using a Spontaneous Potential Network, in Proc. 19th Annual Symposium on the Application of Geo physics to Engineering and Environmental Problems (SAGEEP), EEGS, Seattle, USA., 2-6 April 2006, pp. 202–209, 2006~~ O., Garambois, S., Jongmans, D., Wathelet, M., Chatelain, J. L. and Vengeon, J. M.: Application of geophysical methods for the investigation of the large gravitational mass movement of Séchilienne, France, Can. Geotech. J., 42(4), 1105–1115, doi:10.1139/t05-034, 2005.

Meric, O., Garambois, S. and Orengo, Y.: Large Gravitational Movement Monitoring Using a Spontaneous Potential Network, in Proc. 19th Annual Symposium on the Application of Geophysics to Engineering and Environmental Problems, pp. 202–209, EEGS, Seattle, USA., 2006.

Mudry, J. and Etievant, K.: Synthèse hydrogéologique du versant instable des Ruines de Séchilienne, Unpublished report, UMR Chrono-Environnement, University of Franche-Comté., 2007.

Musy, A. and Higy, C.: Hydrology: A Science of Nature, English ed., CRC Press ; Science Publishers, Boca Raton, FL. : Enfield, N.H., 2011.

Noverraz, F., Bonnard, C., Dupraz, H. and Huguenin, L.: Grands glissements de terrain et climat, VERSINCLIM - Comportement passé, présent et futur des grands versants instables subactifs en fonction de l'évolution climatique, et évolution en continu des mouvements en profondeur, Rapport final PNR31 (Programme National de Recherche), vdf Hochschulverlag AG an der ETH Zürich, Zürich, Switzerland., 1998.

Pachepsky, Y. and Rawls, W. J.: Development of pedotransfer functions in soil hydrology, Elsevier, Amsterdam; New York., 2004.

~~Padilla, C., Onda, Y., Iida, T., Takahashi, S. and Uchida, T.: Characterization of the groundwater response to rainfall on a hillslope with fractured bedrock by creep deformation and its implication for the generation of deep-seated landslides on Mt. Wanitsuka, Kyushu Island, Geomorphology, 204, 444–458, 2014.~~

Patwardhan, A., Nieber, J. and Johns, E.: Effective Rainfall Estimation Methods, Journal of Irrigation and Drainage Engineering, 116(2), 182–193, doi:10.1061/(ASCE)0733-9437(1990)116:2(182), 1990.

Pisani, G., Castelli, M. and Scavia, C.: Hydrogeological model and hydraulic behaviour of a large landslide in the Italian Western Alps, Nat. Hazards Earth Syst. Sci., 10(11), 2391–2406, doi:10.5194/nhess-10-2391-2010, 2010.

Ponziani, F., Pandolfo, C., Stelluti, M., Berni, N., Brocca, L. and Moramarco, T.: Assessment of rainfall thresholds and soil moisture modeling for operational hydrogeological risk prevention in the Umbria region (central Italy), Landslides, 9(2), 229–237, doi:10.1007/s10346-011-0287-3, 2012.

Priestley, C. H. B. and Taylor, R. J.: On the Assessment of Surface Heat Flux and Evaporation Using Large-Scale Parameters, Monthly Weather Review, 100(2), 81–92, doi:10.1175/1520-0493(1972)100<0081:OTAOSH>2.3.CO;2, 1972.

Prokešová, R., Medveďová, A., Tábořík, P. and Snopková, Z.: Towards hydrological triggering mechanisms of large deep-seated landslides, Landslides, 10(3), 239–254, doi:10.1007/s10346-012-0330-z, 2013.

Rochet, L., Giraud, A., Antoine, P. and Évrard, H.: La déformation du versant sud du ~~mont-sec~~Mont-Sec dans le secteur des ruines de Séchilienne (Isère), Bulletin of the International Association of Engineering Geology, 50(1), 75–87, doi:10.1007/BF02594959, 1994.

Le Roux, O., Jongmans, D., Kasperski, J., Schwartz, S., Potherat, P., Lebrouc, V., Lagabrielle, R. and Meric, O.: Deep geophysical investigation of the large Séchilienne landslide (Western Alps, France) and calibration with geological data, Engineering Geology, 120(1–4), 18–31, doi:10.1016/j.enggeo.2011.03.004, 2011.

Rutqvist, J. and Stephansson, O.: The role of hydromechanical coupling in fractured rock engineering, Hydrogeology Journal, 11(1), 7–40, doi:10.1007/s10040-002-0241-5, 2003.

~~Samani, Z.: Estimating Solar Radiation and Evapotranspiration Using Minimum Climatological Data, Journal of Irrigation and Drainage Engineering, 126(4), 265–267, doi:10.1061/(ASCE)0733-9437(2000)126:4(265), 2000.~~

Shahidian, S., Serralheiro, R., Serrano, J., Teixeira, J., Haie, N. and Santos, F.: Hargreaves and Other Reduced-Set Methods for Calculating Evapotranspiration, in Evapotranspiration - Remote Sensing and Modeling, edited by A. Irmak, pp. 60–80, InTech, Rijeka, Croatia., 2012.

Sivaprakasam, S., Murugappan, A. and Mohan, S.: Modified Hargreaves equation for estimation of ETo in a Hot and Humid Location in Tamilnadu State, India, Int. Journal of Engineering Science and Technology, 3, 592–600, 2011.

~~Stirzaker, R., Biggs, H., Roux, D. and Cilliers, P.: Requisite Simplicities to Help Negotiate Complex Problems, Ambio, 39(8), 600–607, doi:10.1007/s13280-010-0075-7, 2010.~~

Tabari, H., Grismer, M. E. and Trajkovic, S.: Comparative analysis of 31 reference evapotranspiration methods under humid conditions, Irrigation Science, 31(2), 107–117, doi:10.1007/s00271-011-0295-z, 2013.

Tabari, H. and Talaee, P. H.: Local Calibration of the Hargreaves and Priestley-Taylor Equations for Estimating Reference Evapotranspiration in Arid and Cold Climates of Iran Based on the Penman-Monteith Model, Journal of Hydrologic Engineering, 16(10), 837–845, doi:10.1061/(ASCE)HE.1943-5584.0000366, 2011.

~~Tan, B. Q. and O'Connor, K. M.: Application of an empirical infiltration equation in the SMAR conceptual model, Journal of Hydrology, 185(1–4), 275–295, doi:10.1016/0022-1694(95)02993-1, 1996.~~

Trajkovic, S.: Temperature-Based Approaches for Estimating Reference Evapotranspiration, Journal of Irrigation and Drainage Engineering, 131(4), 316–323, doi:10.1061/(ASCE)0733-9437(2005)131:4(316), 2005.

Trajkovic, S.: Hargreaves versus Penman-Monteith under Humid Conditions, Journal of Irrigation and Drainage Engineering, 133(1), 38–42, doi:10.1061/(ASCE)0733-9437(2007)133:1(38), 2007.

Trajkovic, S. and Stojnic, V.: Effect of wind speed on accuracy of Turc method in a humid climate, Facta universitatis - series: Architecture and Civil Engineering, 5(2), 107–113, doi:10.2298/FUACE0702107T, 2007.

Turc, L.: Evaluation des besoins en eau d'irrigation, évapotranspiration potentielle, formule simplifiée et mise à jour., Annales Agronomiques, 12, 13–49, 1961.

Vengeon, J. M.: Déformation et rupture des versants en terrain métamorphique anisotrope: Apport de l'étude des Ruines de Séchilienne, ~~Ph.D.~~ PhD thesis, Université Joseph ~~Fourrier~~ Fourier I, Grenoble, ~~France,~~ 3 November., 1998.

Verstraeten, W. W., Muys, B., Feyen, J., Veroustraete, F., Minnaert, M., Meiresonne, L. and De Schrijver, A.: Comparative analysis of the actual evapotranspiration of Flemish forest and cropland, using the soil water balance model WAVE, Hydrol. Earth Syst. Sci., 9(3), 225–241, doi:10.5194/hess-9-225-2005, 2005.

Yoder, R. E., Odhiambo, L. O. and Wright, W. C.: Evaluation of methods for estimating daily reference crop evapotranspiration at a site in the humid Southeast United States, Applied Engineering in Agriculture, 21(2), 197–202, 2005.

Zêzere, J. L., Trigo, R. M. and Trigo, I. F.: Shallow and deep landslides induced by rainfall in the Lisbon region (Portugal): assessment of relationships with the North Atlantic Oscillation, Natural Hazards and Earth System Sciences, 5(3), 331–344, doi:10.5194/nhess-5-331-2005, 2005.

~~Zizioli, D., Meisina, C., Valentino, R. and Montrasio, L.: Comparison between different approaches to modeling shallow landslide susceptibility: a case history in Oltrepo Pavese, Northern Italy, Natural Hazards and Earth System Sciences, 13(3), 559-573, doi:10.5194/nhess-13-559-2013, 2013.~~

Appendix A: Equations for evapotranspiration and solar radiation methods

A.1 Equation parameters terms for all equations ~~are defined as follow:~~

~~R_a~~ R_a extraterrestrial solar radiation [MJ m^{-2} day^{-1}]

~~R_s~~ R_s solar radiation [MJ m^{-2} day^{-1}]

~~R_n~~ R_n net solar radiation [MJ m^{-2} day^{-1}]

~~N~~ N maximum possible duration of sunshine [hour]

~~n~~ n actual daily duration of sunshine [hour]

~~T_{avg}~~ T_{avg} average air temperature at 2 m height [°C]

~~T_{min}~~ T_{min} minimum air temperature at 2 m height [°C]

~~T_{max}~~ T_{max} maximum air temperature at 2 m height [°C]

~~G~~ G soil heat flux density [MJ m^{-2} day^{-1}]

~~γ~~ γ psychrometric constant [kPa $°C^{-1}$]

~~u_2~~ u_2 wind speed at 2 m height [m s^{-1}]

~~e_s~~ e_s mean saturation vapour pressure [kPa]

~~e_a~~ e_a actual vapour pressure [kPa]

~~e^o~~ e^o saturation vapour pressure at the air temperature T [kPa]

Δ slope of vapour pressure curve [kPa $°C^{-1}$]

~~RH~~ RH relative humidity [%]

~~The procedure for calculating these equation terms are presented in detail in the FAO-56 guidelines for computing crop water requirements (Allen et al., 1998).~~

α cloud cover adjustment factor [unitless]

The procedure for calculating these equation terms are given in the FAO-56 guidelines for computing crop water requirements (Allen et al., 1998).

A.2 Solar radiation (R_S)~~:~~

The solar radiation ~~$BC\ R_s$~~ $BC\ R_s$ ~~obtained from the Bristow-Campbell method:~~

~~$BC\ R_s = A_{BC}\ Ra\ 1 - exp\left(-B_{BC}(\alpha\,\Delta T)^{C_{BC}}\right)$ with $\Delta T_{BC} = T_{max(j)} - \frac{T_{\min(j)+}T_{\min(j+1)}}{2}$ (A1)~~

~~The solar radiation $HS\ R_s$ obtained from the Hargreaves-Samani method:~~

~~$HS\ R_s = A_{HS} Ra\left(\Delta T_{HS}\right)^{B_{HS}}$ with~~ is obtained from the Bristow-Campbell method (Bristow and Campbell, 1984):

$$BC\,R_s = A_{BC}\ Ra\left[1 - exp\left(-B_{BC}(\alpha\,\Delta T_{BC})^{C_{BC}}\right)\right] \text{ with } \Delta T_{BC} = T_{max(j)} - \frac{T_{\min(j)+}T_{\min(j+1)}}{2} \qquad \text{(A1)}$$

The solar radiation ~~$\Delta T_{HS} = T_{max(j)} - T_{\min(j)}$~~ $HS\ R_s$ ~~(A2)~~

obtained from the Hargreaves-Samani method (Hargreaves and Samani, 1985):

$$HS\ R_s = A_{HS} Ra\left(\Delta T_{HS}\right)^{B_{HS}} \text{ with } \Delta T_{HS} = T_{max(j)} - T_{\min(j)} \qquad \text{(A2)}$$

where:

j is for the current target day and j+1 is for the following day

~~A_{BC}, B_{BC}, C_{BC}~~ A_{BC}, B_{BC}, C_{BC} are the Bristow-Campbell empirical coefficients (no default values)

~~A_{HS}, B_{HS}~~ A_{HS}, B_{HS} are the Hargreaves-Samani empirical coefficients ~~$(A_{HS} = 0.16\ and\ B_{HS} = 0.5)$~~ $(A_{HS} = 0.16\ and\ B_{HS} = 0.5)$

~~R_S can also be calculated with the Angström formula using sunshine duration data recorded at a weather station (FAO-56 guidelines (Allen et al., 1998)):~~

In this study, the modified forms of R_S equation of Bristow-Campbell and Hargreaves-Samani are implemented: (i) a constant is added to take into account the possibility of a R_S estimation shift, (ii) the ΔT from the Bristow-Campbell method is used in both equations, and (iii) a cloud cover adjustment factor α is applied to ~~$R_s = \left(a_s + b_s \frac{n}{N}\right) R_a$~~ ΔT ~~(A3)~~

~~where:~~ since, for cloudy conditions, ~~$a_s + b_s$~~ ΔT ~~is~~ can produce an estimate larger than the incoming solar radiation (Bristow and Campbell, 1984).

Bristow-Campbell modified equation ($BC_{mod}\ R_s$):

$$BC_{mod}\,R_s = A_{BC}\ Ra\left[1 - exp\left(-B_{BC}\ (\alpha\Delta T)^{C_{BC}}\right)\right] + D_{BC} \qquad \text{(A3)}$$

Hargreaves-Samani modified equation ($HS_{mod}\ R_s$):

$$HS_{mod}\, R_s = A_{HS}\, Ra\left(\alpha \Delta T\right)^{B_{HS}} + C_{HS} \qquad \text{(A4)}$$

with $\Delta T = T_{max(j)} - \dfrac{T_{\min(j)} + T_{\min(j+1)}}{2}$

where:

j is for the current day and j+1 is for the following day

$A_{BC}, B_{BC}, C_{BC}, D_{BC}$ are the Bristow-Campbell regional calibration coefficients

A_{HS}, B_{HS}, C_{HS} are the Hargreaves-Samani regional calibration coefficients

The α coefficient is applied for the two first rain-event days since, for a rain period longer than two days, the value of the Rs estimated from ΔT and the actual R_S value become almost identical. If ΔT on the day before a rain event (ΔT_{j-1}) is less than ΔT_{j-2} by more than 2°C, the coefficient α is also applied assuming that cloud cover was already significantly present. For the remaining days, α is not applied (α = 1). A 2°C threshold and a 2-day period is used (Bristow and Campbell, 1984). In this study, the calibration of α is based on the principle that if this adjustment is not relevant, a calibrated α coefficient would be equal to 1 (no effect).

R_S can also be calculated with the Angström formula using sunshine duration data recorded at a weather station (FAO-56 guidelines, Allen et al., 1998):

$$R_s = \left(a_s + b_s \frac{n}{N}\right) R_a \qquad \text{(A5)}$$

where: $a_s + b_s$ is the fraction of extraterrestrial solar radiation reaching the ~~earth~~Earth surface on clear days~~. By~~ (default values, a_s=0.25 and b_s = 0.5~~ (without calibration~~).

A.3 Reference vegetation evapotranspiration (ET$_0$~~):~~)

The reference vegetation evapotranspiration ~~FAO-56 PM ET$_0$ obtained from the Penman-Monteith method modified form from the FAO paper number 56:~~

$$FAO-56\ PM\ ET_0 = \frac{0.408\,\Delta\left(R_n - G\right) + \gamma \dfrac{900}{T_{avg} + 273}\, u_2\left(e_s - e_a\right)}{\Delta + \gamma\left(1 + 0.34\, u_2\right)}$$

$FAO-56\,PM\ ET_0$

~~(A4)~~

~~The reference vegetation evapotranspiration $HS\,ET_0$ obtained from the Hargreaves-Samani method:~~

~~$HS\,ET_0 = 0.0135\ 0.408\, Rs\left(T_{avg} + 17.8\right)$ (A5)~~

obtained from the Penman-Monteith method modified form from the FAO paper number 56 (Allen et al., 1998) is:

$$FAO-56\,PM\;ET_0=\frac{0.408\Delta(R_n-G)+\gamma\frac{900}{T_{avg}+273}u_2(e_s-e_a)}{\Delta+\gamma(1+0.34u_2)} \qquad (A6)$$

The reference vegetation evapotranspiration $HS\;ET_0$ obtained from the Hargreaves-Samani method (Hargreaves and Samani, 1985) is:

$$HS\;ET_0=0.0135\;0.408\;Rs\,(T_{avg}+17.8) \qquad (A7)$$

The unit conversion factor 0.408 ~~was~~is added to the original formula in order to compute ~~ET_0~~ ET_0 in mm day^{-1} with R_S in MJ m^{-2} day^{-1}.

The reference vegetation evapotranspiration ~~$Turc\;ET_0$~~ $Turc\;ET_0$ ~~obtained from the Turc method:~~

~~$For\;RH>50\%\,,\quad Turc\;ET_0=0.01333\frac{T_{avg}}{T_{avg}+15}(23.9001\,Rs+50) \qquad (A6)$~~

~~$For\;RH<50\%,\quad Turc\;ET_0=0.01333\frac{T_{avg}}{T_{avg}+15}(23.9001\,Rs+50)\left(1+\frac{50-RH}{70}\right) \qquad (A7)$~~

obtained from the Turc method (Turc, 1961) is:

$$For\;RH>50\%\,,\quad Turc\;ET_0=0.01333\frac{T_{avg}}{T_{avg}+15}(23.9001\,Rs+50) \qquad (A8)$$

$$For\;RH<50\%,\quad Turc\;ET_0=0.01333\frac{T_{avg}}{T_{avg}+15}(23.9001\,Rs+50)\left(1+\frac{50-RH}{70}\right) \qquad (A9)$$

For the Séchilienne landslide, the ~~*Equation (A6)* was~~equation (A8) is preferred to ~~*Equation (A7)*~~the equation (A9) because of an average relative humidity (RH) of the nearby mountain weather stations greater than 50% (Chamrousse, 70%; Saint-Michel-Maur, 66 %; Saint-Jean-Saint-Nicolas, 66 %).

The reference vegetation evapotranspiration ~~$PT\;ET_0$~~ $PT\;ET_0$ ~~obtained from the Priestley-Taylor method:~~

~~$PT\;ET_0=1.26\frac{\Delta}{\Delta+\gamma}(R_n-G) \qquad (A8)$~~

~~The reference vegetation evapotranspiration $M\;ET_0$ obtained from the Makkink method:~~

~~$M\;ET_0=0.61\frac{\Delta}{(\Delta+\gamma)}\frac{R_s}{2.45}-0.012 \qquad (A9)$~~

obtained from the Priestley-Taylor method (Priestley and Taylor, 1972) is:

$$PT\ ET_0 = 1.26 \frac{\Delta}{\Delta + \gamma}\left(R_n - G\right) \qquad (A10)$$

The reference vegetation evapotranspiration $M\ ET_0$ obtained from the Makkink method (Makkink, 1957) is:

$$M\ ET_0 = 0.61 \frac{\Delta}{\left(\Delta + \gamma\right)} \frac{R_s}{2.45} - 0.012 \qquad (A11)$$

The Penman-Monteith reduced-set method which allows to calculate the reference vegetation evapotranspiration ~~$PM_{red}\ ET_0$~~ $PM_{red}\ ET_0$ is identical to the PM FAO-56 method (Eq. ~~A12)~~ (A6)), but humidity and wind speed are estimated according to FAO-56 guidelines ~~(Allen et al., 1998).~~(Allen et al., 1998). The actual vapour pressure is estimated with the ~~Equation (A10).~~equation (A12):

$$\cancel{e_a = e^0\left(T_{min}\right) = 0.611\ exp\ \frac{17.27\ T_{min}}{T_{min} + 237.3} \qquad (A10)}$$

$$e_a = e^0\left(T_{min}\right) = 0.611\ exp\ \frac{17.27\ T_{min}}{T_{min} + 237.3} \qquad (A12)$$

In the case of the Séchilienne landslide, the wind speed ~~was~~is fixed at 1.5 m/s at a 2~~-meters~~-meter height (2 m/s by default), which is the daily average of the nearby mountain weather stations (Chamrousse, 2.33 m/s; Saint-Michel-Maur, 0.95 m/s; Saint-Jean-Saint-Nicolas, 1.26 m/s).

A.4 Practical informations

The ET_0 methods used in this study were developed for irrigation scheduling, for which the scope of application involves positive temperatures (plant water supply during the spring-summer growing period). However, in mountainous sites, winter temperatures are often below 0°C, and ET_0 empirical methods can compute negative ET_0 values. Negative ET_0 computed values do not have any physical meaning and are therefore set to zero for this study.

The Priestley-Taylor and Penman-Monteith ET_0 methods use net solar radiation (R_n) instead of R_S, which can be deduced from R_S following the FAO-56 guideline (Allen et al., 1998).

ET_0 reduce-set methods do not take into account the wind speed variations. By removing saturated air from the boundary layer, wind increases evapotranspiration (Shahidian et al., 2012). Several studies show the influence of the wind speed on ET_0 method performance and therefore on calibration (Itenfisu et al., 2003; Trajkovic, 2005; Trajkovic and Stojnic, 2007). For this study, the days with average wind speed above the 95th percentile of the dataset (extreme values) are disregarded for the calibration.

Appendix B: Temperature estimation at the Mont-Sec weather station

B.1 Method

The temperatures at the Mont-Sec weather station are estimated with the characterisation of the local air temperature gradient using two surrounding weather stations recording the temperatures at a daily rate (Luitel et La Mure weather stations). Once the local air temperature gradient is characterized, one of the station is used to estimate the Mont-Sec temperatures.

The decrease in air density with elevation leads to a decrease in air temperature known as the lapse rate (Jacobson, 2005)~~-~~. A commonly used value of this rate is -6.5 °C / 1000 m. The air temperature can thus be related to elevation. In order to compute a local air temperature gradient, two weather stations surrounding the Séchilienne site ~~were~~are used ~~(weather stations of~~: Luitel and La Mure~~).~~ (Table 1 and Fig. 3). The Luitel station is located on the Séchilienne massif whereas the La Mure station is located about 18 km from the landslide. Both stations have weather conditions similar to the Séchilienne recharge area. Although, the temperature estimation from the Luitel station would probably be more accurate, in order to maximize common interval lengths of ~~temperature~~temperatures with displacement ~~record~~records from 1994 to 2012, the La Mure station with ~~record~~records from 1992 to 2012 ~~was selected as a reference~~is preferred to estimate ~~temperature~~temperatures at Mont-Sec.

The local air temperature gradient in relation to elevation is defined by Equation ~~(B1).~~(B1). The La Mure station temperatures (minimum and maximum) are used to estimate the temperatures at Luitel in relation to elevation, over their common recording period. A linear regression between ~~temperature~~temperatures measured at La Mure and Luitel ~~was~~is performed to determine the *a* and *b* coefficients. The b coefficient, which ~~gather together~~gathers the lapse rate (λ) and the elevation difference, ~~was~~is then divided by the elevation difference of the two stations used for the calibration.

$$\cancel{T_{(Station)} = aT_{(Mure)} + b = aT_{(Mure)} + \lambda \, Diff_{elevation} \quad \text{with} \quad Diff_{elevation} = Elevation_{Mure} - Elevation_{Station}} \quad \cancel{(B1)}$$

$$T_{(Station)} = aT_{(Mure)} + b = aT_{(Mure)} + \lambda \, Diff_{elevation}$$

$$\text{with } Diff_{elevation} = Elevation_{Mure} - Elevation_{Station} \qquad (B1)$$

where:

a and b	regional calibration coefficients
T	temperature minimum or maximum [°C]
λ	temperature lapse rate [°C m^{-1}]
$Diff_{elevation}$	difference of elevation between two weather stations [m]
Elevation	weather station elevation [m asl]
Station	target station (Luitel for ~~the~~ calibration, Mont-Sec for computation)

B.2 Results

The recording period used for temperature calibration is from 06 July 2006 to 23 July 2012 (2193 records). This is a common data interval for the two weather stations used (La Mure and Luitel). The estimation of the local air temperature gradient shows a very good performance with R² equal to 0.895 (LBCI at 5% level = 0.826) and 0.916 (LBCI at 5% level = 0.850), and ~~RE~~RMSE equal to 2.12 and 2.48 respectively for minimum and maximum daily temperature calibration. ~~Equation (B2)~~ The equations (B2) and ~~(B3)~~(B3) are used to estimate temperatures at Mont-Sec with temperatures measured at La Mure. ~~Instead of~~Rather than taking the elevation of the Mont-Sec weather station (1147 m), the average elevation of recharge area (1200 m) is used, resulting in a difference of elevation with La Mure of 319 m. ~~The recording period used for temperature calibration was from 06 July 2006 to 23 July 2012 (2193 records). This is a common data interval for the two weather stations used (La Mure, Luitel).~~ The estimated local air temperature gradient is 0.7°C per 100 meters of elevation (the average of the λ of the two following equations).

~~$T_{min\,(Mont\ Sec)} = 0.911\ T_{min\,(Mure)} - 0.0056 \times 319$ (B2)~~

~~$T_{max\,(Mont\ Sec)} = 0.928\ T_{max\,(Mure)} - 0.0087 \times 319$ (B3)~~

~~The absence of reliable temperature records at the Mont-Sec weather station increases the estimation of R_S and ET_0 uncertainty.~~

$$T_{min\,(Mont\ Sec)} = 0.911\ T_{min\,(Mure)} - 0.0056 \times 319 \quad (B2)$$

$$T_{max\,(Mont\ Sec)} = 0.928\ T_{max\,(Mure)} - 0.0087 \times 319 \quad (B3)$$

Appendix C: Rainfall-displacement relationship in the case of the Séchilienne landslide

The rainfall-displacement relationship is hereafter discussed for the precipitation and the R_{LRIW} signals. Although the R^2 values are significantly variable from one station to another, the 2.5th and 97.5th percentiles and the observed value of the NH2 test are rather constant for the four displacement stations (respectively about 0.145, 0.250 and 0.325, Fig. 10A). These results show that the improvement of the correlation performance by using recharge rather than precipitation has the same order of magnitude for the four stations, whereas R^2 values vary considerably between the four stations. This may be explained by the fact that groundwater hydrodynamics probably triggers the entire Séchilienne landslide while the displacement velocity response depends on the damage level of the rock at the location of the displacement station. This interpretation is supported by the variability of the cumulative period, the shift factor, the weighting factor and the R^2 value, especially between G5 and the three others stations (Table 2).

The cumulative period and the shift factor deduced from the antecedent cumulative sum allow to determine the response-time of the Séchilienne landslide to rainfall events. Displacement stations located in the high motion zone show homogenous time delays with shift factors of 2 to 3 days. The average cumulative periods beyond which precipitation or R_{LRIW} have no longer any influence on the landslide destabilisation are estimated at about 50 days for precipitation and 75 days for R_{LRIW}. The station G5 shows significantly different time delays and cumulative periods, whatever the precipitation or R_{LRIW} data used. This difference can be explained by the low signal-to-noise ratio which makes the correlations difficult to interpret.

Concerning the A16 extensometer, regarding precipitation R^2 is better for the recent-short testing interval (0.343) than for the former-long interval of the sensitivity analysis (0.311). Conversely, regarding the recharge, R^2 is better for the former-long interval (0.618) than for the recent-short testing interval (0.586). This could be the consequence of a degradation of the near-surface rock mechanical properties of the Séchilienne landslide (as suggested by the displacement trend, Fig. 4), which makes the landslide more sensitive to precipitation events in the recent period.

Lastly, the best correlations from the sensitivity analysis suggest that infiltration structures could gather a large proportion of the flow (up to 68% for SAWC = 45 mm; NH4 LBCI <0) with respect to their recharge surface area (24%, Table 5). If so, fractures can play an important role in the groundwater drainage from the massif towards the landslide aquifers.

Table 1~~.~~: Summary of weather datasets ~~used in this study~~ with parameters used (●) at ~~each location~~the various locations. Distance is the ~~distance~~measured from the Séchilienne landslide, R_S is the solar radiation, N is the sunshine duration, W is the wind speed, H is the humidity, T is the temperature and P is the ~~precipitations.~~precipitation depth

Station Name	Elevation (m asl)	Distance (km)	From	To	R_S	N	W	H	T	P	Number of days with data
Saint-Jean-Saint-Nicolas	1210	55	01 ~~January~~Jan. 2004	01 ~~January~~Jan. 2012	●	●	●	●	●		2876
Saint-Michel-Maur	698	54	01 ~~January~~Jan. 2004	01 ~~January~~Jan. 2012		●	●	●	●		2864
Grenoble-Saint-Geoirs	384	51	08 ~~July~~Jul. 2009	01 ~~January~~Jan. 2012	●	●	●	●	●		907
Chamrousse	1730	9	12 ~~September~~Sep. 2002	01 ~~March~~Mar. 2012			●	●			3261
La Mure	881	18	9 ~~September~~ Sep. 1992	01 ~~January~~Jan. 2012					●		7517
Luitel	1277	4	06 ~~July~~Jul. 2006	23 ~~July~~Jul. 2012					●		2193
Mont-Sec	1148	0.2	9 ~~September~~ Sep. 1992	01 ~~January~~Jan. 2012						●	7517

Table 2~~. R_S (solar radiation) methods: calibration results and performance assessment parameters (average of three weather stations).~~

~~A, B C and D are the calibration coefficients, α is the cloud cover adjustment factor, R^2 is the coefficient of determination of the linear regression (measured *vs.* estimated R_S) and RE is the relative error. HS_{mod} R_S is the solar radiation calculated with the modified form of Hargreaves-Samani method. BC_{mod} R_S is the solar radiation calculated with the modified form of Bristow-Campbell method.~~

: Statistics of the displacement records and results of the best linear correlation between precipitation/R_{LRIW} and displacement records for 4 displacement stations (1101, A13, A16 and G5). The displacement column indicates basic statistics of the displacement records: 1st quartile (Q1), median and 3rd quartile (Q3). Cumulative period (n), shift factor (β) and weighting factor (α) are the terms of the equation (3). P stands for precipitation, R_1 stands for R_{PMNE} and R2 stands for R_{LRIW}.

Station	Displacement mm/day	Cumulative period (n)			Shift factor (β)			Weighting factor (α)			R^2		
~~Method~~	~~A~~Q1/median/ Q3	P	R_1	R_2	P	R_1	R_2	~~B~~P	~~C~~R_1	~~D~~R_2	~~α~~P	~~R^2~~R_1	~~RE~~R_2
~~HS_{mod} R_S~~1101	~~0.106~~1.75 / 2.50 / 3.84	42	54	68	2	2	2	0.~~662~~071	0.~~670~~065	~~-~~0.091	0.~~740~~28	0.~~847~~35	0.~~123~~50
A13	1.18 / 1.75 / 3.41	52	80	82	3	2	2	0.102	0.070	0.091	0.28	0.37	0.52
~~BC_{mod} R_S~~A16	~~0.669~~1.94 / 2.98 / 4.39	64	71	76	2	2	2	0.~~010~~163	~~2.056~~0.125	~~1.733~~0.168	0.~~790~~34	0.~~864~~44	0.~~119~~59
G5	0.02 / 0.05 / 0.08	8	169	132	0	6	6	0.039	0.003	0.011	0.001	0.08	0.24

Table 3: Calibration and performance of the ~~reduced-set~~five tested ET_0 methods relatively to the FAO-56 PM ET_0 standard (Penman-Monteith method defined in the FAO-56 paper). All ~~reduced-set~~the ET_0 methods are detailed in the appendix A.

a, b and R^2 are the results of linear regression between FAO-56 PM ET_0 and ~~reduced-set~~tested ET_0~~, RE~~ methods. RMSE is the ~~relative~~root mean square error~~.~~

Method	a	b	R^2	~~RE~~RMSE
HS Et_0	0.920	0.130	0.917	0.~~24~~548
Turc ET_0	0.880	0.434	0.900	0.~~257~~588
PS ET_0	0.352	0.365	0.919	0.~~231~~533
M ET_0	1.107	-0.018	0.910	0.~~246~~565
PM_{red} ET_0	0.994	0.013	0.932	0.~~221~~505

Table 4~~.~~: Estimation of Kc (vegetation coefficient), SAWC (soil available water capacity) and runoff ~~estimation~~ for the recharge area of the Séchilienne landslide.

Geology and vegetation are the sub-area ~~types~~factors identified and expressed in proportion of the recharge area. ~~Average~~The average slope gradient is the slope gradient for each identified vegetation sub-area ~~type identified~~factor. Kc, ~~runoff~~R_{coeff} and SAWC columns are the estimated values ~~from the spatial dataset or auger holes~~ for each sub-area ~~type~~factor. Kc RA, SAWC RA and ~~runoff~~R_{coeff} RA columns are the contribution of each sub-area ~~type relatively to sub-area surface proportion~~parameter at the scale of the recharge area. ~~Recharge~~ The recharge-area bottom-row stands for the ~~average~~ estimation at ~~whole~~the scale of the recharge area~~.~~

Geology sub-area (%)		Vegetation sub-area (%)	Average slope gradient (°)	Kc min. max.	Kc RA min. max.	~~Runoff~~R_{coeff} (%)	~~Runoff~~R_{coeff} RA (%)	SAWC (mm)	SAWC RA (mm)
Micaschist	3	Pasture 23	14.0	0.85 1	0.256 0.301	22	5.1	173	5
Sedimentary	9							100	9
Superficial formations	11							112	12
Micaschist	12	Forest 53	20.6	0.745 0.935	0.521 0.654	15	7.7	254	30
Sedimentary	11							81	9
Superficial formations	30							133	41
Outcrop no soil	24	24	-	-	-	0	0	0	0
Recharge area	100	100	-	-	0.777 0.955	-	12.8	-	106

Table ~~5:~~5: Sensitivity analysis results of the best correlation between precipitation/~~recharge~~R_{LRIW} and A16 extensometer detrended displacement.

IS ~~are the~~is for infiltration structures. SAWC is the soil~~-~~-available water~~-~~-capacity. LBCI is the lower bound of the confidence interval. R^2 row is the R^2 computed from recharge~~-~~-area parameters indicated in each table row. Cumulative period (n), shift factor (β) and weighting factor (α) are the terms of the ~~Equation (5).~~equation (3). Null hypothesis ~~NH1~~NH2 test: R^2_{row}-$R^2_{precipitation}$. Null hypothesis ~~NH2~~NH4 test: $R^2_{SAWC\ 105}$-R^2_{row}~~.~~

SAWC mm	~~Runoff coeff. %~~R_{coeff} %	IS %	Cumulative Period (n) day	Shift factor (β) day	Weighting factor (α)	R^2	LBCI of R^2	LBCI of ~~NH1~~NH2	LBCI of ~~NH2~~NH4
0	0.0	100	56	1	0.1697	0.311	0.230	0	0.241
5	0.6	96	92	1	0.1362	0.426	0.335	0.073	0.139
15	1.8	89	101	1	0.1226	0.522	0.435	0.158	0.055
25	3.0	82	104	1	0.1259	0.563	0.481	0.194	0.022
35	4.2	75	104	1	0.1317	0.585	0.508	0.214	0.005
45	5.4	68	103	1	0.1374	0.599	0.525	0.227	-0.004
55	6.6	61	102	1	0.143	0.608	0.537	0.234	-0.008
65	7.8	53	101	1	0.1484	0.613	0.544	0.238	-0.009
75	9.0	46	100	1	0.155	0.616	0.548	0.240	-0.009
85	10.3	39	98	1	0.1609	0.618	0.551	0.242	-0.007
95	11.5	32	94	1	0.1648	0.618	0.552	0.242	-0.004
105	12.8	24	92	1	0.1689	0.618	0.552	0.241	0.000
115	13.9	18	89	1	0.1727	0.617	0.551	0.240	-0.002
125	15.1	10	86	1	0.1745	0.614	0.549	0.237	-0.003

135	16.3	3	82	1	0.1746	0.611	0.545	0.235	-0.003
145	16.3	-	77	1	0.1731	0.609	0.543	0.234	-0.003

~~Table 6: Results of the best linear correlation between precipitation or recharge and displacement records for 4 displacement stations (1101, A13, A16 and G5). Displacement column indicates basic statistics of the displacement records (1st quartile (Q1), median and 3rd quartile (Q3)). Cumulative period (n), shift factor (β) and weighting factor (α) are the terms of the Equation (5). LBCI is the lower bound of the confidence interval. Null hypothesis NH1 test: $R^2_{recharge}$-$R^2_{precipitation}$.~~

			~~← Precipitation / recharge →~~			
~~Extenso-meter~~	~~Displacement Q1/median/Q3 mm/day~~	~~LBCI of NH1~~	~~Cumulative period (n) day~~	~~Shift factor (β) day~~	~~Weighting factor (α)~~	~~R^2~~
~~1101~~	~~1.75 / 2.50 / 3.84~~	~~0.124~~	~~42 / 68~~	~~2 / 2~~	~~0.0714 / 0.0914~~	~~0.284 / 0.495~~
~~A13~~	~~1.18 / 1.75 / 3.41~~	~~0.145~~	~~52 / 82~~	~~3 / 2~~	~~0.1019 / 0.091~~	~~0.275 / 0.520~~
~~A16~~	~~1.94 / 2.98 / 4.39~~	~~0.163~~	~~64 / 76~~	~~2 / 2~~	~~0.1628 / 0.1682~~	~~0.343 / 0.586~~
~~G5~~	~~0.02 / 0.05 / 0.08~~	~~0.144~~	~~8 / 132~~	~~0 / 6~~	~~0.0394 / 0.0110~~	~~0.0006 / 0.243~~

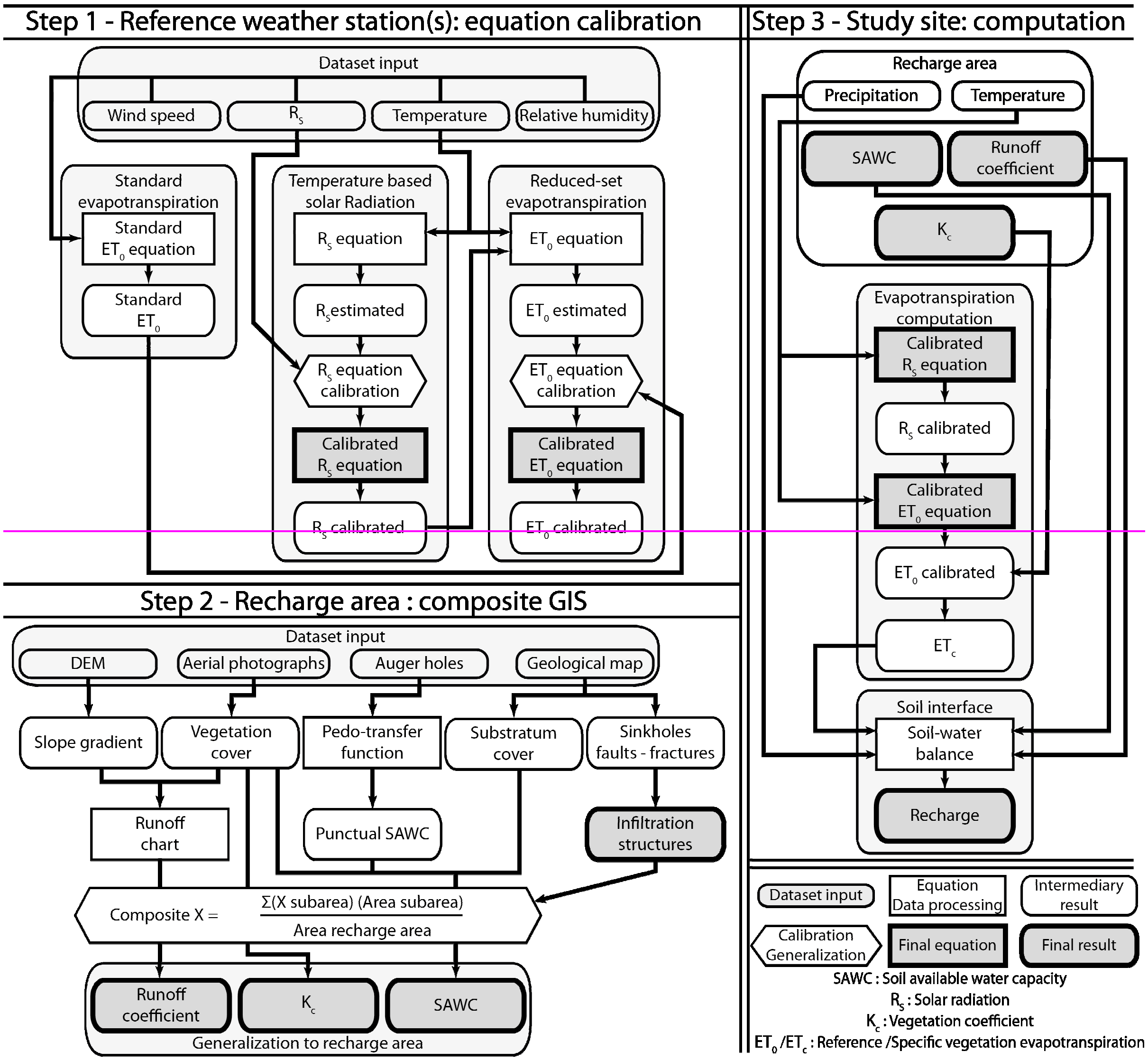
Step 1 - Reference weather station(s): equation calibration
Dataset input
Wind speed
R$_s$
Temperature
Relative humidity
Standard evapotranspiration
Standard ET$_0$ equation
Standard ET$_0$
Temperature based solar Radiation
R$_s$ equation
R$_s$ estimated
R$_s$ equation calibration
Calibrated R$_s$ equation
R$_s$ calibrated
Reduced-set evapotranspiration
ET$_0$ equation
ET$_0$ estimated
ET$_0$ equation calibration
Calibrated ET$_0$ equation
ET$_0$ calibrated
Step 2 - Recharge area : composite GIS
Dataset input
DEM
Aerial photographs
Auger holes
Geological map
Slope gradient
Vegetation cover
Pedo-transfer function
Substratum cover
Sinkholes faults - fractures
Runoff chart
Punctual SAWC
Infiltration structures
Composite X = Σ(X subarea) (Area subarea) / Area recharge area
Runoff coefficient
K$_c$
SAWC
Generalization to recharge area
Step 3 - Study site: computation
Recharge area
Precipitation
Temperature
SAWC
Runoff coefficient
K$_c$
Evapotranspiration computation
Calibrated R$_s$ equation
R$_s$ calibrated
Calibrated ET$_0$ equation
ET$_0$ calibrated
ET$_c$
Soil interface
Soil-water balance
Recharge
Dataset input
Equation Data processing
Intermediary result
Calibration Generalization
Final equation
Final result
SAWC : Soil available water capacity
R$_S$: Solar radiation
K$_c$: Vegetation coefficient
ET$_0$ /ET$_c$: Reference /Specific vegetation evapotranspiration

~~Figure 1:~~

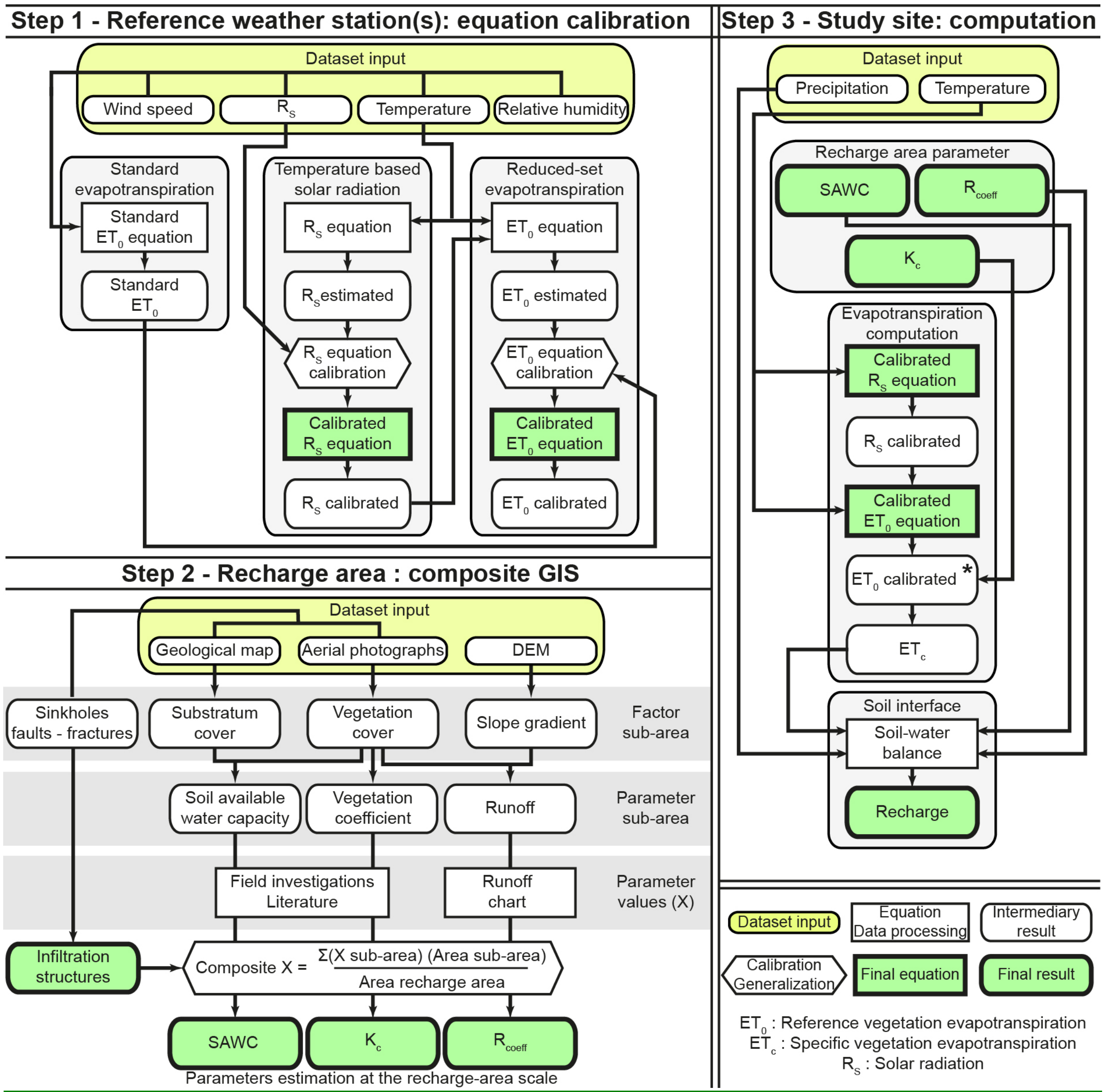

Fig. 1: Landslide Recharge ~~method workflow.~~ Input Workflow (LRIW) diagram. Step 1: calibration of standard ET_0 ~~(reference vegetation evapotranspiration)~~ and R_S ~~(solar radiation)~~ methods.

Step 2: estimation of recharge~~-~~-area parameters required for the soil-water balance (~~runoff coefficient, vegetation coefficient~~R_{coeff}, K_c and SAWC) and the infiltration structures.

Step 3: computation of the recharge with the soil-water balance.

~~Reference~~ *In the case of a landslide having a weather station recording the full set of parameters, the first step can be skipped and the ET_0 ~~method matches with Penman-Monteith method defined in the~~ of step 3 can be estimated directly at the study site with the standard ET_0 (FAO-56 ~~paper and reduced-set ET_0 method with ET_0 methods requiring minimal meteorological data inputs.~~PM method)

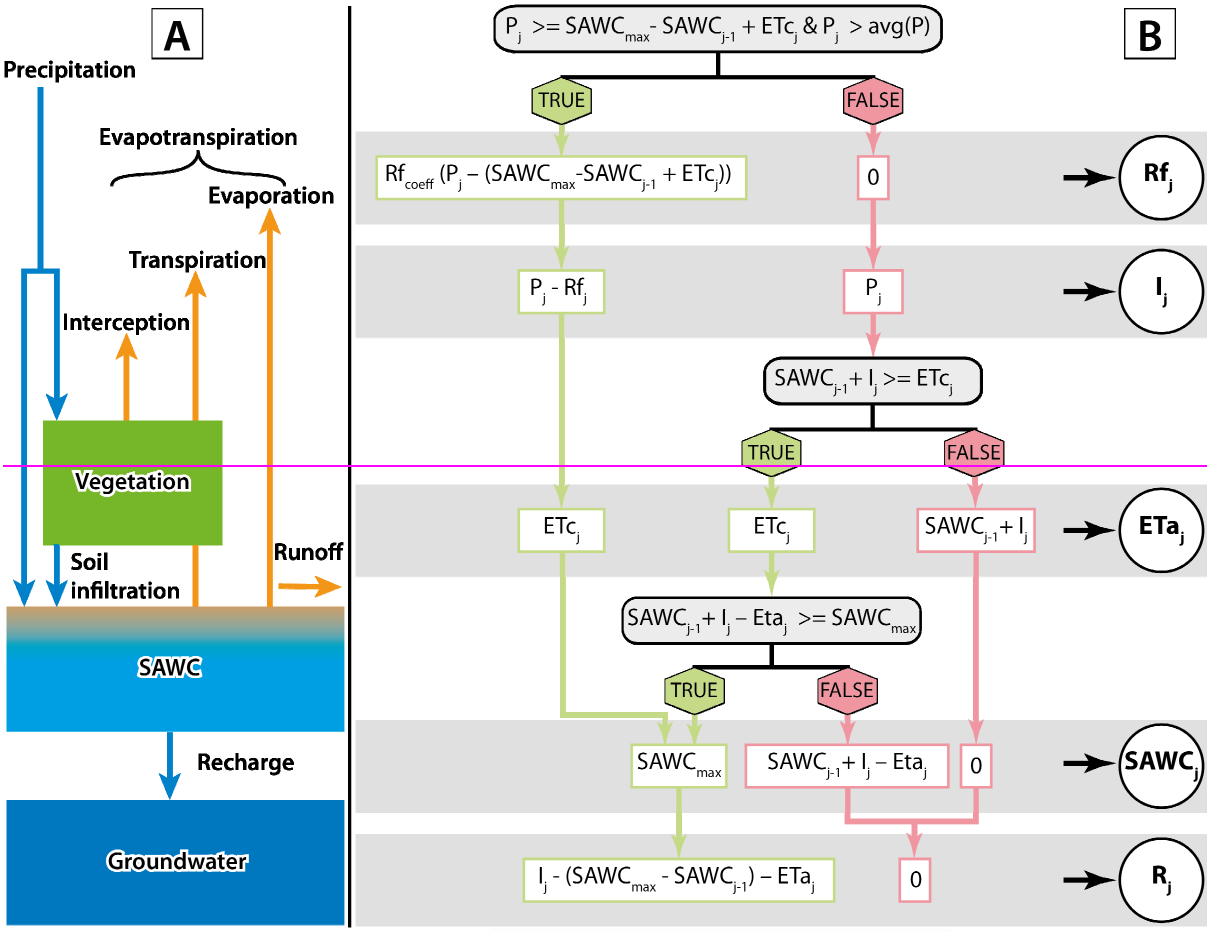
A
Precipitation
Evapotranspiration
Evaporation
Transpiration
Interception
Vegetation
Soil infiltration
Runoff
SAWC
Recharge
Groundwater
B
$P_j >= SAWC_{max} - SAWC_{j-1} + ETc_j \; \& \; P_j > avg(P)$
TRUE
FALSE
$Rf_{coeff} (P_j – (SAWC_{max} - SAWC_{j-1} + ETc_j))$
0
Rf_j
$P_j - Rf_j$
P_j
I_j
$SAWC_{j-1} + I_j >= ETc_j$
TRUE
FALSE
ETc_j
ETc_j
$SAWC_{j-1} + I_j$
ETa_j
$SAWC_{j-1} + I_j – Eta_j >= SAWC_{max}$
TRUE
FALSE
$SAWC_{max}$
$SAWC_{j-1} + I_j – Eta_j$
0
$SAWC_j$
$I_j - (SAWC_{max} - SAWC_{j-1}) – ETa_j$
0
R_j

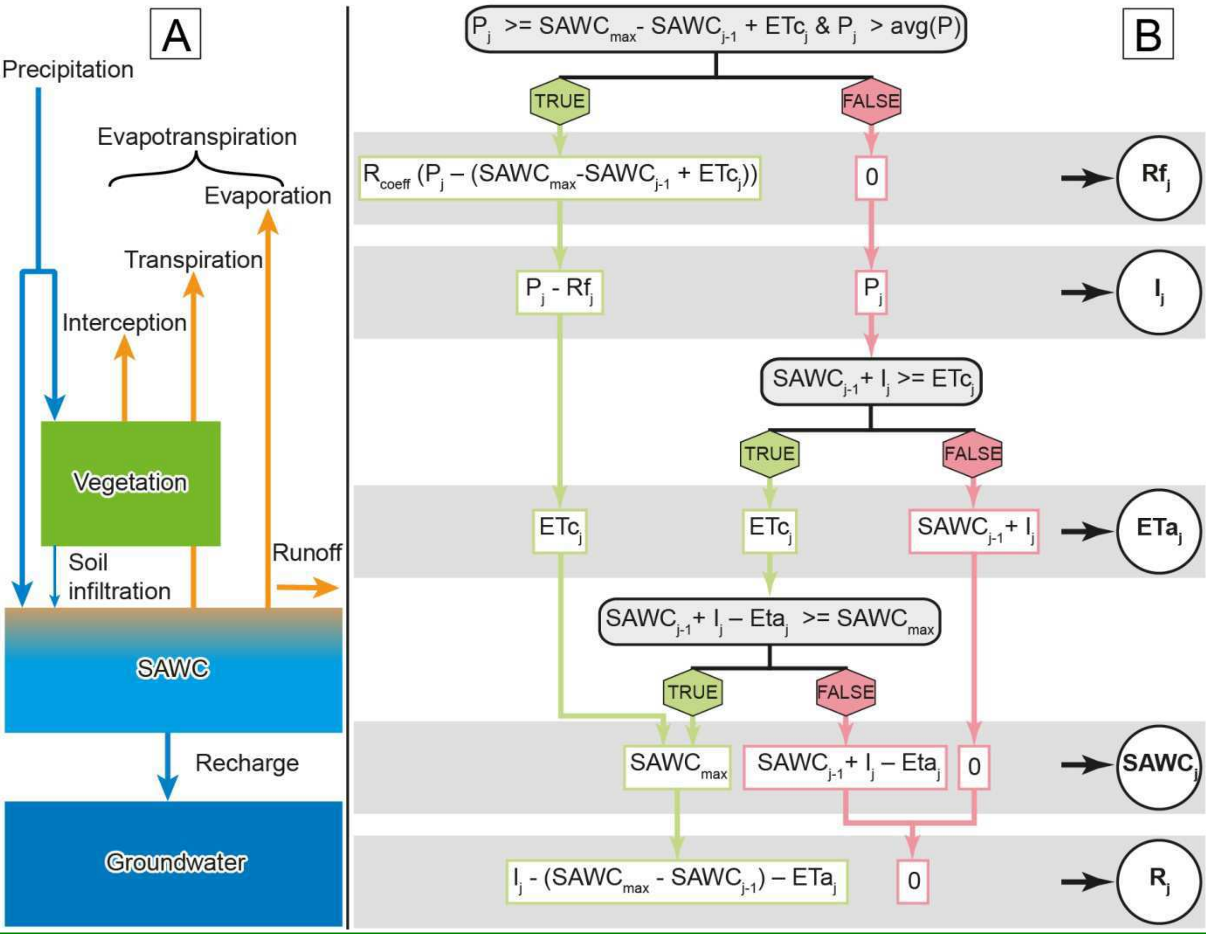
A
Precipitation
Evapotranspiration
Evaporation
Transpiration
Interception
Vegetation
Soil infiltration
Runoff
SAWC
Recharge
Groundwater
B
$P_j >= SAWC_{max} - SAWC_{j-1} + ETc_j \; \& \; P_j > avg(P)$
TRUE
FALSE
$R_{coeff} (P_j – (SAWC_{max} - SAWC_{j-1} + ETc_j))$
0
Rf_j
$P_j - Rf_j$
P_j
I_j
$SAWC_{j-1} + I_j >= ETc_j$
TRUE
FALSE
ETc_j
ETc_j
$SAWC_{j-1} + I_j$
ETa_j
$SAWC_{j-1} + I_j – Eta_j >= SAWC_{max}$
TRUE
FALSE
$SAWC_{max}$
$SAWC_{j-1} + I_j – Eta_j$
0
$SAWC_j$
$I_j - (SAWC_{max} - SAWC_{j-1}) – ETa_j$
0
R_j

~~Figure 2:~~ Fig. 2: Soil-water balance: (A) soil-water balance conceptual representation and (B) soil-water balance diagram used for recharge computation on a daily frequency. SAWC: soil~~-~~-available water~~-~~-capacity, $SAWC_{max}$: SAWC threshold (possible maximum), P: precipitation (rainfall + snow melt), avg (P): precipitation average of the entire record, I: part of precipitation which infiltrate the soil, Rf: surface runoff, ~~Rf_{coeff}~~R_{coeff}: runoff coefficient, ET_c: specific vegetation evapotranspiration, ET_a: actual vegetation evapotranspiration, and R: recharge. Units: mm of water, except R_{coeff} in percent. ~~J~~Subscript j is the computation day and subscript j-1 is the day before. TRUE and FALSE are the answers of the conditional inequality statements~~.~~

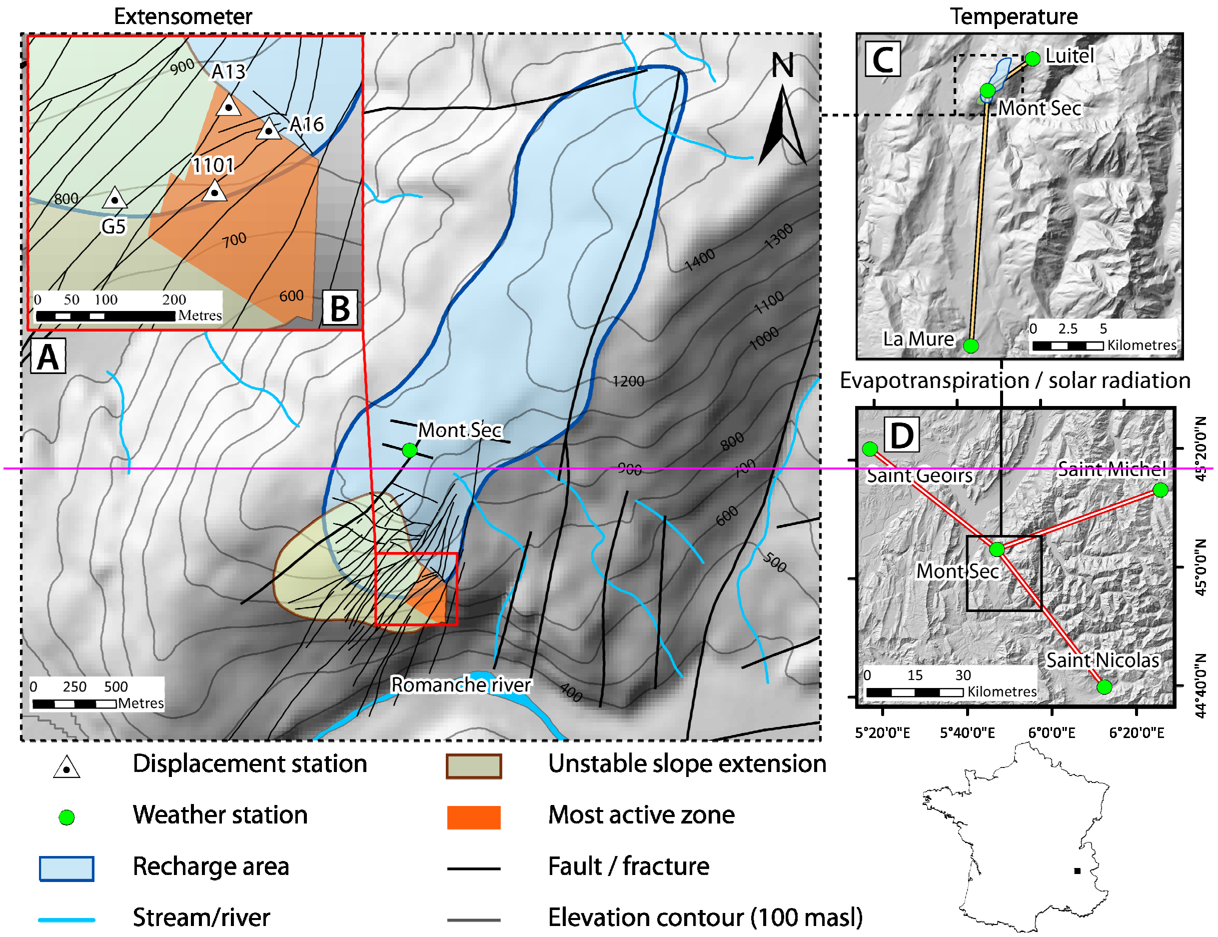

Extensometer
Temperature
A13
A16
1101
G5
900
800
700
600
0 50 100 200 Metres
B
A
N
Mont Sec
Romanche river
1400
1300
1100
1000
1200
900
800
700
600
500
400
0 250 500 Metres
C
Luitel
Mont Sec
La Mure
0 2.5 5 Kilometres
Evapotranspiration / solar radiation
D
Saint Geoirs
Saint Michel
Mont Sec
Saint Nicolas
0 15 30 Kilometres
45°20'0"N
45°0'0"N
44°40'0"N
5°20'0"E
5°40'0"E
6°0'0"E
6°20'0"E
Displacement station
Weather station
Recharge area
Stream/river
Unstable slope extension
Most active zone
Fault / fracture
Elevation contour (100 masl)

1

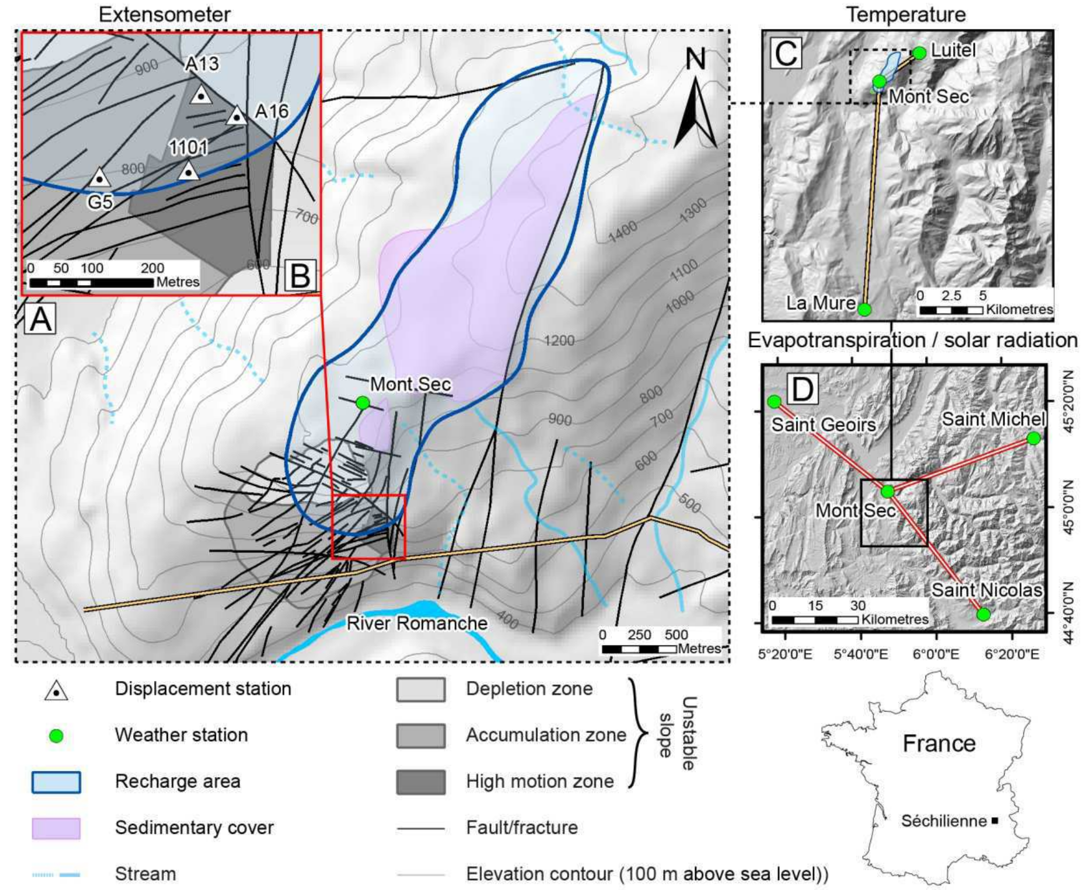

Extensometer
Temperature
A13
A16
1101
G5
900
800
700
600
0 50 100 200 Metres
B
A
N
Mont Sec
River Romanche
1400
1300
1100
1000
1200
900
800
700
600
500
400
0 250 500 Metres
C
Luitel
Mont Sec
La Mure
0 2.5 5 Kilometres
Evapotranspiration / solar radiation
D
Saint Geoirs
Saint Michel
Mont Sec
Saint Nicolas
0 15 30 Kilometres
45°20'0"N
45°0'0"N
44°40'0"N
5°20'0"E
5°40'0"E
6°0'0"E
6°20'0"E
Displacement station
Weather station
Recharge area
Sedimentary cover
Stream
Depletion zone
Accumulation zone
High motion zone
Unstable slope
Fault/fracture
Elevation contour (100 m above sea level))
France
Séchilienne

2

~~Figure 3:~~ **Fig. 3: Location map of the ~~studied~~ Séchilienne landslide.**

A: Map of the Séchilienne unstable slope and recharge area ~~showing the~~ with Mont-Sec weather station ~~used for recharge computation.~~

. B: Enlarged map of the most active area showing displacement stations ~~used.~~

. C: Map showing the weather stations used for the temperature estimation at Mont-Sec.

D: Map showing the weather stations used for evapotranspiration and solar radiation method calibration~~.~~

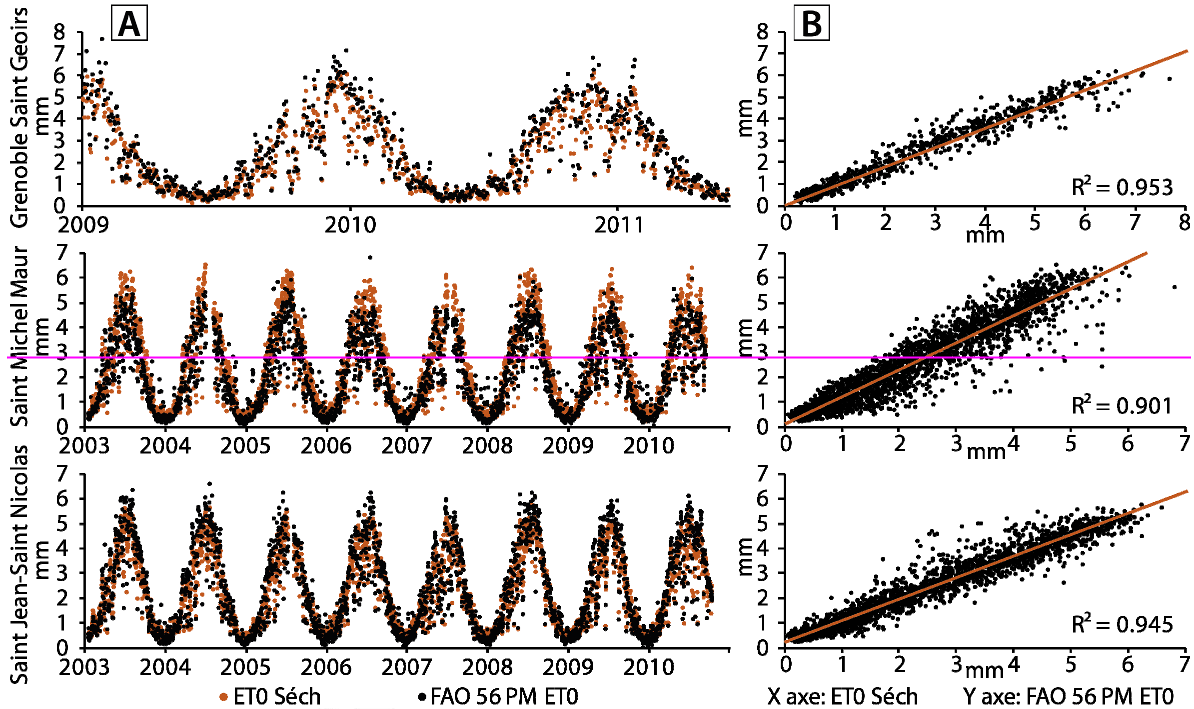

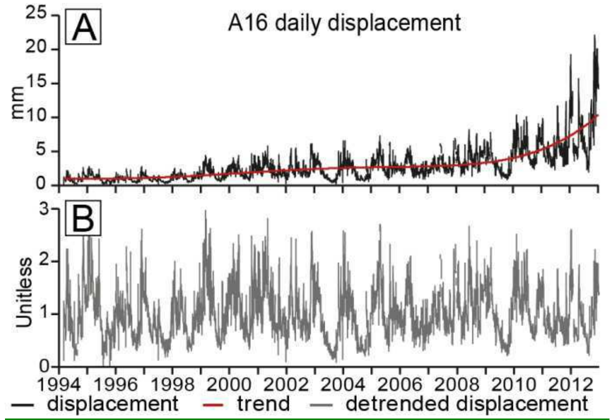

~~Figure 4: ET_0 (reference vegetation evapotranspiration) regional calibration results at the three reference weather stations (Grenoble-Saint-Geoirs, Saint-Jean-Saint-Nicolas, Saint-Michel-Maur).~~

~~A: $ET_{0\ Séch}$ and FAO-56 PM ET_0 as a function of time.~~

~~B: linear regression between $ET_{0\ Séch}$ (X axis) and FAO-56 PM ET_0 (Y axis).~~

~~FAO-56 PM ET_0 stands for ET_0 computed with Penman-Monteith method defined in the FAO-56 paper. $ET_{0\ Séch}$ stands for ET_0 computed with the combination of calibrated ET_0 Penman-Monteith reduced-set method and R_S (solar radiation) modified Bristow-Campbell method.~~

Mis en fo

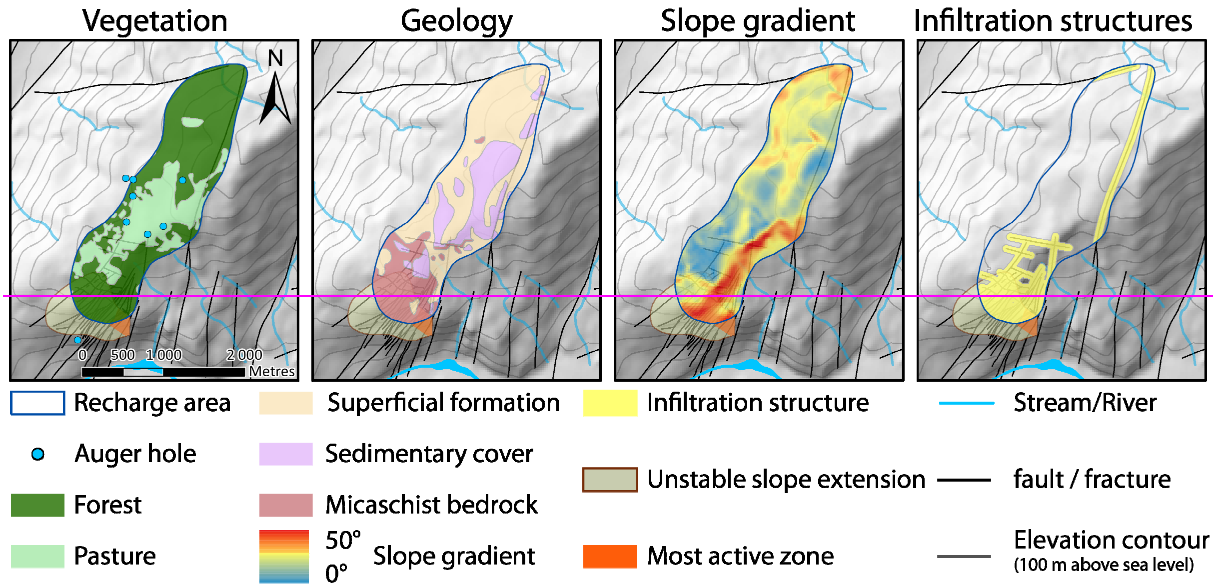

~~Figure 5: Interpreted spatial dataset used for the estimation of recharge area parameters.~~

Mis en fo

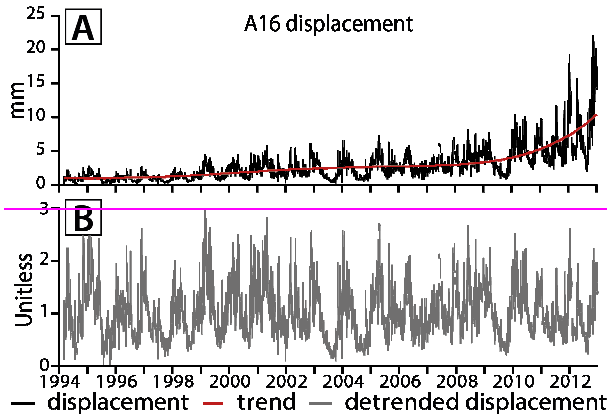

~~Figure 6:~~ Fig. 4: Trend removal of A16 extensometer displacement data~~ with~~. A: A16 displacement data and the fourth order polynomial curve fitting considered as the displacement trend; B: A16 detrended data (unitless) ~~which correspond~~corresponding to A16 displacement data for which the trend ~~was~~is removed by a multiplicative method~~.~~

Mis en fo
: 0 pt

Mis en fo

Mis en fo

Mis en fo

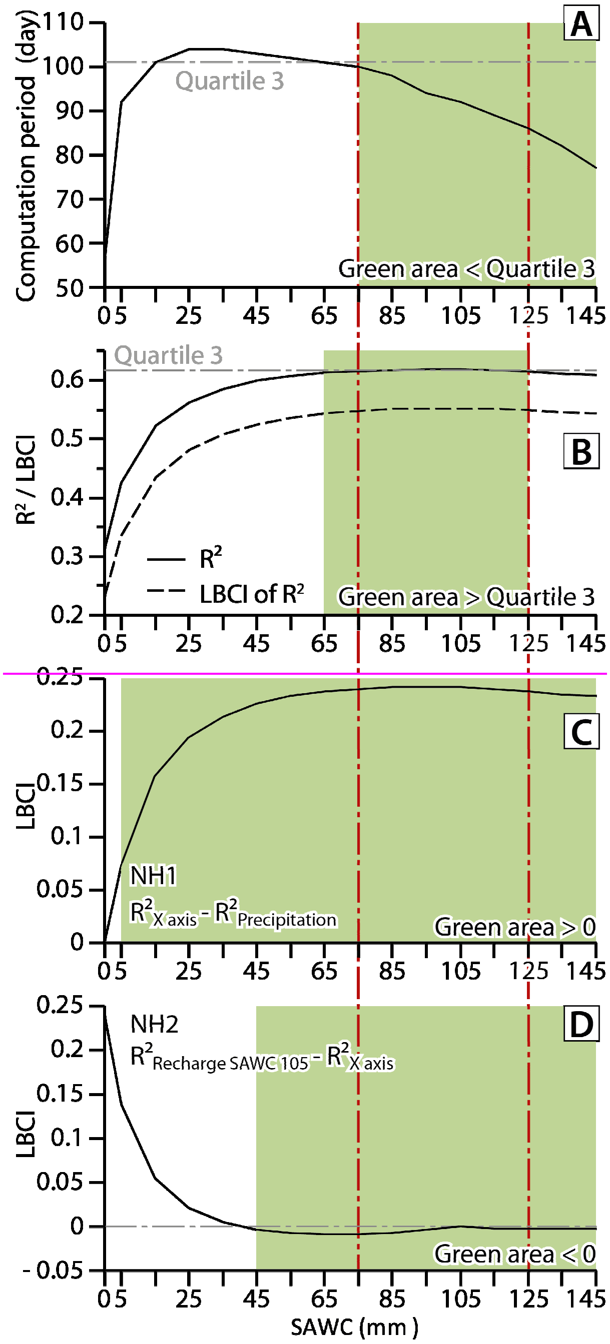
A
Computation period (day)
Quartile 3
Green area < Quartile 3
B
R² / LBCI
Quartile 3
R²
LBCI of R²
Green area > Quartile 3
C
LBCI
NH1
R²X axis - R²Precipitation
Green area > 0
D
LBCI
NH2
R²Recharge SAWC 105 - R²X axis
Green area < 0
SAWC (mm)

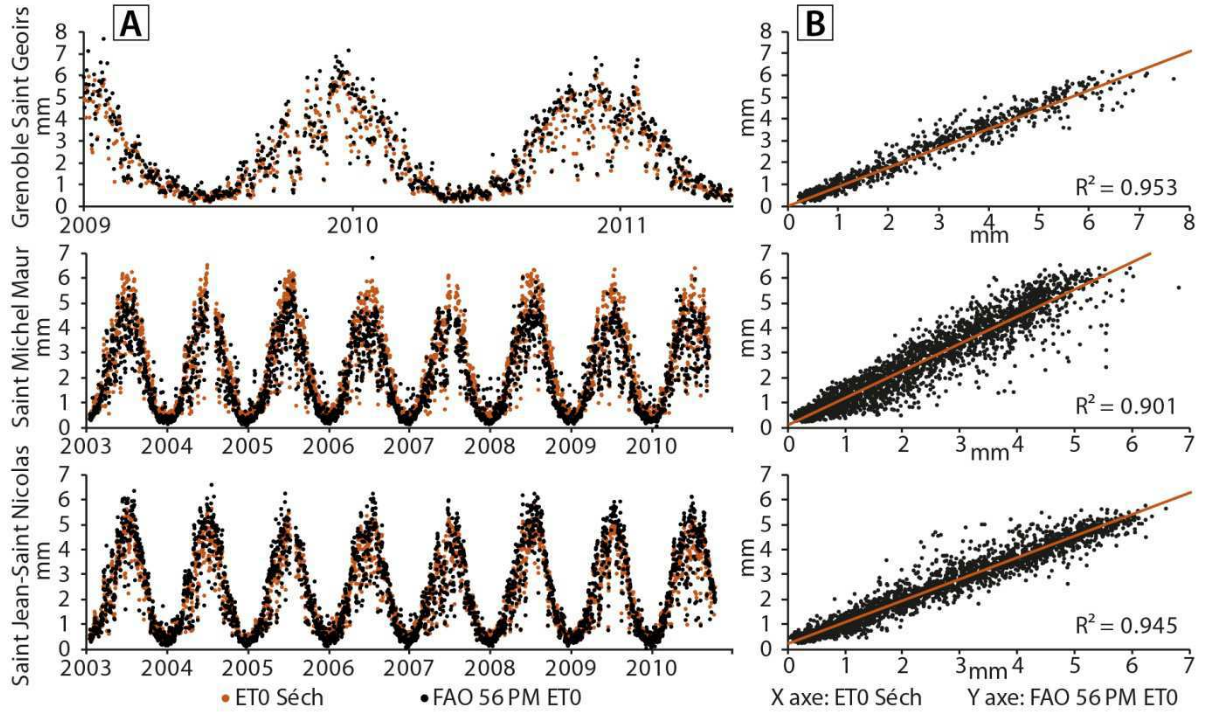

~~**Figure 7:**~~ Fig. 5: ET_0 regional calibration results at the three reference weather stations (Grenoble-Saint-Geoirs, Saint-Jean-Saint-Nicolas and Saint-Michel-Maur). A: $ET_{0\ Séch}$ and FAO-56 PM ET_0 as a function of time. B: linear regression between $ET_{0\ Séch}$ (X axis) and FAO-56 PM ET_0 (Y axis). $ET_{0\ Séch}$ stands for ET_0 computed with the combination of calibrated ET_0 Penman-Monteith reduced-set method and calibrated R_S modified Bristow-Campbell method

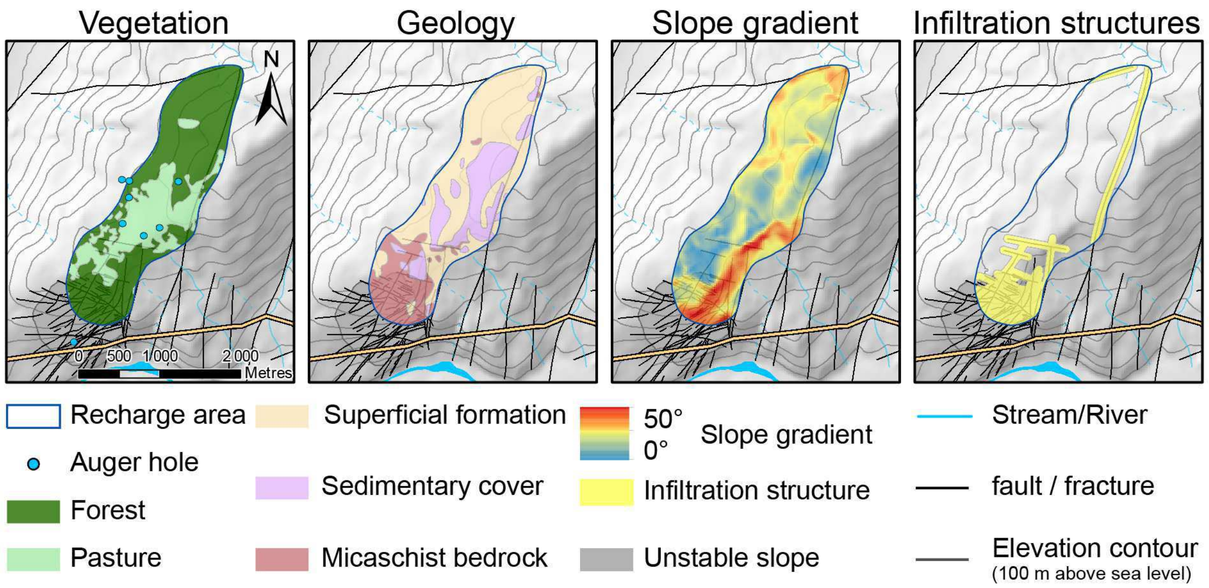

Fig. 6: Factor sub-areas, auger holes and infiltration structures used for the estimation of recharge-area parameters

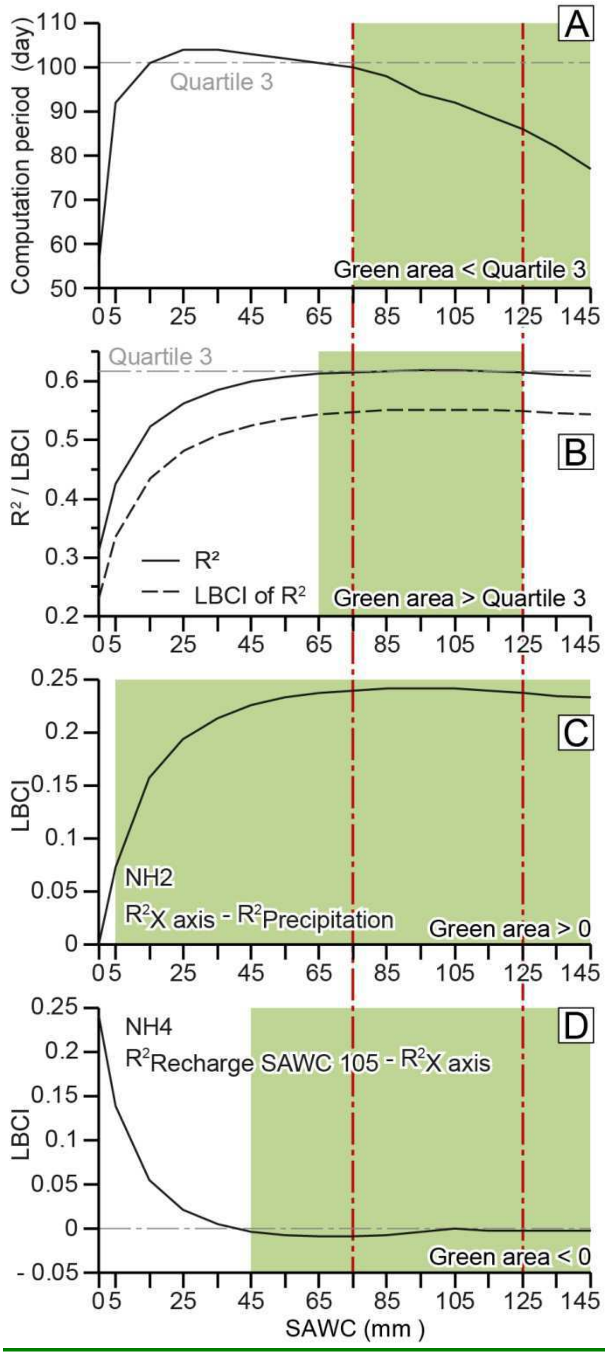

Fig. 7: Results of the sensitivity analysis relative to SAWC (soil-available water-capacity) for (A) the computation period, (B) the R^2 and the LBCI of R^2, (C) the LBCI of the null hypothesis ~~NH1~~NH2 and (D) the LBCI of the null hypothesis ~~NH2~~NH4. LBCI is the lower bound of the confidence interval.

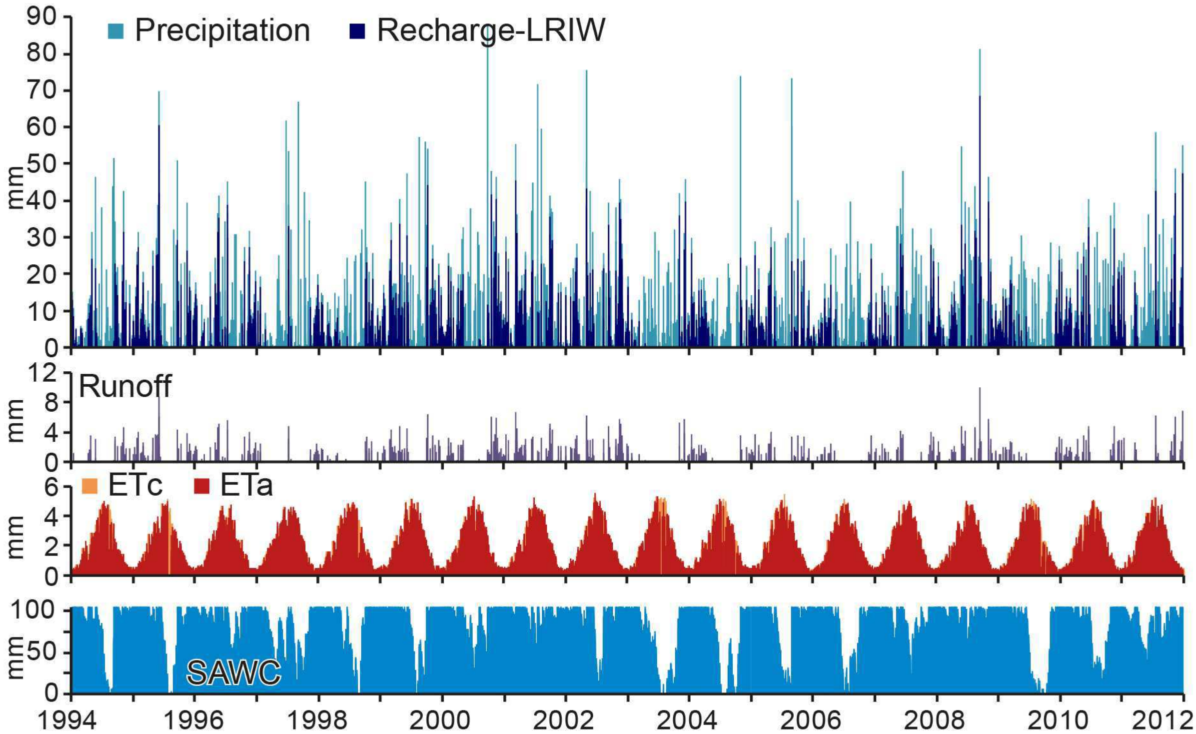

~~Figure 8: Best linear correlation for precipitation and recharge (IS: infiltration structures, SAWC: soil available water capacity).~~

~~A: Linear regression between precipitation/recharge and A16 detrended displacement as a function of time.~~

~~B: Correlation between precipitation/recharge and A16 detrended displacement relatively to time as a function of time.~~

Mis en fo
Crénage 1

Mis en fo

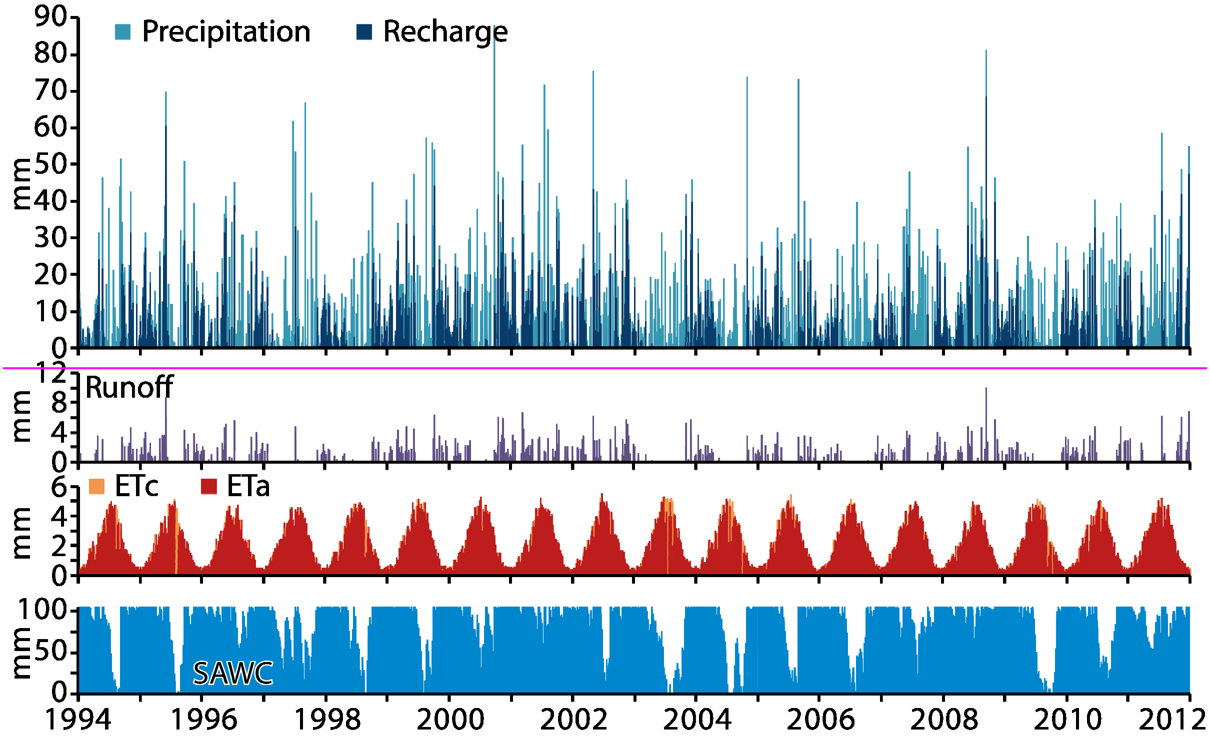

~~Figure 9:~~ Fig. 8: Recharge computation with the LRIW method at Séchilienne with an SAWC of 105 mm and a runoff coefficient of 12.8%. ET_c: specific vegetation evapotranspiration; ET_a: actual vegetation evapotranspiration, SAWC: soil-available water capacity.

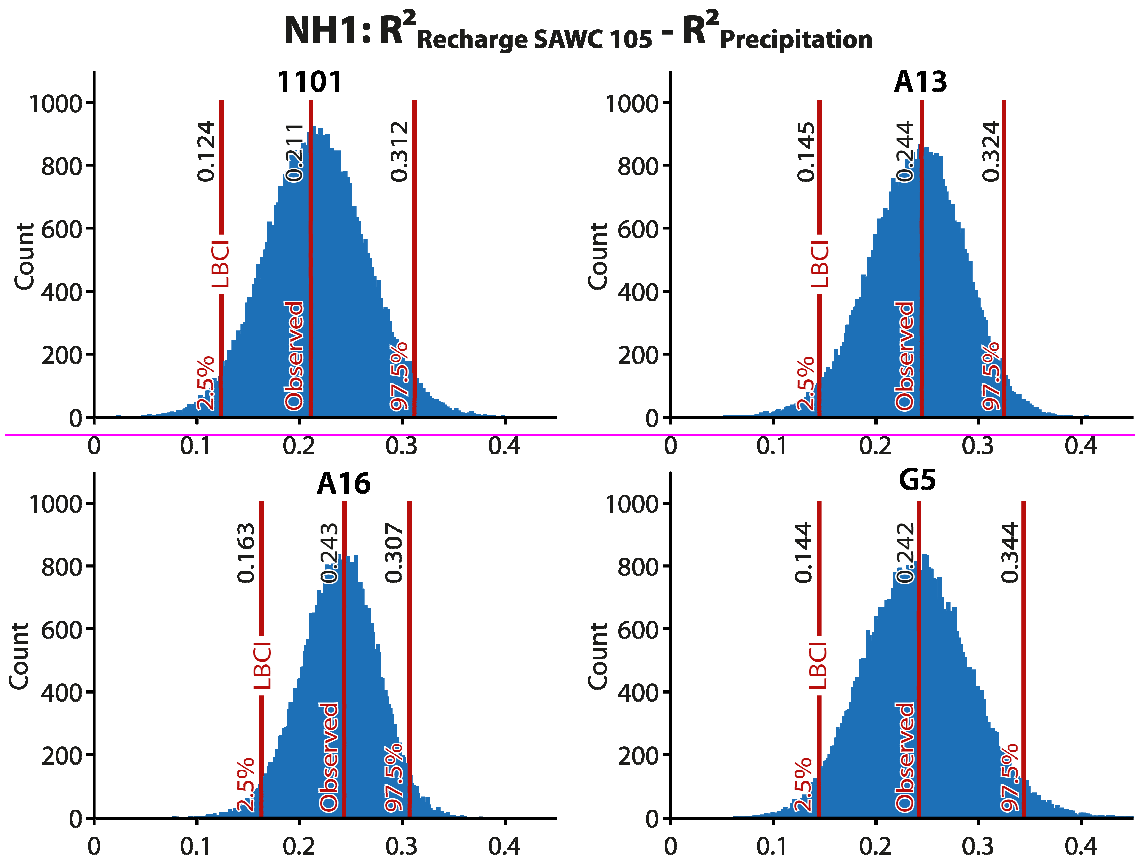

NH1: $R^2_{Recharge\ SAWC\ 105}$ - $R^2_{Precipitation}$
1101
A13
A16
G5
Count
0.124
0.211
0.312
0.145
0.244
0.324
0.163
0.243
0.307
0.144
0.242
0.344
LBCI
Observed
2.5%
97.5%

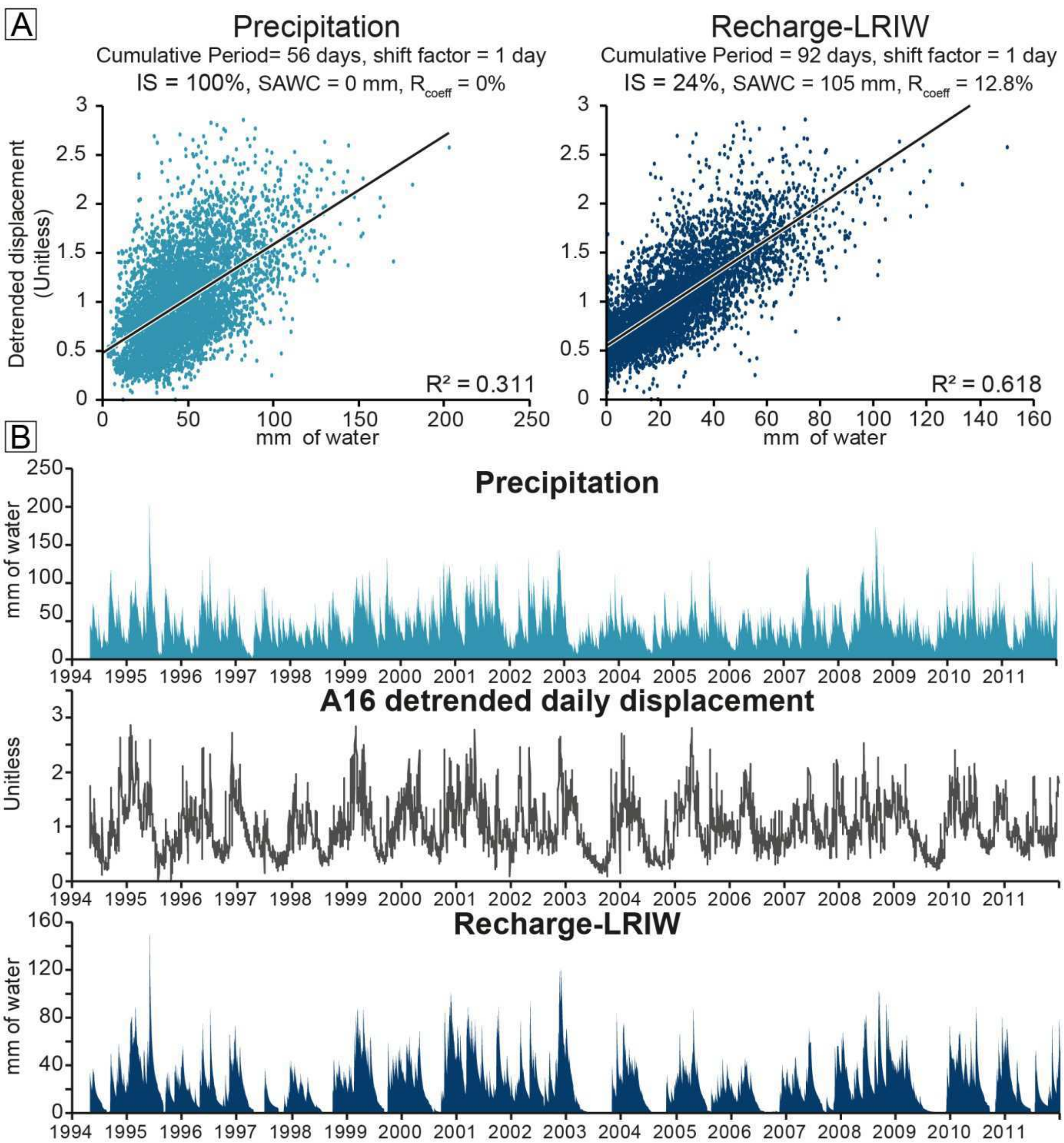

~~Figure 10~~Fig. 9: Best linear correlation for precipitation and recharge computed with the LRIW method. IS is for infiltration structures. SAWC is soil-available water-capacity. Cumulative period (n) and shift factor (β) are the terms of the equation (3). A: Linear regression between precipitation/R_{LRIW} and A16 detrended displacement. B: Correlation between precipitation/R_{LRIW} and A16 detrended displacement as a function of time

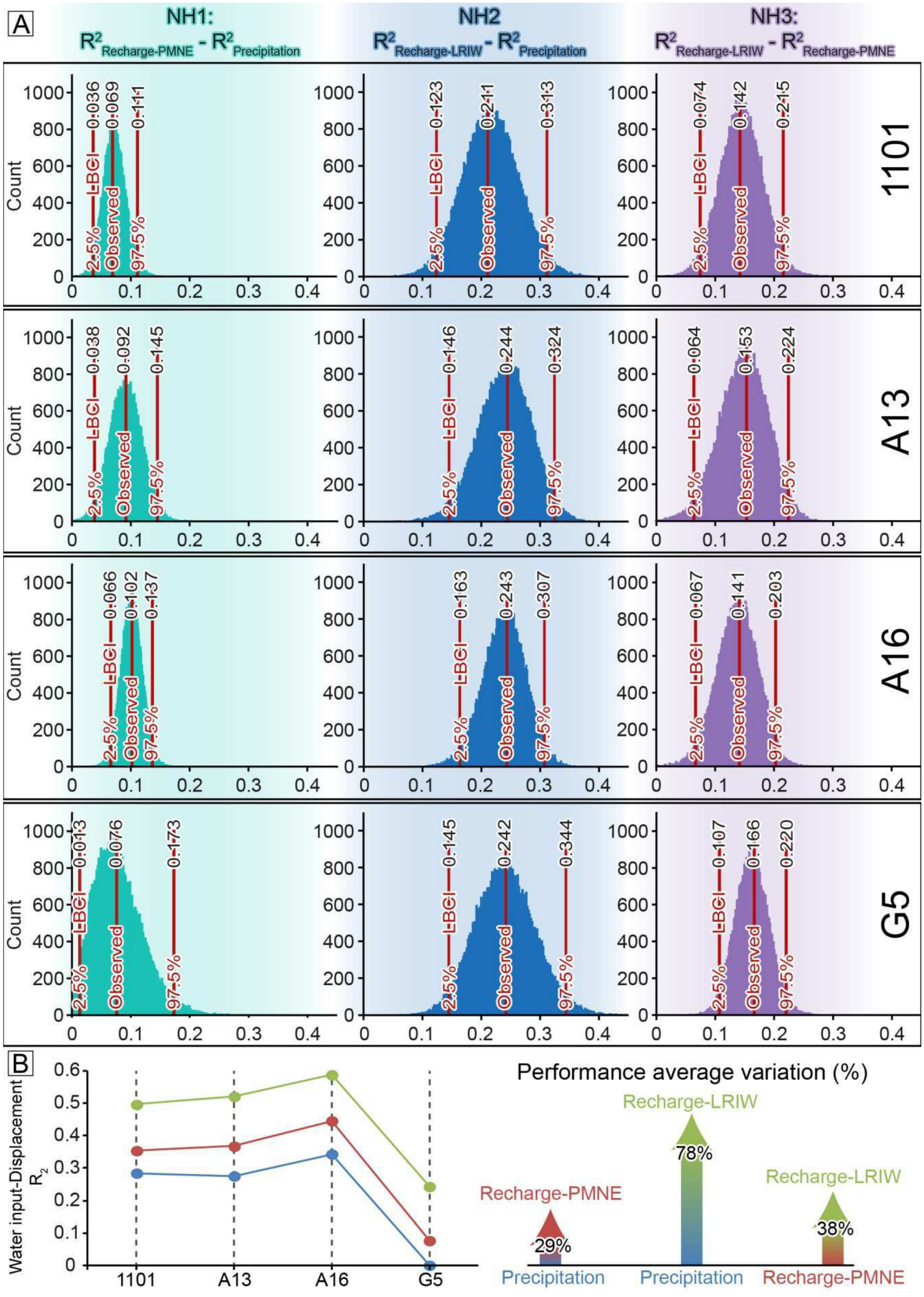

<ins>Fig. 10: Performance of the LRIW workflow. A</ins>: Bootstrap distribution of null hypothesis NH1 ~~test~~<ins>, NH2 and NH3 tests</ins> for four displacement recording stations. LBCI is the lower bound of the confidence interval. ~~Null hypothesis NH1 test: $R^2_{recharge}$ - $R^2_{precipitation}$~~<ins>B: R^2 values for the four displacement recording stations obtained with the precipitation, recharge-PMNE, and recharge-LRIW. LBCI is the lower bound of the confidence interval. G5 station is disregarded in the calculation of the performance average variation calculation since the R^2 value obtained at G5 from precipitation is close to 0, therefore leading to a non-representative variation</ins>.

Mis en fo

Mis en fo